

1
2
3
4
5
6
7
8
9

The Early Proterozoic Matachewan Large Igneous Province: Geochemistry, Petrogenesis, and Implications for Earth Evolution

10 T. Jake. R. Ciborowski*^{1, 2}, Andrew C. Kerr², Richard E. Ernst³, Iain McDonald², Matthew J.
11 Minifie², Stephen S. Harlan⁴, Ian L. Millar⁵

12
13 ¹ Earth and Ocean Sciences, School of Natural Sciences, National University of Ireland,
14 Galway, Ireland

15 ² School of Earth and Ocean Sciences, Cardiff University, Park Place, Cardiff, Wales, CF10
16 3AT, UK

17 ³ Department of Earth Sciences, Carleton University, 1125 Colonel Bay Drive, Ottawa,
18 Ontario, K1S 5B6, Canada & Faculty of Geology and Geography, Tomsk State University, 36
19 Lenin Ave, Tomsk 634050

20 ⁴ National Science Foundation, 4201 Wilson Blvd., Arlington, VA 22230, USA

21 ⁵ NERC Isotope Geosciences Laboratory, Keyworth, Nottingham NG12 5GG, UK

22
23
24 * jake.ciborowski@nuigalway.ie
25
26
27
28
29

30
31
32

ABSTRACT

33 The Matachewan Large Igneous Province (LIP) is interpreted to have formed during the early
34 stages of mantle plume-induced continental break-up in the early Proterozoic. When the
35 Matachewan LIP is reconstructed to its original configuration with units from the Superior
36 Craton and other formerly adjacent blocks (Karelia, Kola, Wyoming and Hearne), the dyke
37 swarms, layered intrusions and flood basalts, emplaced over the lifetime of the province,
38 comprise one of the most extensive magmatic provinces recognised in the geological record.
39 New geochemical data allow, for the first time, the Matachewan LIP to be considered as a
40 single, coherent entity and show that Matachewan LIP rocks share a common tholeiitic
41 composition and trace element geochemistry, characterised by enrichment in the most
42 incompatible elements and depletion in the less incompatible elements. This signature,
43 ubiquitous in early Proterozoic continental magmatic rocks, may indicate that the
44 Matachewan LIP formed through contamination of the primary magmas with lithospheric
45 material or, that the early Proterozoic mantle had a fundamentally different composition to the
46 modern mantle. In addition to the radiating geometry of the dyke swarms, a plume origin for
47 the Matachewan LIP is consistent with the geochemistry of some of the suites; these suites are
48
49
50
51
52
53
54
55
56
57

1
2
3 used to constrain a source mantle potential temperature of approximately 1500-1550°C.
4
5 Comparison of these mantle potential temperatures with estimated temperatures for the early
6 Proterozoic upper mantle, are consistent with a hot mantle plume source for the magmatism.
7
8 Geochemical data from coeval intrusions suggest that the plume head was compositionally
9 heterogeneous and sampled material from both depleted and enriched mantle. As has been
10 documented with less ancient, but similarly vast LIPS, the emplacement of the Matachewan
11 LIP likely had a significant impact on the early Proterozoic global environment. Compilation
12 of the best age estimates for individual suites show that the emplacement of the Matachewan
13 LIP occurred synchronously with the Great Oxidation Event. We explore the potential for the
14 eruption of this LIP and the emission of its associated volcanic gases to have been a driver of
15 the irreversible oxygenation of the Earth.
16
17
18
19
20
21
22
23

24 INTRODUCTION

25
26
27 Large Igneous Provinces (LIPs) consist of large volumes ($>1.3 \times 10^6 \text{ km}^3$) of predominantly
28 mafic-ultramafic magma emplaced during short (1-5 Myr) periods of activity over a
29 maximum lifespan of ~50 Myr (Bryan & Ernst, 2008). LIPs are preserved throughout the
30 geologic record (e.g., Kerr et al., 2000; Ernst & Buchan, 2001) and their study has been used
31 to both understand large-scale mantle processes and also constrain pre-Phanerozoic
32 palaeocontinental reconstructions (e.g., Ernst & Buchan, 2004; Coffin & Eldholm, 2005;
33 Bryan & Ferrari, 2013; Ernst et al., 2013; Ernst, 2014). Currently, the majority opinion
34 favours a mantle plume model for the emplacement of most LIPs, and is even described as
35 'endemic' by Jones et al. (2002). However, other processes for LIP formation have also been
36 proposed, including mantle delamination (Anderson, 2000; McHone, 2000; Anderson, 2005;
37 Elkins-Tanton, 2005; 2007), edge-driven convection (King & Anderson, 1995; 1998; King &
38 Ritsema, 2000; King, 2007), bolide impact (Jones et al., 2002; Ingle & Coffin, 2004; Jones,
39 2005) and mantle insulation (Anderson, 1982; Doblas et al., 2002; Coltice et al., 2007; 2009).

40
41
42 Coffin & Eldholm (1994) subdivide individual LIPs into three parts: the extrusive
43 zone, the middle crust zone and the lower crustal body. The extrusive zone is dominated by
44 basaltic flows, with occasional felsic members and is associated with the early and late stages
45 of LIP formation. The flow packages can be extremely large, extending laterally for
46 thousands of kilometres and can be tens of kilometres thick (Ernst, 2007; Kerr & Mahoney,
47 2007). Typically, erosion has removed much of the extrusive zone in older continental LIPs,
48
49
50
51
52
53
54
55
56
57
58
59
60

1
2
3 though remnants are occasionally preserved within intracratonic basin successions (e.g.,
4 Sandeman & Ryan, 2008). The middle crust zone contains the ‘plumbing system’ of the
5 extrusive zone in the form of dykes, sills and layered intrusions. These plumbing systems are
6 only directly observed in LIPs that are sufficiently old to have had the extrusive cover eroded
7 or to have been dissected by later tectonic events. The most easily recognised features of these
8 plumbing systems are the dykes which form linear dyke sets or massive radiating swarms
9 (Ernst & Buchan, 2001; 2004). The lower crustal body of LIPs is rarely exposed, but is
10 inferred from P-wave velocities of 7.0-7.6 km s⁻¹ at the base of the crust beneath more recent
11 LIPs which suggests the presence of an ultramafic underplated layer beneath these systems
12 (Coffin & Eldholm, 2005).

13
14
15
16
17
18
19 Mafic-ultramafic magmatism occurred on the Superior, Karelia, Kola, Hearne and
20 Wyoming cratons (Fig. 1) during the early Proterozoic (~2.45-2.48 Ga). When these cratons
21 are reconstructed as part of the supercraton, ‘Superia’, the individual igneous suites of the
22 magmatic event comprise a coherent LIP, known as the Matachewan (Bleeker, 2003; Bleeker
23 & Ernst, 2006; Ernst & Bleeker, 2010). This reconstructed Matachewan LIP includes
24 radiating dyke swarms, suites of layered intrusions, sill complexes and flood basalts (Heaman,
25 1997; Dahl et al., 2006; Van Boening & Nabelek, 2008; Söderlund et al., 2010), which
26 themselves appear to have been emplaced in a series of pulses (Table 1). The layered
27 intrusions are of particular interest because of their economic potential for Ni-Cu-platinum
28 group element (PGE) sulphide mineralisation (Peck et al., 2001; James et al., 2002; Iljina &
29 Hanski, 2005).

30
31
32
33
34
35
36
37
38 Prior to this study, many of the individual igneous suites which make up the
39 Matachewan LIP were poorly-known in terms of their geochemistry and no attempt had been
40 made to study the entire Matachewan LIP utilizing data from all the component blocks,
41 though some attempts have been made to understand the petrogenesis of several individual
42 suites [e.g., Jolly et al., 1992; Phinney & Halls, 2001; Van Boening & Nabelek, 2008;
43 Ciborowski et al., 2013]. In this study we have analysed new samples and compiled existing
44 geochemical data for the reconstructed Matachewan LIP in order to understand the nature and
45 origin of the mantle sources, the anatomy of the magmatic plumbing system within the
46 lithosphere, and how the emplacement of the LIP may have affected the global environment
47 during the Archean-Proterozoic transition.

58 OVERVIEW OF THE MATACHEWAN LIP

1
2
3
4 The Matachewan LIP is a proposed ~2.48-2.45 Ga reconstructed LIP found on five separate
5 Archean cratonic blocks (Superior, Wyoming, Hearne, Karelia and Zimbabwe) that comprised
6 the supercontinent 'Superia' (Heaman, 1997; Bleeker & Ernst, 2006; Ernst & Bleeker, 2010;
7 Söderlund et al., 2010) (Fig. 2). Tentative correlations involving rocks associated with the
8 Matachewan LIP have been proposed for decades (Blackwelder, 1926; Young, 1988;
9 Patterson & Heaman, 1991; Williams et al., 1991). However, Roscoe & Card (1993) and
10 Aspler & Chiarenzelli (1998) produced the first detailed sedimentary stratigraphy of, and
11 correlation between, the Superior craton and the Wyoming craton. They suggested that these
12 rocks were either deposited in a common, rift-related intracratonic basin during the break-up
13 of an Archean-Early Proterozoic supercontinent (Kenorland) (Roscoe & Card, 1993) or that
14 the sequences formed as part of a contemporaneous rifted passive margin sequence deposited
15 along the southern margin of the Kenorland supercontinent (Aspler & Chiarenzelli, 1998).
16
17

18
19
20
21
22
23
24 Coeval U-Pb ages (~2.47 Ga) led Heaman (1997) to extend this initial reconstruction
25 to include the Karelia craton following the discovery of radiating dyke swarms on the
26 Superior and Karelia cratons, thus implying a cogenetic source for magmatism on the two
27 cratons. Heaman (1997) was also the first to suggest that a mantle plume was responsible for
28 the break-up of the supercontinent Kenorland and the associated magmatism (Fig. 2).
29
30
31
32

33
34 A comparison of the intrusion history and geochemistry of coeval layered intrusions
35 on the Superior and Karelia cratons (Vogel et al., 1998a), found that the igneous history of the
36 two cratons remained similar until ~2.20 Ga, following which coeval intrusions do not occur
37 on both cratons. A comparison of the dyke swarms in the Superior and Karelian cratons
38 indicated similarity until 2100 Ma (Bleeker & Ernst, 2006) suggesting that breakup did not
39 occur until after, or in association with, the 2025-2100 Ma Marathon LIP and 2075 Ma Fort
40 Frances LIP of the Superior craton and corresponding magmatism on Karelia and the other
41 blocks.
42
43
44
45

46
47 Further, geochemical data for the ~2.48 Ga East Bull Lake layered intrusions
48 (Superior craton) and Fennoscandian intrusions (Karelia craton) suggest that these two suites
49 of intrusions were derived from a common mantle source (Vogel et al., 1998a). The potential
50 ~2.5 Ga link between the Superior, Wyoming and Karelia cratons was further strengthened by
51 Ojakangas et al. (2001) who correlated glaciogenic deposits, a palaeosol horizon and
52 carbonate sequences with high $\delta^{13}\text{C}$ values between the different cratons.
53
54
55

56
57 Using the 'Craton Clan' method, Bleeker (2003) grouped the ~35 Archean cratons into
58 3-4 craton clans which existed during the Archean – Early Proterozoic. It was proposed that
59
60

1
2
3 these clans existed as individual continents separated by intervening oceans, with each
4 continent experiencing a common geologic history prior to continental rifting and tectonic
5 dispersal. One such clan, (the 'Superia' clan) is made up of the Superior, Hearne and Karelia
6 cratons. Using geochronology, petrology and earlier palaeomagnetic work, Bleeker (2004)
7 proposed that these cratons were sutured together prior to 2.45 Ga and that the arrival of a
8 mantle plume head at the end of the Archean initiated magmatism on (and rifting of) the
9 'Superia' supercontinent. Harlan (2005) proposed that the Leopard Dykes (so called for their
10 ubiquitous plagioclase megacrysts) of the Wyoming craton may be cogenetic with the
11 similarly textured Matachewan and Kaminak dyke swarms on the Superior and Hearne
12 cratons, respectively. However, unpublished U-Pb data indicate that the Leopard dykes were
13 not coeval with the other potential Matachewan LIP suites (K. Chamberlain, pers. com., 2014)
14 and will not be considered here.

15
16 A U-Pb date of 2480 ± 6 Ma (Dahl et al., 2006) for the Blue Draw Metagabbro, a 1 km
17 thick layered mafic sill exposed in the eastern Wyoming craton (Ciborowski et al., 2013)
18 strengthens a ~2.5 Ga Superior–Wyoming correlation. This age is identical to the similarly-
19 sized mafic intrusions of the East Bull Lake Intrusive Suite on the Superior craton (Krogh et
20 al., 1984) and suggests a ~ 2.5 Ga supercontinent reconstruction which includes the
21 Wyoming, Superior and Karelia cratons.

22
23 Bleeker & Ernst (2006) proposed that temporal matching of the magmatic 'barcodes'
24 for different cratons provides the most robust method for reconstructing ancient continents.
25 Bleeker & Ernst (2006) and also Ernst & Bleeker (2010) and Söderlund et al. (2010)
26 presented such 'barcodes' for the Superior, Hearne and Karelia cratons and suggested that
27 these cratons were part of the same supercontinent (Superia) during the late-Archean and
28 Paleoproterozoic until 'Superia' rifted apart sometime after 2.1 Ga.

29
30 The most recent ~2.5-2.45 Ga supercontinent reconstruction (Ernst & Bleeker, 2010)
31 links volcano-sedimentary sequences, layered intrusions and mafic dyke swarms on the
32 Wyoming, Superior, Karelia and Hearne cratons and interprets these rocks to have formed
33 during rifting of this supercontinent between ~2.5 and ~2.1 Ga. Crucially, the reconstruction
34 reassembles the mafic dyke swarms preserved on the four constituent cratons into one, giant
35 radiating swarm, thought to indicate the focal point a mantle-plume which drove the rifting
36 event (Fig. 2).

37
38
39
40
41
42
43
44
45
46
47
48
49
50
51
52
53
54
55
56
57
58
59
60
MATACHEWAN LIP SUITES

Matachewan LIP dyke swarms

Matachewan dyke swarm

The Matachewan dyke swarm comprises thousands of north-northwest trending dykes which crop out over an area of 300,000 km² in southern Ontario and south western Quebec (Fig. 1). The dykes are sub-vertical and can be up to ~60 m wide, though the majority are ~10-20 m wide (Bates & Halls, 1990; Nelson et al., 1990; Heaman, 1997; Siddorn, 1999). Individual Matachewan dykes can be followed in outcrop over tens of kilometres (Phinney & Halls, 2001), and high resolution aeromagnetic data (West & Ernst, 1991) allows single dykes to be traced in the subsurface for hundreds of kilometres, revealing that they transcend tectonic boundaries between the east-west trending Archean granite-greenstone and metasedimentary terranes which make up the Superior craton. These Fe-rich quartz tholeiite dykes locally contain distinctive plagioclase megacrysts which can be up to ~20 cm in length (Halls, 1991; Siddorn, 1999). Metamorphism of the Matachewan dyke swarm reached a maximum of lower greenschist facies (Halls, 1991).

The Matachewan dyke swarm can be divided into three sub-swarms, characterised by slight changes in dyke orientation and delineated by intervening areas with a low density of dykes (Bates & Halls, 1990; West & Ernst, 1991; Zhang, 1999). Most workers interpret these sub-swarms as being part of a single fanning system with an arc angle of between ~40-60° which radiates from a focus near Sudbury, Ontario (e.g., Ernst et al., 1995; Park et al., 1995; Zhang, 1999; Phinney & Halls, 2001; Halls et al., 2005; Halls et al., 2007). Ages of ~2473 Ma and ~2446 Ma have been obtained for the central and western subswarms, respectively (Heaman, 1997). Halls et al. (2005) also dated a Matachewan dyke from west of Kapuskasing (U-Pb baddeleyite) that gave a discordant age of 2459 ± 5 Ma which falls within the range determined by Heaman (1997).

Kaminak dyke swarm

The Kaminak dyke swarm is made up of hundreds of north-northeast trending dykes which crop out over an area of 20,000 km² in southern Nunavut (Buchan & Ernst, 2004), approximately 100 km west of Hudson Bay (Fig. 1). The dykes are Fe-rich quartz tholeiites (Christie et al., 1975; Sandeman & Ryan, 2008), range in texture from aphyric to plagioclase porphyritic and locally, can contain abundant megacrysts (~10 cm wide) of plagioclase (Bleeker, 2004). The metamorphism of the bulk of the Kaminak dyke swarm reached a maximum of lower greenschist facies.

1
2
3
4
5 The Kaminak dykes are generally vertical and vary from ~1-40 m in thickness, but are
6 typically 5-10 m thick. The dykes tend to form resistant ridges which can be traced over tens
7 of kilometres before being truncated by younger faults (Christie et al., 1975; Sandeman &
8 Ryan, 2008; Sandeman et al., 2013). The N-NE trend of the dykes bisects the dominant
9 tectonic boundaries between the Archean supracrustal and granitoid rocks which make up the
10 hosting Ennadai-Rankin greenstone belt (Aspler et al., 2000). The trends of the Kaminak
11 dykes have been described as radiating, with an arc angle of ~40° by Ernst & Bleeker (2010)
12 or as a linear array (Sandeman & Ryan, 2008). Age data suggests that the Kaminak swarm
13 consists of two pulses of tholeiitic dykes, at 2450 ± 2 Ma and 2498 ± 1 Ma (Heaman, 2004;
14 Sandeman & Ryan, 2008; Sandemann et al., 2013). The older age is more consistent with a
15 link with the 2500 Ma Mistassini LIP of the southeastern Superior craton rather than with the
16 Matachewan LIP (Ernst & Bleeker, 2010). However, the younger age can be linked to the
17 Matachewan LIP.
18
19
20
21
22
23
24
25

26 Based on field relationships and geochemical similarities, the Kaminak dyke swarms
27 have been interpreted to be feeders to the continental tholeiitic basalts of the Spi Group which
28 crop out in the core of a syncline, preserved in the modern day Spi basin (Patterson, 1991;
29 Sandeman & Ryan, 2008).
30
31
32
33

34 Viianki dyke swarm

35 Mafic dyke swarms preserved on the Karelia craton (Fig. 1) are poorly defined. Preliminary
36 analysis of the ages of these Paleoproterozoic mafic dykes (Kulikov et al., 2010; see also
37 Vuollo & Huhma, 2005) indicates that the craton experienced at least 3-4 mafic igneous
38 events between 2.4-2.5 Ga which broadly overlap the ages of mafic dykes preserved on the
39 other Superia cratons. Unlike the events on the other cratons, very few attempts have been
40 made to sub-divide the dated Karelia dykes into separate swarms which share a consistent
41 trend, appearance, mineralogy and chemistry.
42
43
44
45
46
47

48 One of the few Paleoproterozoic swarms to be identified is the Viianki dyke swarm,
49 which has been proposed as the likely feeder of the ~2.44 Ga layered mafic intrusions on the
50 craton (Vogel et al., 1998a). Vogel et al. (1998a) characterised the Viianki swarm as a
51 northwest trending swarm of tholeiitic basalt and andesite dykes. The Viianki dykes are likely
52 to be equivalent to the Karelia dykes described by Mertanen et al. (1999) based on the similar
53 ages, trends and geographic locations of the dykes. Mertanen et al. (1999) describe the
54 Karelia dykes as northwest trending and subvertical, varying in thickness from 6 cm - 200 m
55
56
57
58
59
60

1
2
3 with compositions which range from Fe-tholeiitic and tholeiitic to calc-alkaline. However,
4 these are likely intermixed with c. 1980 Ma dykes and c. 2100 Ma dykes of approximately
5 similar trend (Vuollo & Huhma, 2005).
6
7

8 9 10 Matachewan LIP flood basalts

11 12 Thessalon Formation

13
14 The Huronian Supergroup is a 5-12 km thick volcanic-sedimentary succession which sits
15 unconformably on the Archean basement rocks of the southern Superior Province. The
16 Huronian crops out discontinuously west from the east shore of Lake Superior, through
17 Sudbury to Lake Timiskaming (Fig. 1).
18
19

20
21 The lowest lithostratigraphic formation in the Huronian Supergroup (Elliot Lake),
22 contains the only ~2.45 Ga volcanic rocks preserved within the supergroup (Krogh et al.,
23 1984; Corfu & Easton, 2000; Ketchum et al., 2013). These volcanic rocks are found in the
24 Thessalon Formation and are preserved in three discrete regions across southern Ontario
25 within which the volcanic rocks range in thickness from 500 – 1200 m (Ketchum et al.,
26 2013).
27
28

29
30 The Thessalon Formation volcanic rocks are predominantly composed of fine-medium
31 grained basaltic, basaltic-andesitic, andesitic and subordinate rhyolitic flows (Jolly, 1987a;
32 Bennett et al., 1991), which have undergone greenschist facies metamorphism. Bennett et al.
33 (1991) reported both ashfall tuffs and pillow basalts within the Thessalon Formation,
34 indicating that eruptions were both subaerial and subaqueous.
35
36
37
38
39

40 41 Spi Group

42
43 The Spi Group is limited to the areally restricted (~8 km²) Spi Basin in southern Nunavut
44 (Fig. 1), which is interpreted to have formed during the same extension event that resulted in
45 the emplacement of the underlying Kaminak dykes (Sandeman & Ryan, 2008). The lower Spi
46 Group is dominated by the Spi Formation, a 75-150 m thick package of plagioclase
47 porphyritic, basaltic flows with intercalated sediments. The Spi Formation basalts are
48 interpreted to be the eruptive equivalents of the Kaminak dyke swarm (Sandeman et al.,
49 2013). The flows predominantly erupted subareally, though localised, poorly developed
50 pillow structures indicate that at least some were erupted subaqueously.
51
52

53
54 Based on similar appearances and geochemical signatures, the Spi Formation lavas
55 have been tentatively correlated with other similar plagioclase porphyritic basalts preserved in
56
57
58
59
60

1
2
3 other remote basins across southern Nunavut (Carpenter, 2003). This may suggest that the Spi
4 Formation represents the erosional remnants of a much larger flood basalt province, although
5 included fragments have not been found in the unconformably overlying sediments
6
7 (Sandeman & Ryan, 2008).
8
9

10 Seidorechka Formation

11
12 Reconstruction of the Huronian and Karelia Supergroups involve correlations of ~2.45 Ga
13 volcanic rocks that form the base of the Sumi-Sariola Group, here referred to collectively as
14 the Seidorechka Formation (Melezhik, 2006) (see Hanski et al. (2001) for a further discussion
15 on the nomenclature and timing of coeval formations). These ~2.45 Ga rocks are preserved in
16 several basins adjacent to the White Sea in northwest Russia and northern Finland (Fig. 1).
17 The Seidorechka Formation is ~3000 m thick and composed of amygdaloidal komatiitic,
18 basaltic and basaltic-andesitic flows at the base and dacitic-rhyolitic flows at the top
19 (Melezhik & Sturt, 1994; Puchtel et al., 1997) that are metamorphosed to lower greenschist
20 facies (Chashchin et al., 2008; Puchtel et al., 1997). Individual flows can be up to ~150 m
21 thick (Puchtel et al. 1996) and the original areal extent of the Seidorechka Formation has been
22 estimated to be between 100,000-700,000 km² (Melezhik, 2006).
23
24
25
26
27
28
29
30
31

32 Matachewan LIP layered intrusions

33 East Bull Lake Suite

34
35 The East Bull Lake intrusive suite is the name given to several 2491 – 2475 Ma, layered
36 gabbro-noritic to gabbroic-anorthositic intrusions which occur along the margin of the
37 Superior Craton with the Southern Province. The areal extent of individual East Bull Lake
38 Suite intrusions varies from 1 to ~100 km². The largest, and most completely preserved of the
39 suite is the 2100 m thick Agnew Lake intrusion, approximately 70 km west of Sudbury,
40 Ontario (Vogel et al., 1998a).
41
42
43
44
45
46
47

48 The East Bull Lake Suite intrusions are dominated by leucogabbro-noritic and
49 gabbro-noritic rocks, though more mafic, melanogabbro-norites, troctolites and olivine
50 gabbro-norites are found in the lower levels of the intrusions (James et al., 2002). In the most
51 completely preserved East Bull Lake Suite intrusion at Agnew Lake, the stratigraphy at the
52 very top of the intrusion is composed of ferrosyenites and alkali-feldspar granites. Field and
53 geochemical studies of the East Bull Lake suite (Vogel et al., 1998b; 1999) identified the
54 most likely feeder dykes to be the gabbro-noritic (An₇₈) Streich dykes. The breccia zones
55
56
57
58
59
60

1
2
3 which are found at the base of many of the East Bull Lake Suite intrusions host contact-style
4 Cu-Ni-PGE mineralisation which has been the focus of continual exploration since the 1980s.
5
6

7 8 Blue Draw Metagabbro

9
10 The 2480 ± 6 Ma Blue Draw Metagabbro is an 800 m thick (~ 6 km² outcrop area) layered
11 amphibolite sill (Dahl et al., 2006) which crops out in the Black Hills uplift, South Dakota,
12 west of Nemo township (Fig. 1). The Black Hills of the Wyoming craton were uplifted during
13 the ~ 75 -35 Ma Laramide Orogeny and expose a complex sequence of basal
14 metaconglomerates and quartzites which are overlain by quartzites, graywackes, iron
15
16 metaconglomerates and quartzites which are overlain by quartzites, graywackes, iron
17
18 formations, metavolcanics, gabbros, schists, phyllites and slates which have been deformed
19
20 during at least three to five separate events (Redden et al., 1990; Hill, 2006). The Blue Draw
21 Metagabbro intrudes the Boxelder Creek Quartzite
22

23
24 Initial work on the Blue Draw Metagabbro by Woo (1952) and Marante (1979)
25 described the intrusion as a 1 km thick layered sill with serpentinite at the base which grades
26 into hornblende, plagioclase gabbrodiorite, biotite granodiorite and discontinuous dioritic
27 pegmatite. A series of dominantly NW-SE trending faults have removed the side-wall
28 contacts of the intrusion and have otherwise dismembered the Blue Draw Metagabbro such
29 that slivers of metamorphosed gabbro thought to be correlative with it crop out at several
30 locations throughout the area (Dahl et al., 2006).
31
32

33
34 Recent work by Ciborowski et al. (2013) resampled the Blue Draw Metagabbro and
35 produced a new stratigraphy for the intrusion, that divided it into a 130 m thick peridotite unit
36 which is successively overlain by a ~ 100 m thick olivine melagabbro unit and a ~ 250 m
37 thick gabbro unit. The gabbro is overlain by an ~ 60 m, locally pegmatitic, quartz
38 gabbro unit. Unlike its proposed counterparts in the East Bull Lake Suite, no
39 appreciable Ni-Cu-PGE mineralisation has been observed in the Blue Draw Metagabbro.
40
41
42
43
44

45 46 Fennoscandian Suite

47
48 The Fennoscandian suite of layered intrusions is composed of ~ 20 individual intrusions which
49 crop out in northern Finland and northwest Russia (Fig. 1). These c. 2500-2430 Ma layered
50 intrusions are preserved in two discontinuous belts which transect the Karelia craton (Iljina &
51 Hanski, 2005). The east-west trending Tornio-Näränkävåara Belt crosses Sweden, Finland
52 and Russia between the tip of the Gulf of Bothnia to the White Sea. The second belt trends
53 northwest-southeast across Finland between Kasivarsi and Lake Onega. The rocks are
54 intruded mostly along the contact between Archean tonalitic gneisses and early
55
56
57
58
59
60

1
2
3 Paleoproterozoic volcanic-sedimentary greenstone belts (Alapieti et al., 1990; Weihed et al.,
4 2005). Further north a belt of similar trend occurs along the Kola Peninsula (Kola craton).

5
6 These intrusions can be divided into two groups, both spatially and in terms of age,
7 and correlations with different LIPs on the Superior craton (e.g., Kulikov et al., 2010; Ernst &
8 Bleeker, 2010): The older mainly c. 2.50 Ga group of intrusions (including Mt Generalskaya,
9 Monchepluton, Main Ridge and Fedorov-Pansky complex) is restricted to the northernmost
10 belt in the Kola Peninsula, and can be linked to the Mistassini LIP of the eastern Superior
11 craton, Canada. The younger, 'Matachewan-age' c. 2.45 Ga suite of layered intrusions is
12 mainly restricted to the two belts crossing Karelia and can be correlated with the Matachewan
13 magmatism of the Superior craton.
14
15
16
17
18
19

20 21 Summary

22 Although the most widely accepted mechanism for the formation of the Matachewan Large
23 Igneous Province is the impingement of a mantle plume beneath an Archean supercontinent,
24 this is not universally accepted. Volcanic arcs, failed rifts and normal continental and ocean
25 spreading have all been suggested to have formed different component igneous packages of
26 the proposed Matachewan LIP [e.g., Jolly (1987); Van Boening & Nabelek (2008)].
27
28
29
30

31 Thus far, geochronology has been key to the development of the Matachewan LIP
32 model, with the most precise ages resulting from U-Pb analyses of baddeleyite. The ages
33 recorded define a period of mafic magmatism which ranges in age between ~2498-2441 Ma
34 that has been interpreted as being pulsatory in nature (Ernst & Bleeker 2010).
35
36
37
38
39
40

41 GEOCHEMISTRY

42
43
44 This study represents the first attempt to collate representative geochemical data for all of the
45 constituent suites of the Matachewan LIP. These data comes from a mixture of sources
46 including both published and unpublished work, as well as new data collected during this
47 study. The data sources for the Matachewan LIP suites are summarised in Table 2. The
48 following sections describe the analytical methods used to collect the new data, how all of the
49 data were screened for alteration and how each of the suites was classified.
50
51
52
53
54

55 Analytical procedures

56
57
58
59
60

1
2
3 Sample preparation and analysis for the new geochemical data presented in this paper were
4 carried out at Cardiff University. Weathered surfaces and veins were removed with a rock saw
5 prior to analysis. The samples were then crushed into ~5 mm chips using a steel jaw crusher
6 and powdered in an agate planetary ball mill. Approximately 2 g of the milled powder was
7 ignited in a furnace at 900 °C for two hours in order to determine loss on ignition values.
8
9

10
11 Whole-rock major element, trace element and rare earth element (REE) data were
12 obtained following Li metaborate fusion (see Minifie et al., 2013). Major element and Sc
13 abundances were determined using a JY Horiba Ultima 2 Inductively Coupled Plasma Optical
14 Emission Spectrometer (ICP-OES). Trace elements were analysed using a Thermo X Series 2
15 Inductively Coupled Plasma Mass Spectrometer (ICP-MS). International reference material
16 JB-1A was run with each sample batch to constrain the accuracy and precision of the
17 analyses. Relative standard deviations show precision of 1–5% for most major and trace
18 elements for JB-1A. 2σ values encompass certified values for the vast majority of elements. A
19 summary of the whole-rock major element and trace element data for the each of the
20 Matachewan LIP suites is presented in Table 3. Full analytical results including repeat runs of
21 standard basalt JB-1A can be found in Supplementary Data Electronic Appendix 1.
22
23

24
25 To augment the published radiogenic isotope data for the Matachewan LIP
26 (Supplimentary Data Electronic Appendix 2), we analysed 18 samples for Sm-Nd and Lu-Hf
27 isotopes from the Blue Draw Metagabbro and East Bull Lake Suite layered intrusions. This
28 work was carried out at the NERC Isotope Geosciences Laboratory in Keyworth, UK. 150-
29 200 mg of sample was weighed into 15ml Savillex Teflon beakers. Mixed ^{149}Sm - ^{150}Nd and
30 ^{176}Lu - ^{177}Hf isotope tracers were added to the samples prior to dissolution using HF-HNO₃.
31 Primary columns consisting of 2 ml of Eichrom AG50x8 cation exchange resin in 10ml
32 Biorad Poly-Prep columns were used to separate bulk high field strength elements (HFSE: Ti,
33 Hf, Zr), an aliquot containing Sr, Ca and Rb, and a bulk rare-earth element (REE) fraction.
34 Sm, Nd and Lu were separated from the bulk REE fraction using columns consisting of 2 ml
35 of LN-SPEC ion exchange resin, again in Biorad Poly-Prep columns. Hafnium separation
36 followed a procedure adapted from Münker et al. (2001) using EICHROM LN-SPEC ion
37 exchange resin in Biorad Poly-Prep columns.
38
39

40
41 Lu fractions were dissolved in 1 ml of 2% HNO₃ prior to analysis on a Thermo-
42 Electron Neptune mass spectrometer, using a Cetac Aridus II desolvating nebuliser. Hf
43 fractions were dissolved in 1 ml of 2% HNO₃ + 0.1M HF, prior to analysis with a Thermo-
44 Electron Neptune mass spectrometer, using A Cetac Aridus II desolvating
45 nebuliser. Replicate analysis of the BCR-2 rock standard across the time of analysis gave a
46
47
48
49
50
51
52
53
54
55
56
57
58
59
60

1
2
3 mean Lu concentration of $0.49 \text{ ppm} \pm 0.0001 \text{ ppm}$ (1-sigma, n=21) while replicate analysis of
4 the JMC475 rock standard across the time of analysis gave a mean Hf concentration of 14.63
5 $\text{ppm} \pm 0.32 \text{ ppm}$ (1-sigma, n=21) and $^{176}\text{Hf}/^{177}\text{Hf}$ of 0.282150 ± 0.000005 .
6
7

8 Sm and Nd fractions were loaded onto one side of an outgassed double Re filament
9 assembly using dilute HCl, and analysed in a Thermo Scientific Triton mass spectrometer.
10 Replicate analysis of the BCR-2 rock standard across the time of analysis gave a mean Sm
11 concentration of $6.34 \pm 0.06 \text{ ppm}$ (1-sigma, n=7), while replicate analyses of the La Jolla
12 standard across the time of analysis standard gave a $^{143}\text{Nd}/^{144}\text{Nd}$ of 0.511845 ± 0.000007
13 (10.4 ppm, 1-sigma).
14
15
16
17

18 19 20 Element mobility

21 As many of the Matachewan LIP suites have experienced at least greenschist facies
22 metamorphism (Nelson, 1990; Sandeman & Ryan, 2008), and samples typically show
23 considerable alteration, the effects of secondary element remobilisation must be considered.
24 At metamorphic conditions above lower amphibolite facies the normally immobile high field
25 strength elements (HFSE) including the REE may become more mobile (Pearce, 1996).
26 Therefore, any scatter observed in plots involving these elements for the different
27 Matachewan LIP suite samples may reflect post-solidus changes brought about by their
28 metamorphic history.
29
30
31
32
33
34

35 To assess if this metamorphism caused secondary element remobilisation of
36 Matachewan LIP lavas, each element was plotted versus Zr. Immobile elements that are
37 incompatible in the main rock-forming minerals should fall on correlated, linear arrays when
38 plotted against Zr for a suite of unaltered rocks formed from a common fractionating magma,
39 whereas secondary remobilisation of elements is likely to result in a scattered trend (Cann,
40 1970). We quantify the strength of the correlations using Pearson's product moment
41 correlation coefficient (R). Elements which have $R^2 \geq 0.75$ are referred to as having a good
42 correlation with Zr; elements with an $0.75 > R^2 \geq 0.5$ are referred to as having a moderate
43 correlation with Zr, and; Elements with an $R^2 < 0.5$ are referred to as having a poor
44 correlation with Zr. Elements whose scatter cannot be explained by a petrogenetic
45 mechanism, or by carrying out statistics on small populations, are inferred to have been
46 remobilised by sub-solidus fluids and are not used to assess petrogenetic processes. A
47 representative subset of these graphs is shown in (Fig. 3) and a summary of the R value
48 classes for each element in each suite is given in Supplementary Data Electronic Appendix
49 3. It should be noted that some of the Matachewan LIP suites (e.g., the Matachewan dykes,
50
51
52
53
54
55
56
57
58
59
60

1
2
3 and Thessalon Formation) are composite formations made up of two or more geochemically
4 distinct groups which can be defined on the basis of different incompatible trace element
5 ratios (Fig. 4). These are indicated in Table 3 and R^2 values have been calculated for each
6 distinct group.
7
8

9 10 11 Classification

12 The TAS diagram (LeBas et al. 1986) uses K_2O and Na_2O contents to classify igneous rocks.
13 Consequently, the applicability of the TAS diagram for classifying the Matachewan suites
14 (which in certain cases have been metamorphosed to amphibolite facies) is questionable, as
15 these elements have been remobilised in some of the suites. Instead, the Zr/Ti vs. Nb/Y
16 diagram (Pearce, 1996) is potentially more useful as it is based on immobile trace elements.
17 On this diagram the majority of the Matachewan LIP suites plot as overlapping clusters within
18 the subalkaline basalt and basaltic andesite fields. Only the Seidorechka Formation samples
19 plot on a trend of increasing Nb/Y with increasing Zr/Ti between the subalkaline basaltic field
20 and the rhyolite field (Fig. 5).
21
22
23
24
25
26
27

28 29 30 Geochemical Variation

31 The most magnesian rocks of the Matachewan LIP belong to the Seidorechka Formation and
32 Viianki dykes, which contain up to 21 wt % MgO . The remaining Matachewan LIP suites
33 contain significantly less MgO (<10 wt %). When plotted on major element bivariate
34 diagrams (Fig. 6), all of the Matachewan suites fall on trends interpreted by Peterson &
35 Moore (1987) to be the result of the initial fractional crystallisation of olivine and subsequent
36 precipitation and removal of plagioclase and clinopyroxene.
37
38
39
40

41 All of the Matachewan LIP suites show positive correlations between MgO and
42 elements that are compatible during normal basaltic differentiation such as Cr , Ni , Co and Sc
43 (Fig. 6). Conversely, the incompatible elements (e.g., La , Sm , Yb and Nb) display negative
44 correlations with MgO in all suites. Subtle, yet consistent variations in these trends within
45 individual suites suggest that several of the suites are actually composite formations. These
46 include the Thessalon Formation and Matachewan dykes. Chondrite-normalised REE patterns
47 for the individual Matachewan LIP suites are remarkably similar in that all of the suites show
48 enrichments in the LREE relative to the HREE, that most resemble modern OIB (Fig. 7). In
49 contrast to the majority of Matachewan LIP suites, which have slightly negative Eu anomalies
50 (likely related to fractionation and removal of plagioclase from the primary magma), the
51 Striech dykes have slightly positive anomalies. These anomalies have been interpreted by
52
53
54
55
56
57
58
59
60

1
2
3 Vogel et al. (1998b) to be a consequence of megacrystic plagioclase in some of the samples.
4 The parallel nature of the REE patterns of the suites may suggest derivation from a
5 compositionally similar mantle source, albeit via varying degrees of partial melting or
6 fractional crystallisation.
7
8

9
10 The trace element geochemistry of the Matachewan LIP suites are generally more
11 enriched in the most incompatible elements relative to the least incompatible elements on
12 Primitive Mantle-normalised multi-element diagrams (Fig. 8). All of the suites studied have
13 sizeable negative Nb-Ta and Ti anomalies (where $Nb/Nb^* = Nb_N / [(Th_N + La_N) / 2]$, $Ti/Ti^* =$
14 $Ti_N / [(Gd_N + Sm_N) / 2]$, where $_N$ denotes primitive mantle normalised value), the largest of
15 which are observed in the Thessalon Formation. Variable anomalies in Zr and Y ($Y/Y^* = Y_N /$
16 $[(Dy_N + Ho_N) / 2]$) are also observed in some of the Matachewan LIP suites, however, these
17 anomalies are not ubiquitous. For example, variably negative Zr anomalies are observed in six
18 of the eleven suites studied, while in the remaining five suites (including all of the layered
19 intrusion parental magma compositions), no appreciable Zr anomalies are observed. More
20 variable still are the Y anomalies which are found in ten of the Matachewan suites and may be
21 either slightly negative or positive (Y/Y^* range = 0.8-1.1). Their broadly similar trace
22 element geochemistry means that the Matachewan LIP suites consistently plot as overlapping
23 clusters on tectonic discrimination diagrams within fields defined by volcanic-arc basalts, and
24 occasionally (depending on the trace element ratios used) within fields defined by oceanic
25 plateau basalts and mid ocean ridge basalts (Fig. 9).
26
27
28
29
30
31
32
33
34
35
36

37 Isotopic data

38 Seventeen samples were analysed for Nd-Hf isotopes (Table 4). Six samples were selected
39 from the Blue Draw Metagabbro while four were selected from the East Bull Lake and
40 Agnew intrusions and a further three from the River Valley intrusion. Complimentary whole-
41 rock geochemical data for these samples are available in Table 5.
42
43
44
45
46

47 The $\epsilon Nd_{(i)}$ (where $i = 2460$ Ma) values of the Blue Draw Metagabbro samples range between -
48 15.4 and -2.3 while the East Bull Lake and River Valley samples range from -3.54 to -0.14
49 and from -1.00 to -0.57 respectively. Three Agnew samples have a narrow range of $\epsilon Nd_{(i)}$
50 values between -0.61 and -1.81 whereas another Agnew sample has an $\epsilon Nd_{(i)}$ value of -9.78.
51
52
53
54
55
56
57
58
59
60

1
2
3 The majority of the other Matachewan LIP suites for which isotopic data is available are also
4 characterised by similarly negative ϵNd_i values (Fig. 10a) which have been widely interpreted
5 to be the result of the primary magmas of the province having been derived from an enriched
6 mantle source (e.g., Sandeman and Ryan 2008) . Only the Matachewan dyke swarm shows
7 significantly positive ϵNd_i values (up to +3.07) thought to represent the variable
8 contamination of primary magmas derived from partial melting of depleted mantle with
9 Archean crustal material during fractionation in subsurface chambers (Boily and Ludden
10 1990).

11
12
13 The Blue Draw Metagabbro samples exhibit the largest range in $\epsilon\text{Hf}_{(i)}$ range between -2.3 and
14 +52.6. The East Bull Lake suite intrusions define much smaller ranges such that the East Bull
15 Lake intrusion samples display $\epsilon\text{Hf}_{(i)}$ ranges between -7.6 and +6.3 while the Agnew and
16 River Valley intrusions show even smaller ranges of +3.0 to +5.9 and +2.6 to +5.2
17 respectively (Fig. 10b).

28 DISCUSSION

29 Determination of primary magma composition

30
31 The relatively evolved nature of the majority of the Matachewan LIP suites (MgO commonly
32 ≤ 9 wt %) suggests that even the most primitive rocks in these suites do not represent primary
33 mantle-derived magmas and have likely evolved through fractionation of olivine \pm pyroxene
34 \pm plagioclase (as discussed below). To characterise the primary magmas of more evolved
35 suites, Herzberg & Asimow (2008) developed the PRIMELT2 software which can model
36 accumulated perfect fractional melting of mantle peridotite in an attempt to produce viable
37 parent magmas for evolved suites of rocks by computing melt fractions which are capable of;
38 (a) being formed by partial melting of mantle peridotite and (b) replicating the major element
39 composition of the evolved lava through fractionation or accumulation of olivine.
40
41
42
43
44
45
46

47 PRIMELT2 is limited in that it is only applicable to peridotite-derived magmas that
48 have been modified by the fractionation or accumulation of olivine. Magmas from pyroxenitic
49 mantle, or those that have undergone fractionation of phases other than olivine, cannot be
50 modelled using PRIMELT2 (Dasgupta et al., 2007; Herzberg & Asimow, 2008).

51
52 All of the samples containing > 7.5 wt % MgO ($n = 42$) from the dyke swarms and
53 flood basalt provinces which make up the Matachewan LIP were assessed using PRIMELT2,
54
55
56

as were parental magmas for the layered intrusions. The results are discussed below. For all

1
2
3 samples studied, $\text{Fe}^{2+}/\Sigma\text{Fe}$ and $\text{Fe}_2\text{O}_3/\text{TiO}_2$ ratios in the mantle peridotite were kept at 0.9 and
4 0.5 respectively. Table 6 shows the major element compositions, degrees of partial melting
5 (F) and potential temperatures (T_p) of all of the primary magmas calculated by PRIMELT2
6 for each of the Matachewan LIP suites.
7
8
9

10 PRIMELT2 results

11 The compositions of magmas parental to the Matachewan LIP layered intrusions have been
12 derived from the compositions of fine-grained, cogenetic dyke feeders (Vogel et al., 1998b;
13 1999; James et al., 2002), or from calculations of the average composition of the whole
14 intrusion (James et al., 2002; Ciborowski et al., 2013).
15
16
17
18

19 PRIMELT2 was able to calculate primary magma compositions for the East Bull Lake
20 Suite parent magmas [sample 234 of Vogel et al. (1998a)]. The calculated primary melt
21 contains 18.7 wt % MgO, which is in equilibrium with olivine of composition $\text{Fo}_{92.4}$. The
22 degree of partial melting required to produce this primary magma from a peridotite of a
23 composition similar to KR-4003 is 30.3%.
24
25
26
27

28 However, PRIMELT2 was unsuccessful in obtaining primary magmas for any of the
29 Thessalon Formation volcanic rocks reported in the literature (Jolly, 1987a; Jolly, 1987b;
30 Jolly et al., 1992; Tomlinson, 1996; Ketchum et al., 2013) or the Seidorechka Formation
31 rocks studied by Chashchin et al. (2008). However, PRIMELT2 successfully calculated a
32 primary magma composition for the Seidorechka Formation lavas (sample 91113; Puchtel et
33 al., 1996). This calculated primary magma contains 17.0 wt % MgO, is in equilibrium with
34 olivine of composition $\text{Fo}_{91.5}$ and requires 31.1% melting of a mantle peridotite similar in
35 composition to KR-4003.
36
37
38
39
40

41 PRIMELT2 was even less successful in calculating primary magmas for the Kaminak
42 or Matachewan dykes analysed in this study or from the literature (Nelson et al., 1990;
43 Phinney & Hall, 2001; Halls et al., 2005; Ernst & Buchan, 2010) and yielded no feasible
44 primary magma. Though disappointing, the low success rate of PRIMELT2 is not surprising
45 given that the majority of the Matachewan LIP lavas contain < 9 wt % MgO and plot on
46 geochemical variation trends indicative of clinopyroxene and plagioclase fractionation (e.g.,
47 Sandeman & Ryan, 2008; Phinney & Halls, 2001). The relatively evolved nature of the
48 Matachewan LIP lavas is likely a product of their intracontinental emplacement setting where,
49 due to limited buoyancy differentials, the primary magmas likely stalled in the lower
50 continental crust (Glazner, 1994; Rudnick & Fountain, 1995) where they fractionated to form
51
52
53
54
55
56

1
2
3 more evolved magmas capable of migrating to higher crustal levels during emplacement of
4 the Matachewan LIP suites studied.
5
6

7 8 Involvement of a Thermal Plume?

9
10 Several lines of evidence have been used to argue for a mantle plume source for the
11 constituent suites of the Matachewan LIP. These include: 1) the radiating patterns of the dyke
12 swarms, resulting from the stresses induced by a plume beneath the lithosphere (Fahrig, 1987;
13 Halls, 1991; Ernst & Buchan, 2001; Phinney & Halls, 2001; Buchan & Ernst, 2004; Ernst &
14 Bleeker, 2010); 2) the coeval nature and sheer volume of magmatism spread across the
15 'Superia' cratons (Heaman, 1997; Vogel et al., 1998a; Dahl et al., 2006); 3) the high MgO
16 content of some of the suites (Puchtel, 1997); and 4) significant amounts of crustal uplift prior
17 to magmatism (Amelin et al., 1995).
18
19
20
21
22

23 Present day and geologically recent mantle plumes are characterised by upper mantle
24 several hundreds of degrees hotter than ambient mantle (e.g., Wolfe et al., 1997; Bijwaard &
25 Spakman, 1999; Li et al., 2000; Cao et al., 2011). The existence of anomalously high
26 temperature magmatism, indicative of a mantle plume can be investigated by examining the
27 geochemistry of the primary magmas and calculating mantle potential temperature (T_p) - the
28 temperature the mantle would reach if it was brought to the surface adiabatically without
29 melting (McKenzie & Bickle, 1988).
30
31
32
33
34

35 Mantle potential temperatures have been calculated using PRIMELT2 for two of the
36 Matachewan LIP suites; the East Bull Lake Suite and the Seidorechka Formation. The
37 primary magma of the East Bull Lake suite has a calculated T_p of 1545°C, while the primary
38 magma of the Seidorechka Formation (as calculated from the analysis of Puchtel et al.
39 (1996)) records a T_p of 1496°C. The total uncertainty in T_p calculated by PRIMELT2 is \pm
40 60°C (2σ) (Herzberg & Asimow, 2008; Herzberg et al., 2010). By comparing these potential
41 temperatures with temperature estimates of the ambient upper mantle at ~2.48-2.45 Ga, we
42 can determine whether the Matachewan LIP magmatism was derived from an anomalously
43 hot upper mantle (i.e., plume) as predicted by mantle plume theory (Campbell, 2007), and
44 confirmed by observations of active mantle plumes (Bijwaard & Spakman, 1999; Li et al.,
45 2000; Montelli et al., 2004; Waite et al., 2006).
46
47
48
49
50
51
52

53
54 Secular cooling models of the mantle suggest that the Paleoproterozoic mantle was
55 significantly hotter than it is today, though by exactly how much is a point of contention.
56
57
58
59
60

Richter (1988) proposed two cooling models where the starting temperature of the upper

1
2
3 mantle at 4.5 Ga was either 2500°C or 2000°C and cooling proceeded at a continuously
4 decreasing rate to reach a present day value of 1350°C. Regardless of the two starting
5 temperatures used by Richter (1988), his models predict that at ~2.48-2.45 Ga the upper
6 mantle was at ~1500°C. Abbot et al. (1994) proposed a cooling history of the upper mantle
7 using fifteen, 3750 Ma samples thought to record N-MORB compositions and calculated the
8 most primitive liquidus temperature for each studied suite. Their model suggests that the
9 upper mantle cooled from ~1700°C at 4 Ga to ~1450°C today. In more recent study,
10 Korenaga (2008) presented a model in which the upper mantle is characterised by an initial
11 increase in temperature from ~1650°C at 4.5 Ga to ~1700°C at 3.6 Ga. This initial increase is
12 followed by an increasingly rapid drop, cooling to a present day value of 1350°C. Subsequent
13 work by Davies (2009) favoured a model of constantly decreasing temperature from an initial
14 upper mantle temperature of 1800°C at 4.5 Ga to reach a modern day temperature of 1300°C.
15 In contrast, Herzberg et al. (2010) proposed a model similar to that of Korenaga (2008)
16 whereby an initial warming of the mantle (facilitated by 'sluggish' convection) during the
17 Hadean and Archean led to a mantle temperature maximum at 2.5 – 3.0 Ga that was followed
18 by a continual cooling to reach a modern day temperature of ~1350°C.
19
20
21
22
23
24
25
26
27
28
29
30

31 The secular cooling models described above are shown in Fig. 11. The T_p of the two samples
32 which yield primary magma estimates with PRIMELT2 are also plotted. Seidorechka
33 Formation sample 91113 of Puchtel et al. (1996) records a T_p of 1496°C, which is very close
34 to the temperature of the upper mantle at 2.46 Ga predicted by Richter (1988), but ~120°C
35 hotter than the prediction of Davies (2009). The highest T_p sample is the East Bull Lake Suite
36 feeder dyke [sample 234 of Vogel et al. (1998a)] which has a calculated T_p of 1545°C. This
37 T_p is 161-57°C higher than the temperature of the upper mantle as modelled by Davies (2009)
38 and Richter (1988) respectively, but lower than that modelled by Korenaga (2008), Herzberg
39 et al. (2010) and Abbot et al. (1994).
40
41
42
43
44
45

46 The two most recent cooling models from Davies (2009) and Herzberg et al. (2010) –
47 the latter being very similar to that published by Korenaga (2008) – differ hugely (~350°C) in
48 their estimates of T_p during the early Proterozoic. The disparity in these two models stems
49 from the different model parameters used. Davies (2009) argued that some of the assumptions
50 made by Korenaga (2008) regarding plate thickness, Urey ratio (mantle heat production
51 divided by heat loss) and plate curvature at subduction zones appear to be incorrect (Davies,
52 2009; Karato, 2010). In contrast, Herzberg et al. (2010) contend that the high Urey ratio
53
54
55
56
57
58
59
60

1
2
3 employed in the model of Davies (2009) is in conflict with cosmochemical constraints on the
4 amount of radiogenic elements in the mantle.
5

6 Determining which of the cooling models presented in Figure 11 is more correct is
7 beyond the scope of this work. Indeed, we argue that until more work is carried out to
8 constrain factors such as Urey ratio, effective lithosphere viscosity, secular changes in plate
9 thickness and the radius of curvature for plate bending (upon which such cooling models
10 depend), questions regarding the manner of Earth's secular cooling remain open (Lenardic et
11 al., 2011; Herzberg et al., 2010; Karato, 2010; Davies, 2009).
12
13
14
15
16

17 Fractional Crystallisation

18 Although, fractional crystallisation can be modelled using the most primitive sample from
19 each suite (i.e., highest MgO and lowest incompatible element concentration), the most
20 primitive sample is unlikely to be a primary magma given the evolved nature of many of the
21 Matachewan LIP suites (Fig. 6). However, the most primitive sample is assumed to be the
22 closest estimate of the primary magma for the suite.
23
24
25
26
27

28 The major element geochemical trends for each of the dyke swarms and flood basalt
29 provinces has been modelled using the PELE computer program (Boudreau, 1999) under five
30 different scenarios (Table 7): Model 1: fractional crystallisation at 1 kbar (anhydrous); Model
31 2: fractional crystallisation at 1 kbar (1% H₂O); Model 3: fractional crystallisation at 3 kbar
32 (anhydrous); Model 4: fractional crystallisation at 7 kbar (anhydrous) and Model 5: fractional
33 crystallisation at 10 kbar (anhydrous). All models use a quartz-fayalite- magnetite (QFM)
34 oxygen buffer and calculate the composition of the liquid at 10% crystallisation intervals.
35 The model which best predicts the major element geochemical trends observed in each of the
36 dyke swarms and flood basalt suites is further tested by fractional crystallisation modelling of
37 incompatible trace elements using the mineral assemblages predicted by PELE during
38 crystallisation and the empirically derived mineral/melt partition coefficients given in
39 Supplementary Data Electronic Appendix 4.
40
41
42
43
44
45
46
47

48 Where fractional crystallisation fails to accurately model the incompatible element
49 geochemical trends observed in the different Matachewan LIP suites, AFC modelling has
50 been attempted. This modelling uses the mineral assemblages predicted by PELE to form
51 during crystallisation and the empirically derived mineral/melt partition coefficients in
52 Supplementary Data Electronic Appendix 4, the composition of felsic crust (Rudnick &
53 Fountain 1995), and the ratio of assimilation/crystallisation which is taken to be 0.3. Table 8
54 summarises the results of this petrogenetic modelling.
55
56
57
58
59
60

1
2
3 The majority of the models consistently show that the geochemical trends observed in
4 the Matachewan LIP suites are indicative of AFC processes involving a felsic crustal
5 contaminant (Fig. 12). FC models do not predict the presence of, or changes in, the magnitude
6 of the Nb-Ta and Ti anomalies observed in the majority of the Matachewan LIP suites
7 (Ciborowski et al., 2014). Increasing normalised LREE/HREE ratios are predicted by both the
8 FC and AFC models, though the rate of increase is greater for AFC models and also fits the
9 Matachewan LIP data more convincingly.
10
11
12
13

14 In contrast, the trace element geochemistry of the numerous Matachewan Group 1
15 dykes is best modelled by simple fractional crystallisation with little contamination of the
16 fractionating magmas. However, the significantly negative but variable Ti and Nb anomalies
17 in the Group 1 Matachewan dykes are not predicted by the FC model and may be the product
18 of in situ crustal contamination of individual dykes possibly after, or in the later stages of,
19 emplacement.
20
21
22
23
24
25

26 Mantle Source Composition

27 Despite the significant amount of field and other evidence that argues for a mantle plume
28 origin for the Matachewan LIP, the geochemical signatures recorded by the constituent suites
29 are more commonly associated with magmas formed in subduction zone settings (Pearce &
30 Peate, 1995). Indeed, these signatures, characterised by significant enrichments in the LREE
31 and LILE, significant negative Nb-Ta and Ti anomalies, and variable Eu anomalies, have
32 been used to argue against a mantle plume mechanism for the petrogenesis of some of the
33 Matachewan LIP suites (e.g., Van Boening & Nabelek, 2008; Jolly, 1987).
34
35
36
37
38
39

40 In other Paleoproterozoic suites that record field evidence that precludes their having
41 formed in a volcanic arc environment, alternative proposed mechanisms (other than a
42 fundamentally different asthenospheric mantle source) for their arc-like geochemistry include
43 either partial melting of subduction-modified sub-continental lithospheric mantle (SCLM)
44 (Sandeman & Ryan, 2008; Neumann et al., 2011), or, the contamination of mantle melts by
45 continental crust during fractionation in deep crustal magma chambers (e.g., Nelson et al.,
46 1990; Neumann et al., 2011; Jowitt & Ernst, 2013). Below, we attempt to determine whether
47 the action of one of these two mechanisms (mixing of partial melts of the lithospheric mantle
48 vs. crustal contamination) on primary magmas derived from a known mantle reservoir can
49 explain the trace element compositions of the Matachewan LIP suites. This question can be
50 investigated by again looking at the PRIMELT2 data and the degrees of partial melting and
51 fractional crystallisation required to produce the primary magmas of the suites. By applying
52
53
54
55
56
57
58
59
60

1
2
3 these parameters to mantle reservoirs of known composition, potential mantle sources for the
4 Matachewan LIP magmatism may be identified.

5
6 Three mantle reservoirs are modelled (Table 9): Depleted MORB Mantle (DMM),
7 Enriched Mantle (EM) and Primitive Mantle (PM). The composition of DMM has been
8 constrained by Workman & Hart (2005) from the trace element depletion trends of abyssal
9 peridotites. The composition of the EM1 reservoir is estimated from inverse modelling of the
10 compositions of EM1 ocean island basalts (Willbold & Stracke, 2006). The composition of
11 PM is derived from studies of chondritic meteorites and refractory element ratios of mantle
12 peridotites (McDonough & Sun, 1995). It should be noted that projecting the existence of
13 these reservoirs, predominantly recognised from modern intraplate basaltic rocks, back into
14 the Palaeoproterozoic is questionable. However, these reservoir compositions can be used to
15 characterise the enriched, depleted or chondritic nature of the Matachewan LIP mantle source
16 region(s).
17
18
19
20
21
22
23

24 The ~30% partial melting needed to form the Matachewan LIP primary magmas (as
25 predicted by PRIMELT2) can be modelled using batch melting of spinel lherzolite (Johnson
26 et al., 1990) from the different mantle reservoirs. Spinel lherzolite was chosen for the models
27 as all of the Matachewan LIP suites have relatively flat HREE patterns (Fig. 7) which
28 indicates that mantle melting probably occurred within the spinel stability field, or that, if
29 melting occurred deeper, it melted out all of the garnet in the source.
30
31
32
33
34
35

36 Crustal Contamination

37 PRIMELT2 predicts that, following partial melting, the Matachewan LIP magmas
38 fractionated variable amounts (7.3–32.3%) of olivine to form the most primitive compositions
39 observed in the suites today. Crustal contamination of these ~30% partial melts of spinel
40 lherzolite can be modelled using the AFC (assimilation fractional crystallisation) equation of
41 DePaolo (1981), the average continental crust composition of Rudnick & Gao (2003) and the
42 degrees of fractionation predicted by PRIMELT2.
43
44
45
46
47

48 Primitive Mantle-normalised multi-element patterns for Seidorechka sample 91113
49 and East Bull Lake Suite feeder 234, for which PRIMELT2 was able to define partial melting
50 and fractionation parameters, are shown in Supplementary Data Electronic Appendix 5.
51 Also plotted are the modelled compositions of magmas formed by AFC of primary magmas
52 derived from melting of spinel lherzolites from the DMM, EM1 and PM mantle reservoirs
53 using the parameters of melting and fractionation listed in Table 6. The models consistently
54 show that with larger amounts or higher rates of AFC, primary mantle melts from any of the
55
56
57
58
59
60

1
2
3 reservoirs studied can form magmas which replicate aspects of the trace element
4 geochemistry of the Matachewan suites (negative Nb-Ta and Ti anomalies and LILE-LREE
5 enrichment relative to the HREE). However, for sample 91113, all of the models predict
6 lower La/Sm ratios and much higher HREE contents than those observed in the sample,
7 whereas for the East Bull Lake Suite feeder dyke (sample 234), all of the models predict
8 much greater abundances of HREE than in the sample.
9
10
11
12

13 14 15 Interaction with SCLM

16 To determine whether mixing of primary mantle melts with low degree partial melts of
17 subduction-modified SCLM can replicate the trace element composition of the Matachewan
18 LIP suites (as suggested by Sandeman & Ryan, 2008), we have modelled mixing of the
19 primary mantle melts derived from the different mantle reservoirs (Table 9) with varying
20 amounts (0.1-5%) of low degree partial melts of subduction-modified SCLM using simple
21 binary mixing. Fractionation of olivine from the resulting mixtures was then modelled to the
22 degree predicted by PRIMELT2.
23
24
25
26
27

28 The estimate for partial melts of the subduction-modified SCLM was taken from an
29 average of 113 analyses of ~1.88 Ga ultrapotassic igneous rocks (minette-lamproite) of the
30 Christopher Island Formation, preserved on the Hearne craton (Sandeman et al., 2003).
31 Despite being significantly younger than the Matachewan LIP magmatism, Sandeman &
32 Ryan (2008) and Cousens et al. (2001) argue that the rocks of the Christopher Island
33 Formation represent low degree partial melts of a subcontinental lithospheric mantle source
34 which developed beneath the Hearne and Superior cratons during the Archean and which was,
35 thus, an available source for the Paleoproterozoic Matachewan LIP magmatism. These
36 models show that the mixing of partial melts from the modelled mantle reservoirs with small
37 amounts (~5%) of low degree partial melt from subduction modified SCLM is a viable
38 mechanism for producing the general trace element signatures observed in the Matachewan
39 LIP rocks (LREE enrichment relative to HREE, significant negative Nb-Ta and Ti
40 anomalies). Indeed, the trace element chemistry of Seidorechka Formation sample 91113
41 (Puchtel et al., 1996), can be closely approximated by a mixture of ~8% SCLM partial melt
42 and 92% DMM partial melt (Fig. 13). In contrast though, the SCLM mixing models produce
43 HREE concentrations that are at least 2-3× higher than those observed in the East Bull Lake
44 Suite feeders (Supplementary Data Electronic Appendix 6).
45
46
47
48
49
50
51
52
53
54
55
56

57 58 Two-stage Melting 59 60

1
2
3 The two types of model described above attempt to determine whether the trace element
4 signatures observed in the Matachewan LIP suites are better explained by contamination of
5 primary magmas by crustal material during fractionation of the magma in lower crustal
6 bodies, or through mixing of primary magmas with low-degree partial melts of subduction
7 modified SCLM. The models show that the two mechanisms can broadly reproduce the
8 geochemical signatures of the Matachewan LIP samples. This modelling shows that the
9 composition of Seidorechka Formation basalt 91113 can be replicated by a mixture of ~8%
10 SCLM partial melt and 92% DMM partial ($F = 0.3$) melt. However, for the East Bull Lake
11 Suite feeders, both sets of models over-estimate the abundance of the HREE in the samples
12 studied by a factor of ≥ 3 . Instead, the modelling suggests that in order to produce primary
13 magmas with the HREE contents observed in the East Bull Lake Suite feeder samples (~5.5×
14 chondritic values), partial melting of the DMM spinel lherzolite would need to exceed ~45%
15 which is well in excess of the extent of melting predicted by PRIMELT2.
16
17

18 Thus, if we assume that the modelled mantle reservoirs are applicable to the ~2.48-
19 2.45 Ga Matachewan LIP suites, then the degrees of melting predicted by PRIMELT2 are too
20 low. Alternatively, if we assume that the degrees of partial melting predicted by PRIMELT2
21 are correct then the trace element compositions of the mantle reservoirs modelled are not
22 representative of the sources of the Matachewan LIP magmatism. The inference is that the
23 Matachewan LIP mantle source was more depleted than any of those modelled.
24

25 The existence of a strongly depleted mantle source for the Matachewan LIP
26 magmatism may be inferred by the presence of the ~2.7 Ga greenstone belts (including the
27 Abitibi and Ennadai-Rankin belts of the Superior and Hearne cratons) which host many of the
28 Matachewan LIP suites. These greenstone belts contain large amounts of komatiitic lavas
29 which have been interpreted by Sproule et al. (2002) to have formed through ~30% partial
30 melting of the mantle. This partial melting event would have depleted the mantle in
31 incompatible elements such that any further melting events would produce melts with much
32 lower incompatible element contents than the komatiitic lavas of the greenstone belts. If such
33 a residual mantle source persisted beneath the Superia supercontinent (Bleeker, 2003) from its
34 accretion at ~2.7 Ga to the period of melting which formed the Matachewan LIP magmas at
35 ~2.48 Ga, it may have been a source for the Matachewan LIP magmatism.
36
37

38 To test whether melting of such a depleted source is a potential mechanism for
39 producing the trace element compositions observed in the Matachewan LIP suites, models
40 similar to those shown in Supplementary Data Electronic Appendices 5 and 6 were
41
42
43
44
45
46
47
48
49
50
51
52
53
54
55
56
57

constructed, this time using the trace element composition of residues of DMM, EM1 and

Two-stage Melting

1
2
3 PM spinel lherzolite formed through 30% batch partial melting as suggested by Sproule et al.
4 (2002) and Maier et al. (2003). The compositions of these residues are shown in Table 9.

5
6 AFC models (Fig. 14) based on ~30% partial melts of these previously-melted mantle
7 sources in the same way as those in Supplementary Data Electronic Appendix 5 show that
8 such a mechanism is capable of producing the trace element geochemistry of the Matachewan
9 LIP suites for a previously-melted DMM source which was contaminated by continental crust
10 with an assimilation/fractionation ratio of ~0.4-0.5. Sample 234 is less likely to have been
11 derived from a previously melted EM1 or PM source as it has a $(La/Sm)_N$ ratio higher than
12 those predicted by the model for these reservoirs.
13
14
15
16
17

18 Models which mix partial melts of Archean SCLM with partial melts of previously-
19 melted sources (Fig. 15) in the same way as those shown in Supplementary Data Electronic
20 Appendix 6 also show that this mechanism is capable of producing the trace element
21 geochemistry of the Matachewan LIP suites using several, but not all of the starting
22 reservoirs. The trace element geochemistry recorded by the East Bull Lake Suite feeder dyke
23 is not compatible with derivation from a previously-melted DMM source, as mixing of partial
24 melts from this source with low degree partial melts of Archean SCLM does not yield
25 mixtures with the observed HREE contents or La/Yb ratios. Alternatively, East Bull Lake
26 Suite feeder dyke 234 may have been derived by mixing of melts of a previously-melted
27 Enriched- or Primitive- Mantle source with low degree partial melts of Archean SCLM in the
28 ratio of ~19:1.
29
30
31
32
33
34
35
36
37

38 Isotopic considerations

39 Due to the effects of secondary remobilisation (Fig. 3), Rb-Sr isotopic data cannot be used
40 with confidence when assessing the petrogenesis of the Matachewan LIP. Instead, the Nd-Sm
41 and Lu-Hf systems, which are less susceptible to alteration (Gaffney et al., 2011) are used in
42 the remainder of this study.
43
44
45

46 Previously published Nd isotopic data for the majority of the Matachewan LIP suites
47 record negative ϵNd_i values, indicating derivation from enriched mantle sources. New Nd
48 isotopic data for the East Bull Lake suite also records significantly negative ϵNd_i values,
49 similar in magnitude to the other Matachewan LIP suites, and may be evidence of the
50 intrusions having been derived from similarly enriched primary magmas, or contaminated by
51 continental crust. In terms of the latter, equivalent data for the Blue Draw Metagabbro have
52 the widest range of ϵNd_i in the Matachewan LIP suites ($-15.09 > \epsilon Nd_i < -2.46$), the most
53
54
55
56

1
2
3 formed the intrusion, and unrelated to in situ AFC processes (Ciborowski et al., 2013). This is
4 evidenced by the fact that the earliest formed, and most primitive cumulates have the most
5 extreme ϵNd_i values, while those rocks with trace element compositions consistent with in
6 situ contamination by host-rock material are also the samples with the most positive ϵNd_i
7 values.
8
9

10
11 Unfortunately the only Lu-Hf data available for the province is that analysed during
12 this study. Our data show that the majority of the East Bull Lake suite samples have positive
13 ϵHf_i values of $\sim+4.0$ which suggests that the intrusions were derived from a depleted mantle
14 source. Again, the Blue Draw Metagabbro samples have the most extreme isotopic values
15 ($\epsilon\text{Hf}_i < 53$). Such extreme values are rare in the published literature; however, they have been
16 reported in peridotite mantle xenoliths from the island of O'ahu, Hawai'i. These xenoliths
17 have been interpreted to be derived from ancient (>2 Ga) depleted mantle lithosphere caught
18 up in the upwelling Hawaiian plume (Bizimis et al., 2007).
19
20
21
22
23
24

25
26 Invoking a similar reservoir for the Blue Draw Metagabbro is, however, problematic since the
27 O'ahu xenoliths are also characterised by significantly positive ϵNd values (Fig. 16) in
28 contrast to the negative ϵNd in the Blue Draw Metagabbro samples. Instead, the Blue Draw
29 Metagabbro (and potentially the East Bull Lake suite) were likely derived from a mantle
30 reservoir not recognised in the modern mantle. This reservoir was characterised by high
31 $^{176}\text{Hf}/^{177}\text{Hf}$ and low $^{143}\text{Nd}/^{144}\text{Nd}$ ratios relative to the Bulk Earth at 2.46 Ga that cannot be
32 adequately modelled by mixing depleted mantle, similar in composition to the O'ahu
33 xenoliths, with more enriched crustal material.
34
35
36
37
38
39

40 While seemingly rare in the mantle, extremely positive ϵHf values (with concomitant
41 negative ϵNd values) have been observed in kimberlite-hosted Archean-Proterozoic mafic
42 granulites from the Kaapvaal craton (e.g., Schmitz et al., 2004). In these rocks, the apparent
43 decoupling of the Lu-Hf and Sm-Nd isotope systems is argued to be a result of partial melting
44 in the presence of titanomagnetite and ilmenite, but absence of rutile, which itself acts to
45 buffer against Hf depletion in the residue. Assimilation of such material by the primary
46 magmas of the intrusion, prior to its in situ fractionation within the Boxelder Creek Quartzite,
47 may explain the extreme ϵHf values recorded by the Blue Draw Metagabbro. This
48 mechanism, may also help explain the arc-like trace element compositions of the Blue Draw
49 Metagabbro and other related Matachewan LIP suites. To date, however, no such potential
50 contaminants have been documented within the Black Hills uplift which hosts the Blue Draw
51 extremely negative of which have been shown be a feature of the primary magma which
52
53
54
55
56
57
58
59
60

1
2
3
4
5 Schmitz et al. (2004) also document rutile-bearing felsic granulites that are
6 characterised by $-\epsilon\text{Hf}$ and $+\epsilon\text{Nd}$ values which lie well away from the ‘normal’ lithosphere
7 array (Vervoort et al., 2000). Schmitz et al. (2004) argues that the decoupling of the two
8 isotope systems in these rocks is due to refractory rutile retaining Hf (but not Lu) during low-
9 P, high-T anatexis, creating a residue characterised by subchondritic Lu/Hf and $-\epsilon\text{Hf}$ values
10 and an isotopically complementary liquid fraction. Mixing of such a liquid with the Blue
11 Draw Metagabbro primary magmas may be a more feasible mechanism than partial melting
12 of mafic granulites for producing the isotopic variation observed in the most primitive
13 samples of the intrusion.
14
15
16
17
18
19

20 Another possible explanation for the isotopic compositions observed in the Blue Draw
21 Metagabbro comes from Nebel et al. (2013, 2014) who report significantly positive ϵHf_i
22 values in Archean komatiites from the Yilgarn craton which they interpreted to be inherited
23 during partial melting of an ancient, melt-depleted mantle reservoir. Nebel et al. (2013, 2014)
24 suggest that such a reservoir – which they term the Early Refractory Reservoir (ERR) – would
25 have formed as the residue left over during the formation of the earliest Hadean terrestrial
26 crust that would have been remelted by hot, upwelling mantle plumes to ultimately produce
27 mafic lavas characterised by superchondritic initial $^{176}\text{Hf}/^{177}\text{Hf}$ signatures.
28
29
30
31
32
33
34

35 Summary

36 Trace element modelling has shown that both AFC and magma mixing are potential
37 mechanisms for producing the trace element composition of the Matachewan LIP suites.
38 Although trace element modelling is unable to determine which of these processes ‘fit’ the
39 data better, it suggests that the mantle source for at least the East Bull Lake Suite had been
40 significantly melted prior to its involvement in the formation of the intrusions, potentially
41 during the formation of the 2.8-2.6 Ga greenstone belts which host much of the Matachewan
42 LIP. Alternatively, evidence of this prior melting event may be present in the form of the 2.5
43 Ga Mistassini LIP, most obviously characterised by the Mistassini radiating dyke swarm
44 preserved on the Superior Craton in Quebec (Ernst & Buchan, 2001). In contrast, the
45 Seidorechka Formation magmatism does not require derivation from such a previously melted
46 source region.
47
48
49
50
51
52
53

54 As debate regarding the precise timing of the initiation of plate tectonics and
55 subduction continues (e.g., Harrison et al., 2005; Stern, 2005), the use of reservoirs
56 recognised in the modern mantle which are thought to be related to subduction and recycling
57
58
59
60

1
2
3 [e.g., Willbold & Stracke (2006)] is questionable. Instead, previous workers have suggested
4 that rather than being the product of contamination or mantle mixing, that the trace element
5 chemistry of the Matachewan LIP, which is ubiquitous in Paleoproterozoic continental
6 magmatic rocks (e.g., Buchan et al., 2007) is due to a fundamental difference in the
7 geochemistry of the ancient mantle compared to the modern mantle.
8
9

10
11 This explanation was proposed by Vogel et al. (1998b) who, when studying the
12 Agnew intrusion of the East Bull Lake suite, noted that the arc-like trace element
13 geochemistry of the East Bull Lake suite feeder dykes is shared by all magmatic rocks coeval
14 with the intrusions on the Superior Craton. Further, global analysis of greenstone belt
15 volcanic rocks and mafic dyke swarms (Condie, 1994; Ernst & Bleeker, 2010) shows that this
16 signature is ubiquitous in such rocks older than ~2 Ga. Vogel et al. (1998b) suggest that the
17 ubiquity of this signature in mafic continental intrusions in the Archean-Paleoproterozoic is
18 due to a fundamental difference in the composition of the ancient mantle compared to the
19 modern. Vogel et al. (1998b) speculate that this arc-like signature may have been caused by
20 the slow, upward migration of LILE- and LREE-enriched fluids through the mantle during
21 early differentiation of the Earth. They argue that such a process would have metasomatised
22 the entire mantle so that any subsequent partial melts would have a subduction-like
23 geochemical signature. Vogel et al. (1998b) argue that continued continental growth,
24 subduction (and recycling) of slabs and partial melting could have obliterated this ephemeral
25 signature by the end of the Paleoproterozoic. The existence of such a mantle reservoir may be
26 recorded by the Nd-Sm and Lu-Hf isotope systematics of the Blue Draw Metagabbro, which
27 are unlike any of the components recognised in the modern mantle.
28
29

30
31 Potentially more feasible mechanisms for explaining the Nd-Sm and Lu-Hf isotope
32 systematics of the Blue Draw Metagabbro (and perhaps other Matachewan LIP suites), than
33 the cryptic global metasomatism advocated by Vogel et al. (1998b) involve the incorporation
34 of material from some sort of lithospheric component, either through assimilation of material
35 produced during Low-P, high-T anatexis of lithospheric material (Schmitz et al., 2004) or
36 through involvement of an 'Early Refractory Reservoir' (Nebel et al., 2014) residual from the
37 partial melting of the mantle during initial terrestrial crust formation in the Hadean.
38
39

40
41 In conclusion, the trace element geochemical signatures recorded by the Matachewan
42 LIP suites are common to the majority of Archean-Paleoproterozoic intracontinental
43 magmatic rocks. The debate regarding the mantle source of such widespread magmatic rocks,
44 which retain signatures more associated with modern subduction-related rocks, is ongoing
45
46
47
48
49
50
51
52
53
54
55
56
57

1
2
3 Sandeman & Ryan, 2008) and not something this study aims to resolve. However, the
4 geochemical modelling presented here suggests that crustal contamination of primary magmas
5 during prolonged residence in the continental crust, or, mixing of the primary magmas from
6 known mantle reservoirs with low degree partial melts of subduction-modified SCLM are
7 potential mechanisms for producing the trace element signatures of the Matachewan LIP
8 suites (assuming the mantle reservoir had already been significantly melted). The models do
9 not require the input of an alternate Archean-Paleoproterozoic mantle reservoir, one which
10 was defined by higher LILE and LREE concentrations relative to HFSE and HREE, but nor
11 do the models rule out the input (or existence) of such a reservoir.
12
13
14
15
16
17

18 Several LIPs preserved throughout the geological record, including the Siberian Traps,
19 Emeishan LIP and Deccan Traps, have been linked to periods of great environmental
20 upheaval (e.g., Keller et al., 2009; Zhou et al., 2002; Campbell et al., 1992). As such, a
21 review of the Matachewan LIP would not be complete without at least exploring such an
22 avenue. To this end, below we present a discussion of the Matachewan LIP and its potential
23 relationship with the Great Oxidation Event (GOE) which is widely cited to be the first
24 sustained appearance of free oxygen in Earth's atmosphere.
25
26
27
28
29
30
31
32

33 The Matachewan LIP – a cause of the Great Oxidation Event?

34 It has been proposed that the GOE was a fundamental factor in the evolution of complex
35 multicellular life on Earth (Sessions et al., 2009) and is widely interpreted to have occurred
36 relatively abruptly as evidenced by a number of secular changes in the geological record. One
37 such change relates to the widespread preservation of reduced detrital mineral species in
38 surficial deposits in rocks deposited prior to the Archean-Proterozoic transition, but
39 subsequent absence in sediments younger than the transition (Frimmel, 2005; Sverjensky &
40 Lee, 2010). A second, equally well-documented line of evidence for the GOE may be deduced
41 from studies of sulphur isotopes preserved within sedimentary rocks (e.g., Bekker et al.,
42 2004). Such studies consistently define a transition from mass-independent fractionation of
43 isotopes during the Archean to mass-dependent fractionation in rocks younger than this,
44 which has been argued to signify the stabilisation of ozone (and O₂) in the upper atmosphere
45 (Farquhar & Wing, 2003).
46
47
48
49
50
51
52
53

54 Based on these (and other) lines of evidence, the GOE has been dated to
55 approximately 2450 Ma, that is, hundreds of millions of years after the appearance of
56

1
2
3 photosynthesis and the oxygenation of the atmosphere, a number of mechanisms have been
4 suggested. These include: a partial cessation of ultramafic volcanism towards the end of the
5 Archean eon, leading to reduced nickel supply to the oceans and concomitant methanogenic
6 bacteria stress (Konhauser et al., 2009); widespread continental collision and orogenesis may
7 have increased nutrient supply to the oceans as well as increasing organic carbon burial rates
8 (Campbell & Allen, 2008); episodes of rifting may have increased the size of the early
9 Proterozoic continental shelf seas, thus promoting organic carbon burial (Lenton et al., 2004);
10 the secular loss of H₂ to space (Kasting, 2013) and a change in volcanic gas composition from
11 more reduced compositions during the Archean to more oxidised compositions during the
12 Proterozoic (Kump & Barley, 2007). More recently, it has been proposed that oxygen released
13 by the reduction of SO₂ (as sulphate ions in seawater) derived from early Proterozoic
14 subaerial volcanism may have driven the GOE (Gaillard et al., 2011).

23
24 We argue that against the backdrop of the first emergence of the continents from the oceans
25 during the Archean-Proterozoic transition (Flament et al., 2008), the subaerially erupted lavas
26 of the truly massive Matachewan LIP (Sandeman & Ryan, 2008; Ketchum et al., 2013;
27 Melezhik, 2006) would have resulted in considerable changes to the ancient atmosphere and
28 biosphere. Given the sheer scale of the province, and the fact that the U-Pb geochronological
29 data for the flood basalt suites define an average age of eruption (Fig. 17) indistinguishable
30 from the best estimates for the GOE, we suggest that the Matachewan LIP warrants further
31 study as a potential driver of the GOE, arguably the most fundamental event in Earth's
32 history.

33 34 35 36 37 38 39 40 41 CONCLUSIONS

42
43
44
45 The Matachewan LIP is composed of late Archean-early Proterozoic dyke swarms, layered
46 intrusions and flood basalt provinces preserved on the Superior, Karelia, Wyoming and
47 Hearne cratons. The magmatism is bracketed by the emplacement of members of the East
48 Bull Lake Suite at 2491 Ma and the eruption of the Seidorechka Formation at 2437 Ma, with
49 the entire LIP having an average age of 2461 Ma.

50
51
52
53
54
55 1. The basaltic dyke swarms can be reconstructed as part of the Superia supercraton to
56 radiate out from a point south of Sudbury, Ontario. This point may mark the centre of
57 photosynthetic cyanobacteria (Sessions et al., 2009). To explain the lag between the onset of
58
59
60

an early Proterozoic mantle plume which initiated the eventual breakup of Superia.

1
2
3 The mantle plume also resulted in the formation of a large volcanic province, the
4 remnants of which are compositionally similar to the dyke swarms and parent magmas
5 of the layered intrusions.
6
7

- 8
9 2. The Matachewan LIP suites all have a broadly similar trace element geochemistry,
10 characterised by enrichment in the most incompatible large ion lithophile and light
11 rare earth elements and depletion in the heavy rare earth and other high field strength
12 elements. This shared geochemistry may suggest the existence of a once widespread
13 mantle reservoir not recognised in the modern mantle that imparted a geochemical
14 signature that is shared by the vast majority of early Proterozoic intracontinental
15 igneous rocks.
16
17 3. Alternatively, trace element modelling involving the Matachewan LIP suites suggests
18 their trace element signature can be explained by the contamination of mantle-derived
19 magmas, either by subduction modified sub-continental lithospheric mantle or
20 continental crust during their ascent from the mantle.
21
22 4. Comparison of the potential temperatures of the Matachewan LIP suites with the
23 estimates of the early Proterozoic upper mantle suggest that at least parts of the
24 province are derived from mantle hotter than 2.45Ga ambient upper asthenosphere.
25 Given the proposed plume origin of the province, this is not unexpected.
26
27 5. The flood basalt volcanism and continental breakup associated with the emplacement
28 of the Matachewan LIP would have caused an enormous perturbation in the Earth's
29 atmosphere. The increase in area of continental shelf on which to bury organic carbon,
30 coupled with a potential sulphur-reducing bacterial bloom initiated by loading the
31 atmosphere with volcanogenic SO₂, could have forced the atmosphere onto a path of
32 irreversible oxygenation, known as the Great Oxidation Event.
33
34
35
36
37
38
39
40
41
42
43
44
45
46
47
48
49
50

51 ACKNOWLEDGEMENTS

52
53 A. Oldroyd, L. Woolley and P. Fisher are thanked for their help in preparation and analysis of
54 samples. Constructive reviews by Oliver Kebl and two anonymous reviewers contributed to
55 significant improvement of the original manuscript
56
57
58
59
60

FUNDING

This study forms part of a Ph.D. dissertation undertaken by T.J.R.C. at Cardiff University, United Kingdom, funded by the School of Earth and Ocean Sciences.

REFERENCES

- Abbott, D., Burgess, L., Longhi, J. and Smith W. H. F., 1994. An empirical thermal history of the Earth's upper mantle. *Journal of Geophysical Research*, 99, 13835–13850
- Alapieti, T. T., 2005. Chapter 1 - Early Palaeoproterozoic (2.5-2.4 Ga) Tornio - Näränkäväära layered intrusion belt and related chrome and platinum-group element mineralization, Northern Finland. In Guide 51a, eds. T. T. Alapieti and A. J. Kärki. Geological Survey of Finland.
- Alapieti, T.T., Filèn, B.A., Lahtinen, J.J., Lavrov, M.M., Smol'kin, V.F. and Voitekhovsky, S.N., 1990. Early Proterozoic layered intrusions in the northeastern part of the Fennoscandian Shield. *Mineral. Petrol.*, 42, pp. 1–22.
- Amelin, Y. V. and Semenov, V. S., 1996. Nd and Sr isotopic geochemistry of mafic layered intrusions in the eastern Baltic shield: implications for the evolution of Paleoproterozoic continental mafic magmas. *Contributions to Mineralogy and Petrology*, 124, 255-272.
- Amelin, Y. V., Heaman, L. M. and Semenov, V. S., 1995. U-Pb geochronology of layered mafic intrusions in the eastern Baltic Shield: implications for the timing and duration of Paleoproterozoic continental rifting. *Precambrian Research*, 75, 31-46.
- Anbar, A. D., Duan, Y., Lyons, T. W., Arnold, G. L., Kendall, B., Creaser, R. A., Kaufman, A. J., Gordon, G. W., Scott, C., Garvin, J. and Buick, R., 2007. A Whiff of Oxygen Before the Great Oxidation Event? *Science*, 317, 1903-1906.
- Anderson, D. L., 1982. Hotspots, polar wander, Mesozoic convection and the geoid. *Nature*, 297, 391-393.
- Anderson, D. L., 2000. The Thermal State of the Upper Mantle; No Role for Mantle Plumes. *Geophysical Research Letters*, 27, 3623-3626.
- Anderson, D. L., 2005. Large Igneous Provinces, Delamination, and Fertile Mantle. *Elements*, 1, 271-275.
- Asimow, P. D., and Ghiorso, M. S., 1998. Algorithmic modifications extending MELTS to calculate subsolidus phase relations. *American Mineralogist*, 83, 1127–1132.
- Aspler, L. B. and Chiarenzelli, J. R., 1998. Two Neoproterozoic supercontinents? Evidence from the Paleoproterozoic. *Sedimentary Geology*, 120, 75-104.
- Aspler, L. B., Armitage, A. E., Ryan, J. J., Hauseux, M., Surmacz, S. and Harvey, B. J. A., 2000. Precambrian geology, Victory and Mackenzie lakes, Nunavut, and significance of 'Mackenzie Lake metasediments', Paleoproterozoic Hurwitz Group. In *Current Research*, 10.
- Baker, J. A., Thirlwall, M. F. and Menzies, M. A., 1996. Sr-Nd-Pb isotopic and trace element evidence for crustal contamination of plume-derived flood basalts: Oligocene flood volcanism in western Yemen. *Geochimica et Cosmochimica Acta*, 60, 2559-2581.
- Balashov, Yu., Bayanova, T. & Mitrofanov, F. 1993 . Isotope data on the age and genesis of layered basic-ultrabasic intrusions in the Kola Peninsula and northern Karelia, northeastern Baltic Shield. *Precambrian Research* 64, 197-205.
- Bayanova, T. & Balashov, Yu. 1995. Geochronology of Palaeoproterozoic layered intrusions and volcanites of the Baltic Shield. *Norges Geologiske Undersøkelse, Special Paper*, 7, 75-80.
- Bates, M. P. and Halls, H. C., 1990. Regional variation in paleomagnetic polarity of the Matachewan dyke swarm related to the Kapuskasing Structural Zone, Ontario. *Canadian Journal of Earth Sciences*, 27, 200-211.

- 1
2
3 Bekker, A., Holland, H. D., Wang, P. L., Rumble, D., Stein, H. J., Hannah, J. L., Coetzee, L. L. and Beukes, N.
4 J., 2004. Dating the rise of atmospheric oxygen. *Nature*, 427, 117-120.
- 5
6 Bennett, G., Dressler, B. O. and Robertson, J. A., 1991. The Huronian Supergroup and associated intrusive
7 rocks. In: Thurston, P.C., Williams, H.R., Sutcliffe, R.H. and Stott, G.M., Editors,, *Geology of Ontario*
8 *Geological Survey, Special Volume*, 549-591.
- 9
10 Bijwaard, H. and Spakman, W., 1999. Tomographic evidence for a narrow whole mantle plume below Iceland.
11 *Earth and Planetary Science Letters*, 166, 121-126.
- 12
13 Bizimis, M., Griselein, M., Lassiter, J. C., Salters, V. J. M. and Sen, G., 2007. Ancient recycled mantle
14 lithosphere in the Hawaiian plume: Osmium–Hafnium isotopic evidence from peridotite mantle xenoliths. *Earth
15 and Planetary Science Letters*, 257, 259-273.
- 16
17 Blackwelder, E., 1926. Precambrian geology of the Medicine Bow Mountains. *Geological Society of America
18 Bulletin*, 37, 617-658.
- 19
20 Bleeker, W., 2003. The late Archean record: a puzzle in ca. 35 pieces. *Lithos*, 71, 99-134.
- 21
22 Bleeker, W., 2004. Taking the pulse of planet Earth: a proposal for a new multi-disciplinary flagship project in
23 Canadian solid Earth sciences. *Geoscience Canada*, 31, 179-190.
- 24
25 Bleeker, W. and Ernst, R., 2006. Short-lived mantle generated magmatic events and their dyke swarms: The key
26 unlocking Earth's paleogeographic record back to 2.6 Ga. In *Dyke Swarms - Time Markers of Crustal Evolution*.
27 Edited by E. Hanski, S. Mertanen, T. Rämö, and J. Vuollo. Taylor, 3-26.
- 28
29 Blichert-Toft, J., Albarède, F., Rosing, M., Frei, R. and Bridgwater, D., 1999. The Nd and Hf isotopic evolution
30 of the mantle through the Archean. results from the Isua supracrustals, West Greenland, and from the Birimian
31 terranes of West Africa. *Geochimica et Cosmochimica Acta*, 63, 3901-3914.
- 32
33 Boily, M. and Ludden, N.J., 1990. Trace-element and Nd isotopic variations in Early Proterozoic dyke swarms
34 emplaced in the vicinity of the Kapuskasing structural zone: enriched mantle or assimilation and fractional
35 crystallization (AFC) process? *Canadian Journal of Earth Sciences*, 28, 26-36.
- 36
37 Boudreau, A. E., 1999. PELE-a version of the MELTS software program for the PC platform. *Comput. Geosci.*,
38 25, 201-203.
- 39
40 Bryan, S. E. and Ernst, R. E., 2008. Revised definition of Large Igneous Provinces (LIPs). *Earth-Science
41 Reviews*, 86, 175-202
- 42
43 Bryan, S.E., & Ferrari, L. 2013. Large igneous provinces and silicic large igneous provinces: Progress in our
44 understanding over the last 25 years: *Geological Society of America Bulletin*, 125, 1053–1078.
- 45
46 Buchan, K. L. and Ernst, R. E., 2004. Diabase dyke swarms and related units in Canada and adjacent regions,
47 Canada and Northern USA. *Geological Survey of Canada*.
- 48
49 Buchan, K. L., Goutier, J., Hamilton, M. A., Ernst, R. E. and Matthews, W. A., 2007. Paleomagnetism, U-Pb
50 geochronology, and geochemistry of Lac Esprit and other dyke swarms, James Bay area, Quebec, and
51 implications for Paleoproterozoic deformation of the Superior Province. *Canadian Journal of Earth Sciences*, 44,
52 643-664.
- 53
54 Buiko, A., Levchenkov, O., Turchenko, S. & Drubetskoi, E. 1995. Geology and isotopic dating of the early
55 Proterozoic Sumian-Sariolian Complex in northern Karelia (Paanajärvi-Tspringa structure). *Stratigraphy,
56 Geological Correlation*, 3, 16-30.
- 57
58 Campbell, I. H. and Allen, C. M., 2008. Formation of supercontinents linked to increases in atmospheric oxygen.
59 *Nature Geoscience*, 1, 554-558.
- 60
61 Campbell, I. H., 2007. Testing the plume theory. *Chemical Geology*, 241, 153-176.
- 62
63 Cann, J. R., 1970. Rb, Sr, Y, Zr and Nb in some ocean floor basaltic rocks. *Earth and Planetary Science Letters*,
64 10, 7-11.

- 1
2
3 Campbell, I. H., Czamanske, G. K., Fedorenko, V. A., Hill, R. I. and Stepanov, V., 2002. Synchronism of the
4 Siberian Traps and the Permian-Triassic Boundary. *Science*, 258, 1760-1763.
- 5
6 Cao, Q., van der Hilst, R. D., de Hoop, M.V. and Shim, S.-H., 2011. Seismic imaging of transition zone
7 discontinuities suggests hot mantle west of Hawaii. *Science*, 332, 1068-1071.
- 8
9 Carpenter, R. L., 2003. Relative and absolute timing of supracrustal deposition, tectonothermal activity and gold
10 mineralization, west Meliadine regio, Rankin Inlet greenstone belt, Nunaut, Canada. London, Ontario: The
11 University of Western Ontario.
- 12
13 Chashchin, V., Bayanova, T. and Levkovich, N., 2008. Volcanoplutonic association of the early-stage evolution
14 of the Imandra-Varzuga rift zone, Kola Peninsula, Russia: Geological, petrogeochemical, and isotope-
15 geochronological data. *Petrology*, 16, 279-298.
- 16
17 Chauvel, C., Hofmann, A. W. and Vidal, P., 1992. HIMU-EM: The French Polynesian connection. *Earth and
18 Planetary Science Letters*, 110, 99-119.
- 19
20 Christie, K. W., Davidson, A. and Fahrig, W. F., 1975. The Paleomagnetism of Kaminak Dikes - No Evidence of
21 Significant Hudsonian Plate Motion. *Canadian Journal of Earth Sciences*, 45, 745-767.
- 22
23 Ciborowski, T.J.R., Kerr, A.C., McDonald, I., Ernst, R.E. and Minifie, M.J., 2013. The geochemistry and
24 petrogenesis of the Blue Draw Metagabbro, *Lithos*, 174, 271-290.
- 25
26 Ciborowski, T.J.R., Kerr, A.C., McDonald, I., Ernst, R.E., Hughes, H.S.R. and Minifie, M.J., 2014. The
27 geochemistry and petrogenesis of the Paleoproterozoic du Chef dyke swarm, Québec, Canada. *Precambrian
28 Research*. 10.1016/j.precamres.2014.05.008
- 29
30 Claire, M. W., Catling, D. C. and Zahnle, K. J., 2006. Biogeochemical modelling of the rise in atmospheric
31 oxygen. *Geobiology*, 4, 239-269.
- 32
33 Cloud, P., 1973. Paleocological Significance of the Banded Iron-Formation. *Economic Geology*, 68, 1135-
34 1143.
- 35
36 Coffin, M. F. and Eldholm, O., 1994. Large Igneous Provinces: Crustal Structure, Dimensions, and External
37 Consequences. *Reviews of Geophysics*, 32.
- 38
39 Coffin, M. F. and Eldholm, O., 2005. Large igneous provinces. In: Selley RC, Cocks R, Plimer IR (Eds).
40 *Encyclopedia of Geology*, 315-323.
- 41
42 Coltice, N., Bertrand, H., Rey, P., Jourdan, F., Phillips, B. R. and Ricard, Y., 2009. Global warming of the
43 mantle beneath continents back to the Archaean. *Gondwana Research*, 15, 254-266.
- 44
45 Coltice, N., Phillips, B. R., Bertrand, H., Ricard, Y. and Rey, P., 2007. Global warming of the mantle at the
46 origin of flood basalts over supercontinents. *Geology*, 35, 391-394.
- 47
48 Condie, K. C., 1994. Chapter 3 Greenstones Through Time. In *Developments in Precambrian Geology*, ed. K. C.
49 Condie, 85-120. Elsevier.
- 50
51 Condie, K. C., 2005. High field strength element ratios in Archean basalts: a window to evolving sources of
52 mantle plumes? *Lithos*, 79, 491-504.
- 53
54 Corfu, F. and Easton, R.M., 2001. U-Pb evidence for polymetamorphic history of Huronian rocks within the
55 Grenville front tectonic zone east of Sudbury, Ontario, Canada. *Chemical Geology*, 172, 149-171.
- 56
57 Cousens, B. L., Aspler, L. B., Chiarenzelli, J. R., Donaldson, J. A., Sandeman, H., Peterson, T. D. and
58 LeCheminant, A. N., 2001. Enriched Archean lithospheric mantle beneath western Churchill Province tapped
59 during Paleoproterozoic orogenesis. *Geology*, 29, 827-830.
- 60
61 Dahl, P. S., Hamilton, M. A., Wooden, J. L., Foland, K. A., Frei, R., McCombs, J. A. and Holm, D. K., 2006.
2480 Ma mafic magmatism in the northern Black Hills, South Dakota: a new link connecting the Wyoming and
Superior cratons. *Canadian Journal of Earth Sciences*, 1579-1600.

- 1
2
3 Dasgupta, R., Hirschmann, M. M. and Smith, N. D., 2007. Partial Melting Experiments of Peridotite + CO₂ at 3
4 GPa and Genesis of Alkalic Ocean Island Basalts. *Journal of Petrology*, 48, 2093-2124.
- 5
6 Davies, G. F., 2009. Effect of plate bending on the Urey ratio and the thermal evolution of the mantle. *Earth and
7 Planetary Science Letters*, 287, 513-518.
- 8
9 DePaolo, D. J., 1981. Trace element and isotopic effects of combined wallrock assimilation and fractional
10 crystallization. *Earth and Planetary Science Letters*, 53, 189-202.
- 11
12 Doblas, M., Lopez-Ruiz, J., Cebria, J.-M., Youbi, N. and Degroote, E., 2002. Mantle insulation beneath the West
13 African craton during the Precambrian-Cambrian transition. *Geology*, 30, 839-842.
- 14
15 Easton, R. M., Davidson, A. and Murphy, E. I., 1999. Tansects across the Southern-Grenville Province boundary
16 near Sudbury, Ontario. In *Guidebook*, 52. Sudbury: Geological Association of Canada.
- 17
18 Easton, R. M., James, R. S. and Jobin-Bevans, L. S., 2010. Geological Guidebook to the Paleoproterozoic East
19 Bull Lake Intrusive Suite Plutons at East Bull Lake, Agnew Lake and River Valley: a field trip for the 11th
20 International Platinum Symposium. In *Open File Report*, 108. Ontario Geological Survey.
- 21
22 Elkins-Tanton, L. T., 2005. Continental magmatism caused by lithospheric delamination, . in Foulger, G.R.,
23 Natland, J.H., Presnall, D.C., and Anderson, D.L., eds., *Plates, plumes, and paradigms*, Geological Society of
24 America Special Paper 388, 449-461.
- 25
26 Elkins-Tanton, L. T., 2007. Continental magmatism, volatile recycling, and a heterogeneous mantle caused by
27 lithospheric gravitational instabilities, *Journal of Geophysical Research*, 112, B03405.
- 28
29 Ernst, R.E., 2014. *Large Igneous Provinces*. Cambridge University Press, in press.
- 30
31 Ernst, R. E. and Bleeker, W., 2010. Large igneous provinces (LIPs), giant dyke swarms, and mantle plumes:
32 significance for breakup events within Canada and adjacent regions from 2.5 Ga to the Present. *Canadian Journal
33 of Earth Sciences*, 47, 695-739.
- 34
35 Ernst, R. E. and Buchan, K. L., 2001. The use of mafic dike swarms in identifying and locating mantle plumes.
36 *Geological Society of America Special Papers*, 352, 247-265.
- 37
38 Ernst, R. E. and Buchan, K. L., 2004. Large Igneous Provinces (LIPs) in Canada and adjacent regions: 3 Ga to
39 Present. *Geoscience Canada*, 31, 103-126.
- 40
41 Ernst, R. E., 2007. Large igneous provinces in Canada through time and their metallogenic potential. in
42 Goodfellow, W.D., ed., *Mineral Deposits of Canada: A Synthesis of Major Deposit-Types, District Metallogeny,
43 the Evolution of Geological Provinces, and Exploration Methods*, Geological Association of Canada, Mineral
44 Deposits Division, Special Publication No. 5, 929-937.
- 45
46 Ernst, R. E., Bleeker, W., Hamilton, M. A. and Söderlund, U., 2008. Continental Reconstructions Back To 2.6
47 Ga Using The Large Igneous Province (LIP) Record, With Implications For Mineral Deposit Targeting And
48 Hydrocarbon Resource Exploration [extended Abstract]. In *Palaeogeography: The Spatial Context for
49 Understanding the Earth System*, ed. R. L. P. Markwick, M. Huber (conveners). Cambridge U.K.
- 50
51 Ernst, R. E., Head, J. W., Parfitt, E., Grosfils, E. and Wilson, L., 1995. Giant radiating dyke swarms on Earth
52 and Venus. *Earth-Science Reviews*, 39, 1-58.
- 53
54 Fahrig, W. F. (1987), The tectonic settings of continental mafic dyke swarms: Failed arm and early passive
55 margin, in *Mafic Dyke Swarms*, Spec. Pap. 34, edited by H. C. Halls and W. F. Fahrig, pp. 331-348, Geol.
56 Assoc. of Can., St. John's
- 57
58 Farquhar, J. and Wing, B. A., 2003. Multiple sulfur isotopes and the evolution of the atmosphere. *Earth and
59 Planetary Science Letters*, 213, 1-13.
- 60
61 Frimmel, H. E., 2005. Archaean atmospheric evolution: evidence from the Witwatersrand gold fields, South
62 Africa. *Earth-Science Reviews*, 70, 1-46.

- 1
2
3 Gaffney, A. M., Borg, L. E., Asmerom, Y., Shearer, C. K. and Burger, P. V., 2011. Disturbance of isotope
4 systematics during experimental shock and thermal metamorphism of a lunar basalt with implications for
5 Martian meteorite chronology. *Meteoritics & Planetary Science*, 46, 35-52.
- 6
7 Gaillard, F., Scaillet, B. and Arndt, N. T., 2011. Atmospheric oxygenation caused by a change in volcanic
8 degassing pressure. *Nature*, 478, 229-232.
- 9
10 Galer, S. J. G. and Mezger, K., 1998. Metamorphism, denudation and sea level in the Archean and cooling of the
11 Earth. *Precambrian Research*, 92, 389-412.
- 12
13 Gallagher, K. and Hawkesworth, C., 1992. Dehydration melting and the generation of continental flood basalts.
14 *Nature*, 358, 57-59.
- 15
16 Gates, T. M., and Hurley, P. M., 1973. Evaluation of Rb-Sr dating methods applied to the Matachewan, Abitibi,
17 Mackenzi, and Sudbury, dike swarms in Canada. *Canadian Journal of Earth Science*, 10, 900-919.
- 18
19 Ghiorso, M. S. and Sack, R. O., 1995. Chemical mass transfer in magmatic processes IV. A revised and
20 internally consistent thermodynamic model for the interpolation and extrapolation of liquid-solid equilibria in
21 magmatic systems at elevated temperatures and pressures. *Contributions to Mineralogy and Petrology*, 119, 197-
22 212.
- 23
24 Halls, H. C., 1991. The Matachewan dyke swarm, Canada: an early Proterozoic magnetic field reversal. *Earth
25 and Planetary Science Letters*, 105, 279-292.
- 26
27 Halls, H. C., Kumar, A., Srinivasan, R. and Hamilton, M. A., 2007. Paleomagnetism and U-Pb geochronology
28 of easterly trending dykes in the Dharwar craton, India: feldspar clouding, radiating dyke swarms and the
29 position of India at 2.37 Ga. *Precambrian Research*, 155, 47-68.
- 30
31 Halls, H. C., Stott, G. M. and Davis, D. W., 2005. Paleomagnetism, geochronology and geochemistry of several
32 Proterozoic mafic dike swarms in northwestern Ontario. Ontario Geological Survey, Open File Report 6171, 59.
- 33
34 Hanski, E., Huhma, H., and Vaasjoki, M., 2001. Geochronology of northern Finland: A summary and discussion.
35 In: Radiometric age determinations from Finnish Lapland and their bearing on the timing of Precambrian
36 volcano-sedimentary sequences (eds) M. Vaasjoki, 255-279. Geological Survey of Finland, Special Paper 33.
- 37
38 Harlan, S. S., 2005. The Paleoproterozoic Leopard Dikes of Montana and Wyoming: A Dismembered fragment
39 of the 2.45Ga Hearst-Matachewan giant radiating dike swarm of the Superior Craton? *Geological Society of
40 America Abstracts with Programs*, 37, p. 50.
- 41
42 Harlan, S. S., Geissman, J. W. and Premo, W. R., 2003. Paleomagnetism and geochronology of an Early
43 Proterozoic quartz diorite in the southern Rind River Range, Wyoming, USA. *Tectonophysics*, 362, 105-122.
- 44
45 Harrison, T. M., Blichert-Toft, J., Müller, W., Albarede, F., Holden, P. and Mojzsis, S. J., 2005. Heterogeneous
46 Hadean Hafnium: Evidence of Continental Crust at 4.4 to 4.5 Ga. *Science*, 310, 1947-1950.
- 47
48 Heaman, L. M., 1997. Global mafic magmatism at 2.45 Ga: Remnants of an ancient large igneous province?
49 *Geology*, 25, 299-302.
- 50
51 Heaman, L. M., 2004. 2.5-2.4 Ga global magmatism: Remnants or supercontinents or products of superplumes. .
52 *Geological Society of America, Abstracts with Programs*, 36, 255.
- 53
54 Heimlich, R. A. and Manzer, G. H., 1972. Flow differentiation within Leopard rock dikes, Bighorn Mountains,
55 Wyoming. *Earth and Planetary Science Letters*, 17, 350-356.
- 56
57 Herzberg, C. and Asimow, P. D., 2008. Petrology of some oceanic island basalts: PRIMELT2.XLS software for
58 primary magma calculation. *Geochemistry, Geophysics, Geosystems*, 9, Q09001.
- 59
60 Herzberg, C., Condie, K. and Korenaga, J., 2010. Thermal history of the Earth and its petrological expression.
Earth and Planetary Science Letters, 292, 79-88.
- Hill, J. C., 2006. Structural geology and tectonics of the paleoproterozoic rocks of the Mount Rushmore

- 1
2
3 Huhma, H., Cliff, R.A., Perttunen, V. and Sakko, M., 1990. Sm–Nd and Pb isotopic study of mafic rocks
4 associated with early Proterozoic continental rifting: the Perö Pohja schist belt in northern Finland. *Contributions*
5 *to Mineralogy and Petrology*, 104, 369-379.
- 6
7 Iljina, M., 1994. The Portimo Layered Igneous Complex. PhD Thesis. Department of Geology, University of
8 Oulu. Pp. 178.
- 9
10 Iljina, M. and Hanski, E., 2005. Chapter 3 Layered mafic intrusions of the Tornio—Näränkäväära belt. In
11 *Developments in Precambrian Geology*, eds. P. A. N. M. Lehtinen and O. T. Rämö, 101-137. Elsevier.
- 12
13 Ingle, S. and Coffin, M. F., 2004. Impact origin for the greater Ontong Java Plateau? *Earth and Planetary Science*
14 *Letters*, 218, 123-134.
- 15
16 Jackson, S. L., 2001. On the structural geology of the Southern Province between Sault Ste. Marie and Espanola,
17 Ontario. Ontario Geological Survey, Open File Report 55.
- 18
19 James, R. S., Easton, R. M., Peck, D. C. and Hrominchuk, J. L., 2002. The East Bull Lake Intrusive Suite:
20 Remnants of a ~2.48 Ga Large Igneous and Metallogenic Province in the Sudbury Area of the Canadian Shield.
21 *Economic Geology*, 97, 1577-1606.
- 22
23 Johnson, K. T. M., Dick, H. J. B. and Shimizu, N., 1990. Melting in the oceanic upper mantle: an ion microprobe
24 study of diopsides in abyssal peridotites. *Journal of Geophysical Research*, 95, 2661-2678.
- 25
26 Jolly, W. T., 1987a. Geology and geochemistry of Huronian rhyolites and low-Ti continental tholeiites from the
27 Thessalon region, central Ontario. *Canadian Journal of Earth Sciences*, 24, 1360-1385.
- 28
29 Jolly, W. T., 1987b. Lithophile elements in Huronian low-Ti continental tholeiites from Canada, and evolution
30 of the Precambrian Mantle. *Earth and Planetary Science Letters*, 85, 401-415.
- 31
32 Jolly, W. T., Dickin, A. P. and Wu, T.-W., 1992. Geochemical stratigraphy of the Huronian continental
33 volcanics at Thessalon, Ontario: contributions of two-stage crustal fusion. *Contributions to Mineralogy and*
34 *Petrology*, 110, 411-428.
- 35
36 Jones, A. P., 2005. Meteorite Impacts as Triggers to Large Igneous Provinces. *ELEMENTS*, 1, 277-281.
- 37
38 Jones, A. P., Price, G. D., Price, N. J., DeCarli, P. S. and Clegg, R. A., 2002. Impact induced melting and the
39 development of large igneous provinces. *Earth and Planetary Science Letters*, 202, 551-561.
- 40
41 Jowitt, S. M. and Ernst, R. E., Geochemical assessment of the metallogenic potential of Proterozoic LIPs of
42 Canada. *Lithos*. 174, 291-307.
- 43
44 Karato, S.-i., 2010. Rheology of the deep upper mantle and its implications for the preservation of the
45 continental roots: A review. *Tectonophysics*, 481, 82-98.
- 46
47 Kasting, J. F., 2013. What caused the rise of atmospheric O₂? *Chemical Geology* 362:13-25.
- 48
49 Kerr, A.C., White, R.V. & Saunders, A.D. 2000. LIP reading: Recognizing oceanic plateaus in the geological
50 record. *Journal of Petrology*, 41, 1041-1056.
- 51
52 Keller, G., Sahni, A. and Bajpai, S., 2009. Deccan volcanism, the KT mass extinction and dinosaurs. *Journal of*
53 *Biosciences*, 34, 709-728.
- 54
55 Kerr, A. C. and Mahoney, J. J., 2007. Oceanic plateaus: Problematic plumes, potential paradigms. *Chemical*
56 *Geology*, 241, 332-353.
- 57
58 Ketchum, K.Y., Heaman, L.M., Bennet, G. and Hughes, D.J., 2013. Age, petrogenesis and tectonic setting of the
59 Thessalon volcanic rocks, Huronian Supergroup, Canada. *Precambrian Research*, 233, 144-172.
- 60
King, S. D. and Anderson, D. L., 1995. An alternative mechanism of flood basalt formation. *Earth and Planetary*
Science Letters, 136, 269-279.

- 1
2
3 King, S. D. and Ritsema, J., 2000. African Hot Spot Volcanism: Small-Scale Convection in the Upper Mantle
4 Beneath Cratons. *Science*, 290, 1137-1140.
- 5
6 King, S. D., 2007. Hotspots and edge-driven convection. *Geology*, 35, 223-226.
- 7
8 Kirschvink, J. L., Gaidos, E. J., Bertani, L. E., Beukes, N. J., Gutzmer, J., Maepa, L. N. and Steinberger, R. E.,
9 2000. Paleoproterozoic snowball earth: extreme climatic and geochemical global change and its biological
10 consequences. *Proceedings of the National Academy of Sciences of the United States of America*, 97, 1400-
11 1405.
- 12
13 Komiya, T., Maruyama, S., Hirata, T., Yurimoto, H. and Nohda, S., 2004. Geochemistry of the oldest MORB
14 and OIB in the Isua Supracrustal Belt, southern West Greenland: Implications for the composition and
15 temperature of early Archean upper mantle. *Island Arc*, 13, 47-72.
- 16
17 Konhauser, K. O., Pecoits, E., Lalonde, S. V., Papineau, D., Nisbet, E. G., Barley, M. E., Arndt, N. T., Zahnle,
18 K. and Kamber, B. S., 2009. Oceanic nickel depletion and a methanogen famine before the Great Oxidation
19 Event. *Nature*, 458, 750-753.
- 20
21 Konhauser, K.O., Lalonde, S.V., Planavsky, N.J., Pecoits, E., Lyons, T.W., Mojzsis, S.J., Rouxel, O.J., Barley,
22 M.E., Ros`ere, C., Fralick, P.W., Kump, L.R. and Bekker, A., 2011. Aerobic bacterial pyrite oxidation and acid
23 rock drainage during the Great Oxidation Event. *Nature*, 478, 369-374.
- 24
25 Korenaga, J., 2008. Urey ratio and the structure and evolution of Earth's mantle. *Reviews of Geophysics*, 46, 1-
26 32.
- 27
28 Krogh, T. E., Davis, D. W. and Corfu, F., 1984. Precise U-Pb zircon and baddelyite ages for the Sudbury area. In
29 *The geology and ore deposits of the Sudbury structure.*, eds. E. G. Pye, A. J. Naldrett and P. E. Giblin, 431-446.
- 30
31 Kulikov, V. S., Bychkova, Y. V., Kulikova, V. V. and Ernst, R., 2010. The Vetreny Poyas (Windy Belt)
32 subprovince of southeastern Fennoscandia: An essential component of the ca. 2.5–2.4 Ga Sumian large igneous
33 provinces. *Precambrian Research*, 183, 589-601.
- 34
35 Kump, L. R. and Barley, M. E., 2007. Increased subaerial volcanism and the rise of atmospheric oxygen 2.5
36 billion years ago. *Nature*, 448, 1033-1036.
- 37
38 Kump, L., Fallick, A., Melezhik, V., Strauss, H. and Lepland, A., 2013. 8.1 The Great Oxidation Event. In
39 *Reading the Archive of Earth's Oxygenation*, eds. V. A. Melezhik, A. R. Prave, E. J. Hanski, A. E. Fallick, A.
40 Lepland, L. R. Kump and H. Strauss, 1517-1533. Springer Berlin Heidelberg.
- 41
42 Lauri, L. S., Mikkola, P. and Karinen, T., 2012. Early Paleoproterozoic felsic and mafic magmatism in the
43 Karelian province of the Fennoscandian shield. *Lithos*, 151, 74-82.
- 44
45 Le Bas, M. J., Le Maitre, R. W., Streckeisen, A. and Zanettin, B., 1986. A Chemical Classification of Volcanic
46 Rocks Based on the Total Alkali-Silica Diagram. *Journal of Petrology*, 27, 745-750.
- 47
48 Lee, K. H., 1996. Structure and geochemistry of the Nemo area Black Hills, South Dakota, United States of
49 America. Lincoln: University of Nebraska.
- 50
51 Lenton, T. M., Schellnhuber, H. J. and Szathmary, E., 2004. Climbing the co-evolution ladder. *Nature*, 431, 913-
52 913.
- 53
54 Levchenkov, O., Nikolaev, A., Bogomolov, E. & Yakovleva, S. 1994. U-Pb ages of Sumian acid magmatic
55 rocks in northern Karelia. *Stratigraphy, Geological Correlation*, 2, 3-9.
- 56
57 Li, X., Kind, R., Priestley, K., Sobolev, S. V., Tilmann, F., Yuan, X. and Weber, M., 2000. Mapping the
58 Hawaiian plume conduit with converted seismic waves. *Nature*, 405, 938-941.
- 59
60 Lobach-Zhuchenko, S. B., N. A. Arestova, V. P. Chekulaev, L. K. Levsky, E. S. Bogomolov, and I. N. Krylov,
1998. Geochemistry and petrology of 2.40-2.45 Ga magmatic rocks in the north-western Belomorian Belt,
Fennoscandian Shield, Russia. *Precambrian Research*, 92, 223-250.

- 1
2
3 Maier, W. D., Roelofse, F. and Barnes, S.-J., 2003. The Concentration of the Platinum-Group Elements in South
4 African Komatiites: Implications for Mantle Sources, Melting Regime and PGE Fractionation during
5 Crystallization. *Journal of Petrology*, 44, 1787-1804.
- 6
7 Manninen, T., Pihlaja, P. & Huhma, H. 2001. U-Pb geochronology of the Peurasuvanto area, northern Finland.
8 In: Vaasjoki, M. (ed.) *Radiometric Age Determinations from Finnish Lapland and Their Bearing on the Timing*
9 *of Precambrian Volcano-Sedimentary Sequences*. Geological Survey of Finland, Special Paper, 33, 189-200.
- 10
11 Maranate, S., 1979. Petrogenesis of a layered amphibolite sill in the Nemo district, Black Hills, South Dakota.
12 60. Rapid City: South Dakota School of Mines and Technology.
- 13
14 McDonough, W. F. and Sun, S. S., 1995. The composition of the Earth. *Chemical Geology*, 120, 223-253.
- 15
16 McHone, J. G., 2000. Non-plume magmatism and rifting during the opening of the central Atlantic Ocean.
17 *Tectonophysics*, 316, 287-296.
- 18
19 McHone, J. G., Anderson, D. L., Beutel, E. K. and Fialko, Y. A., 2005. Giant dikes, rifts, flood basalts, and plate
20 tectonics: A contention of mantle models. In *Plates, plumes, and paradigms*, eds. G. R. Foulger, J. H. Natland, D.
21 C. Presnall and D. L. Anderson, 401-420. Geological Society of America.
- 22
23 McKenzie, D. and Bickle, M. J., 1988. The Volume and Composition of Melt Generated by Extension of the
24 Lithosphere. *Journal of Petrology*, 29, 625-679.
- 25
26 Melezhik, V. A. and Sturt, B. A., 1994. General geology and evolutionary history of the early proterozoic
27 Polmak-Pasvik-Pechenga-Imandra/Varzuga-Ust'Ponoy greenstone belt in the northeastern Baltic Shield. *Earth-*
28 *Science Reviews*, 36, 205-241.
- 29
30 Melezhik, V. A., 2006. Multiple causes of Earth's earliest global glaciation. *Terra Nova*, 18, 130-137.
- 31
32 Mertanen, S., Halls, H. C., Vuollo, J. I., Pesonen, L. J. and Stepanov, V. S., 1999. Paleomagnetism of 2.44 Ga
33 mafic dykes in Russian Karelia, eastern Fennoscandian Shield — implications for continental reconstructions.
34 *Precambrian Research*, 98, 197-221.
- 35
36 Minifie, M. J., Kerr, A. C., Ernst, R. E., Hastie, A. R., Ciborowski, T. J. C., Desharnais, G. and Milliar, I. L.,
37 2013. The northern and southern sections of the western ca. 1880 Ma Circum-Superior Large Igneous Province,
38 North America: The Pickle Crow dyke connection? *Lithos*, 174, 217-235.
- 39
40 Mints, M. V., Glaznev, V. N., Konilov, A. N., Kunina, N. M., Nikitichev, A. P., Raevsky, A. B., Sedikh, Y. N.,
41 Stupak, V. M. and Fonarev, V. I. 1996. *The Early Precambrian of the Northeastern Baltic Shield:*
42 *Palaeogeodynamics, Crustal Structure and Evolution*. Moscow: Nauchny Mir Pub.
- 43
44 Montelli, R., Nolet, G., Dahlen, F. A., Masters, G., Engdahl, E. R., and Hung, S.-H., 2004. Finite-Frequency
45 Tomography Reveals a Variety of Plumes in the Mantle. *Science*, 16, 338-343.
- 46
47 Munker, C., S. Weyer, E. Scherer, and K. Mezger., 2001. Separation of high field strength elements (Nb, Ta, Zr,
48 Hf) and Lu from rock samples for MC-ICPMS measurements, *Geochem. Geophys. Geosyst.*, 2,
49 10.1029/2001GC000183
- 50
51 Neal, C. R., Coffin, M. F., Arndt, N. T., Duncan, R. A., Eldholm, O., Erba, E., Farnetani, C., Fitton, J. G., Ingle,
52 S. P., Ohkouchi, N., Rampino, M. R., Reichow, M. K., Self, S. and Tatsumi, Y., 2008. *Investigating Large*
53 *Igneous Province Formation and Associated Paleoenvironmental Events: A White Paper for Scientific Drilling*.
54 Scientific Drilling.
- 55
56 Nebel, O., Arculus, R. J., Ivanic, T. J. and Nebel-Jacobsen, Y. J., 2013. Lu–Hf isotopic memory of
57 plume–lithosphere interaction in the source of layered mafic intrusions, Windimurra Igneous
58 Complex, Yilgarn Craton, Australia. *Earth and Planetary Science Letters*, 380, 151-161.
- 59
60 Nebel, O., Campbell, I. A., Sossi, P. A. and Van Kranendonk, M. J., 2014. Hafnium and iron isotopes
in early Archean komatiites record a plume-driven convection cycle in the Hadean Earth. *Earth and*
Planetary Science Letters, 397, 111-120.

- 1
2
3 Nelson, D. O., Morrison, D. A. and Phinney, W. C., 1990. Open-system evolution versus source control in
4 basaltic magmas: Matachewan-Hearst dike swarm, Superior Province, Canada. *Canadian Journal of Earth*
5 *Sciences*, 27, 767-783.
- 6
7 Neumann, E.R., Svensen, H., Galerne, C.Y. and Planke, S., 2011. Multistage Evolution of Dolerites in the Karoo
8 Large Igneous Province, Central South Africa. *Journal of Petrology*, 10.1093.
- 9
10 Ohta, H., Maruyama, S., Takahashi, E., Watanabe, Y. and Kato, Y., 1996. Field occurrence, geochemistry and
11 petrogenesis of the Archean Mid-Oceanic Ridge Basalts (AMORBs) of the Cleaverville area, Pilbara Craton,
12 Western Australia. *Lithos*, 37, 199-221.
- 13
14 Ojakangas, R. W., Marmo, J. S. and Heiskanen, K. I., 2001. Basin evolution of the Paleoproterozoic Karelian
15 Supergroup of the Fennoscandian (Baltic) Shield. *Sedimentary Geology*, 141-142, 255-285.
- 16
17 Park, J. K., Buchan, K. L. and Harlan, S. S., 1995. A proposed giant radiating dyke swarm fragmented by the
18 separation of Laurentia and Australia based on paleomagnetism of ca. 780 Ma mafic intrusions in western North
19 America. *Earth and Planetary Science Letters*, 132, 129-139.
- 20
21 Patterson, J. G. and Heaman, L. M., 1991. New geochronologic limits on the depositional age of the Hurwitz
22 Group, Trans-Hudson hinterland, Canada. *Geology*, 19, 1137-1140.
- 23
24 Pearce, J. A. and Peate, D. W., 1995. Tectonic implications of the composition of volcanic arc magmas Annual
25 review of Earth and planetary sciences, 23, 251-285.
- 26
27 Pearce, J. A., 1996. A user's guide to basalt discrimination diagrams. In Trace element geochemistry of volcanic
28 rocks: application for massive sulphide exploration, ed. D. Wyman, 79-113. Winnipeg: Geological Association of
29 Canada, Mineral Deposits Division.
- 30
31 Peck, D. C., Keays, R. R., James, R. S., Chubb, P. T. and Reeves, S. J., 2001. Controls on the Formation of
32 Contact-Type Platinum-Group Element Mineralization in the East Bull Lake Intrusion. *Economic Geology*, 96,
33 559-581.
- 34
35 Peterson, D.W. and Moore, R.B., 1987. Geologic history and evolution of geologic concepts, Island of Hawaii.
36 In: Decker, R.W., Wright, T.L. and Stauffer P.H. (eds.), *Volcanism in Hawaii*. USGS Prof. Paper 1350, 1, pp.
37 149-189.
- 38
39 Phinney, W. C. and Halls, H. C., 2001. Petrogenesis of the Early Proterozoic Matachewan dyke swarm, Canada,
40 and implications for magma emplacement and subsequent deformation. *Canadian Journal of Earth Sciences*, 38,
41 1541-1563.
- 42
43 Puchtel, I. S., Haase, K. M., Hofmann, A. W., Chauvel, C., Kulikov, V. S., Garbe-Schönberg, C. D. and
44 Nemchin, A. A., 1997. Petrology and geochemistry of crustally contaminated komatiitic basalts from the
45 Vetryny Belt, southeastern Baltic Shield: Evidence for an early Proterozoic mantle plume beneath rifted Archean
46 continental lithosphere. *Geochimica et Cosmochimica Acta*, 61, 1205-1222.
- 47
48 Puchtel, I. S., Hofmann, A. W., Mezger, K., Shchipansky, A. A., Kulikov, V. S. and Kulikova, V. V., 1996.
49 Petrology of a 2.41 Ga remarkably fresh komatiitic basalt lava lake in Lion Hills, central Vetryny Belt, Baltic
50 Shield. *Contributions to Mineralogy and Petrology*, 124, 273-290.
- 51
52 Räsänen, J. & Huhma, H., 2001. U-Pb datings in the Sodankylä schist area of the Central Lapland Greenstone
53 Belt. In: Vaasjoki, M. (ed.) *Radiometric Age Determinations from Finnish Lapland and Their Bearing on the*
54 *Timing of Precambrian Volcano-Sedimentary Sequences*. Geological Survey of Finland, Special Paper. 33, 153-
55 188.
- 56
57 Redden, J. A., Peterman, Z. E., Zartman, R. E. and DeWitt, E. R., 1990. U-Th-Pb geochronology and
58 preliminary interpretation of Precambrian events in the Black Hills, South Dakota. In *The Trans-Hudson orogen*.
59 Edited by J.F. Lewry and M.R. Stauffer, Geological Association of Canada Special Paper 37, 229-251.
- 60
61 Richter, F. M., 1988. A Major Change in the Thermal State of the Earth at the Archean-Proterozoic Boundary:
62 Consequences for the Nature and Preservation of Continental Lithosphere. *Journal of Petrology*,

- 1
2
3 Roscoe, S. M. and Card, K. D., 1993. The reappearance of the Huronian in Wyoming: rifting and drifting of
4 ancient continents. *Canadian Journal of Earth Sciences*, 30, 2475-2480.
- 5
6 Rudnick, R. L. and Fountain, D. M., 1995. Nature and composition of the continental crust: a lower crustal
7 perspective. *Reviews of Geophysics*, 33, 267-309.
- 8
9 Rudnick, R. L. and Gao, S., 2003. 3.01 - Composition of the Continental Crust. In *Treatise on Geochemistry*,
10 eds. D. H. Editors-in-Chief: Heinrich and K. T. Karl, 1-64. Oxford: Pergamon.
- 11
12 Sandeman, H. A. and Ryan, J. J., 2008. The Spi Lake Formation of the central Hearne domain, western Churchill
13 Province, Canada: an axial intracratonic continental tholeiite trough above the cogenetic Kaminak dyke swarm.
14 *Canadian Journal of Earth Sciences*, 45, 745-767.
- 15
16 Sandeman, H. A., Cousens, B. L. and Hemmingway, C. J., 2003. Continental tholeiitic mafic rocks of the
17 Paleoproterozoic Hurwitz Group, Central Hearne sub-domain, Nunavut: insight into the evolution of the Hearne
18 sub-continental lithosphere. *Canadian Journal of Earth Sciences*, 40, 1219-1237.
- 19
20 Sandeman, H. A., Heaman, L. M. and LeCheminant, A.N., 2013. The Paleoproterozoic Kaminak dykes, Hearne
21 craton, western Churchill Province, Nunavut, Canada: Preliminary constraints on their age and petrogenesis.
22 *Precambrian Research*, 232, 119-139.
- 23
24 Schmitz, M. D., Vervoort, J. D., Bowring, S. A. and Patchett, P. J., 2004. Decoupling of the Lu-Hf and
25 Sm-Nd isotope systems during the evolution of granulitic lower crust beneath southern Africa.
26 *Geology*, 32, 405-408.
- 27
28 Schopf, J.W., 1993. Microfossils of the Early Archean Apex chert: new evidence of the antiquity of life. *Science*,
29 260, 640-646.
- 30
31 Sessions, A. L., Doughty, D. M., Welander, P. V., Summons, R. E. and Newman, D. K., 2009. The Continuing
32 Puzzle of the Great Oxidation Event. *Current Biology*, 19, R567-R574.
- 33
34 Siddorn, J.P., 1999. Differential uplift of the Archean Basement North of the Sudbury Basins: Petrographic
35 Evidence from the Matachewan Dyke Swarm. 62. University of Toronto.
- 36
37 Söderlund, U., Hofmann, A., Klausen, M. B., Olsson, J. R., Ernst, R. E. and Persson, P.-O., 2010. Towards a
38 complete magmatic barcode for the Zimbabwe craton: Baddeleyite U-Pb dating of regional dolerite dyke
39 swarms and sill complexes. *Precambrian Research*, 183, 388-398.
- 40
41 Sproule, R. A., Leshner, C. M., Ayer, J. A. and Thurston, P. C., 2003. *Geochemistry and metallogenesis of
42 komatiitic rocks in the Abitibi greenstone belt, Ontario*. ed. O. G. Survey, 119.
- 43
44 Stern, R.J., 2005. Evidence from ophiolites, blueschists, and ultrahigh-pressure metamorphic terranes that the
45 modern episode of subduction tectonics began in Neoproterozoic time. *Geology*, 33, 557-560.
- 46
47 Sun, S. s. and McDonough, W. F., 1989. Chemical and isotopic systematics of oceanic basalts: implications for
48 mantle composition and processes. *Geological Society, London, Special Publications*, 42, 313-345.
- 49
50 Sverjensky, D. A. and Lee, N., 2010. The Great Oxidation Event and Mineral Diversification. *ELEMENTS*, 6,
51 31-36.
- 52
53 Tomlinson, K. Y., 1996. The geochemistry and tectonic setting of early Precambrian greenstone belts,
54 Northwestern Ontario, Canada. PhD thesis. pp. 287. University of Portsmouth.
- 55
56 Van Boening, A. M. and Nabelek, P. I., 2008. Petrogenesis and tectonic implications of paleoproterozoic mafic
57 rocks in the Black Hills, South Dakota. *Precambrian Research*, 167, 363-376.
- 58
59 Vervoort, J. D., Patchett, P. J., Blichert-Toft, J. and Albarède, F., 1999. Relationships between Lu-Hf and Sm-
60 Nd isotopic systems in the global sedimentary system. *Earth and Planetary Science Letters*, 168, 79-99.
- 61
62 Vogel, D. C., James, R. S. and Keays, R. R., 1998a. The early tectono-magmatic evolution of the Southern
63 Province: implications from the Agnew Intrusion, central Ontario, Canada. *Canadian Journal of Earth Sciences*,
64 35, 854-870.

- 1
2
3 Vogel, D. C., Vuollo, J. I., Alapieti, T. T. and James, R. S., 1998b. Tectonic, stratigraphic, and geochemical
4 comparisons between ca. 2500-2440 Ma mafic igneous events in the Canadian and Fennoscandian Shields.
5 *Precambrian Research*, 92, 89-116.
- 6 Vogel, D. C., Keays, R. R., James, R. S. and Reeves, S. J., 1999. The Geochemistry and Petrogenesis of the
7 Agnew Intrusion, Canada: A Product of S-Undersaturated, High-Al and Low-Ti Tholeiitic Magmas. *Journal of*
8 *Petrology*, 40, 423-450.
- 9
10 Vuollo, J. and Huhma, H., 2005. Chapter 5 Paleoproterozoic mafic dikes in NE Finland. In *Developments in*
11 *Precambrian Geology*, eds. P. A. N. M. Lehtinen and O. T. Rämö, 195-236. Elsevier.
- 12
13 Waite, G. P., Smith, R. B. and Allen, R. M., 2006. VP and VS structure of the Yellowstone hot spot from
14 teleseismic tomography: Evidence for an upper mantle plume. *Journal of Geophysical Research*, 111, B04303.
- 15
16 Walter, M. J., 1998. Melting of garnet peridotite and the origin of komatiite and depleted lithosphere. *Journal of*
17 *Petrology*, 39, 29-60.
- 18
19 Wehred, P., Arndt, N. T., Billström, K., Duchesne, J.-C., Eilu, P., Martinsson, O., Papunen, H. and Lahtinen, R.,
20 2005. 8: Precambrian geodynamics and ore formation: The Fennoscandian Shield. *Ore Geology Reviews*, 27,
21 273-322.
- 22
23 West, G. F. and Ernst, R. E., 1991. Evidence from aeromagnetism on the configuration of Matachewan dykes and
24 the tectonic evolution of the Kapuskasing Structural Zone, Ontario, Canada. *Canadian Journal of Earth Sciences*,
25 28, 1797-1811.
- 26
27 Willbold, M. and Stracke, A., 2006. Trace element composition of mantle end-members: Implications for
28 recycling of oceanic and upper and lower continental crust. *Geochemistry, Geophysics, Geosystems*, 7, Q04004.
- 29
30 Williams, H., 1991. Anatomy of North America: thematic geologic portrayals of the continent. *Tectonophysics*,
31 187, 117-134.
- 32
33 Wolfe, C. J., Bjarnason, I. T., VanDecar, J. C. and Solomon, S. C., 1997. Seismic structure of the Iceland mantle
34 plume. *Nature*, 385, 245-247.
- 35
36 Woo, C. C., 1952. The Pre-Cambrian geology and amphibolites of the Nemo district, Black Hills, South Dakota.
37 148. Chicago: University of Chicago.
- 38
39 Workman, R. K. and Hart, S. R., 2005. Major and trace element composition of the depleted MORB mantle
40 (DMM). *Earth and Planetary Science Letters*, 231, 53-72.
- 41
42 Xie, Q., Kerrich, R. and Fan, J., 1993. HFSE/REE fractionations recorded in three komatiite-basalt sequences,
43 Archean Abitibi greenstone belt: Implications for multiple plume sources and depths. *Geochimica et*
44 *Cosmochimica Acta*, 57, 4111-4118.
- 45
46 Young, G. M., 1988. Proterozoic plate tectonics, glaciation and iron-formations. *Sedimentary Geology*, 58, 127-
47 144.
- 48
49 Zhang, B., 1999. A Study of Crustal Uplift along the Kapuskasing Zone Using 2.45 Ga Matachewan Dykes. In
50 Department of Geology. Toronto: University of Toronto.
- 51
52 Zhou, M-F., Malpas, J., Song, X-Y., Robinson, P. T., Sun, M., Kennedy, A. K., Leshner, C. M. and Keays, R. R.,
53 2002. A temporal link between the Emeishan large igneous province (SW China) and the end-Guadalupian mass
54 extinction. *Earth and Planetary Science Letters*, 196, 113-122.
- 55
56
57
58
59
60

1
2
3 Figure captions
4
5
6

7 Fig. 1. Maps showing the present day positions of the cratons which make up the
8 reconstructed Archean supercontinent, Superia. Also shown are the locations of the mafic
9 dyke swarms, layered intrusions and volcano-sedimentary rift basins which have been
10 proposed to constitute the reconstructed Matachewan LIP. Volcano-sedimentary rift basins:
11 Snowy Pass Supergroup – SP, Spi Group – SG, Huronian Supergroup – HU, Karelian
12 Supergroup – KS; Layered intrusions: East Bull Lake Suite – EBLs, Blue Draw Metagabbro
13 – BDM, Fennoscandian Intrusions – FI; Mafic dyke swarms: Leopard – LE, Kaminak – KA,
14 Matachewan – MA, Viianki – VI, Streich – ST.
15
16
17
18
19

20 Fig. 2. Early Proterozoic Matachewan LIP reconstruction. The mafic dyke swarms, layered
21 intrusions and volcano-sedimentary rift basins are preserved on the Superior, Wyoming,
22 Hearne, Karelia and Kola cratons. When reconstructed to their inferred primary distribution,
23 the composite radiating dyke swarm defines a mantle plume locus, melting at which triggered
24 the emplacement of the Matachewan LIP. Abbreviations as in Fig. 1. Modified after
25 Söderlund et al. (2010).
26
27
28
29
30

31 Fig. 3. Major and trace element variation diagrams vs Zr for the Matachewan LIP suites.
32
33

34 Fig. 4. Trace element ratio diagrams for the Matachewan dykes and Thessalon Formation
35 basalts. (a) La/Sm vs Gd/Yb; (b) Nb/Th vs La/Yb
36
37
38

39 Fig. 5. Zr/Ti vs Nb/Yb classification diagram (after Pearce, 1996) for the Matachewan LIP
40 suites.
41
42
43

44 Fig. 6. Major and trace element variations vs MgO for the Matachewan LIP suites.
45
46
47

48 Fig. 7. Chondrite-normalised rare earth element patterns for the average composition of each
49 of the Matachewan LIP suites. EMORB, NMORB, OIB values are from Sun & McDonough
50 (1989). Chondrite normalising values from McDonough & Sun (1995).
51
52

57 The compositions have been modified by 7.3% AFC of olivine using the bulk continental
58
59
60

1
2
3 Fig. 8. Primitive mantle-normalised trace element patterns for the average composition of
4 each of the Matachewan LIP suites. EMORB, NMORB, OIB values from Sun & McDonough
5 (1989). Primitive Mantle normalising values from McDonough & Sun (1995).
6
7

8
9 Fig. 9. Zr/Nb vs Nb/Th (a) and Nb/Y vs Zr/Y (b) for the Matachewan LIP suites. Field
10 boundaries and end-member compositions from Condie (2005). Abbreviations: PM =
11 Primitive Mantle, DM = shallow depleted mantle, ARC = arc related basalts, NMORB =
12 normal mid-ocean ridge basalt, OPB = oceanic plateau basalt, OIB = oceanic island basalt,
13 DEP = deep depleted mantle, REC = recycled component.
14
15
16

17
18 Fig. 10. ϵ_{Ndi} (a), and ϵ_{Hfi} (b) variations for the Matachewan LIP suites. Data for East Bull
19 Lake Suite and Blue Draw Metagabbro (BDM) from this study. Sources of data for the other
20 suites are in Table 2. Initial isotope ratios (i) calculated for $t = 2460$ Ma.
21
22
23

24 Fig. 11. Thermal evolution of the upper mantle through times using different models; A –
25 Davies (2009); B – Richter (1988); C – Abbot et al. (1994); D – Korenaga (2008) and
26 Herzberg et al. (2010).
27
28

29 Fig. 12. Crystallisation models used in this study (for the Kaminak dykes). (a) and (b) major
30 element models showing the best fit of Model 4 (7 kbar, anhydrous, QFM) in reproducing the
31 major element variation in the Kaminak dykes. Line markers denote 10% crystallisation
32 intervals of the parent magma. (c) Primitive Mantle-normalised trace element patterns for the
33 Kaminak dykes and range of compositions predicted to form through AFC using the mineral
34 assemblage and degrees of fractionation predicted by Model 4, and the composition of
35 average crust (Rudnick & Fountain 1995) where $r = 0.1$ and $F =$ fraction of liquid remaining.
36 Normalising values from McDonough & Sun (1995).
37
38
39
40
41
42

43 Fig. 13. Primitive Mantle-normalised multi-element patterns for 31.1% partial melt of spinel
44 lherzolite from the DMM (a), EM1 (b) and PM (c) mantle reservoirs which have mixed with
45 between 0.1-5% low degree partial melts of Archaean SCLM (Sandeman et al., 2003) before
46 fractionating 7.31% olivine. Also plotted is the analysis of the Seidorechka Formation basalt
47 91113 (Puchtel et al., 1996). Primitive Mantle normalising values from McDonough & Sun
48 (1995).
49
50
51
52
53
54
55
56
57
58
59
60

53
54
55
56

Fig. 14. Primitive Mantle-normalised multi-element patterns for 30.3% partial melts of spinel lherzolite from DMM (a), EM1 (b) and PM (c) which have been previously melted ($F = 0.3$).

57
58
59
60

The compositions have been modified by 7.3% AFC of olivine using the bulk continental

1
2
3 crust (Rudnick & Gao 2003) as the contaminant for $r = 0.1-0.5$. Also plotted is the analysis of
4 East Bull Lake Suite feeder dyke 234 (Vogel et al., 1998b). Primitive Mantle normalising
5 values from McDonough & Sun (1995).
6
7

8
9 Fig. 15. Primitive Mantle-normalised multi-element patterns for 30.3% partial melts of spinel
10 lherzolite from the DMM, EM1 and PM reservoirs which have been previously melted ($F =$
11 0.3). The compositions have been modified by mixing with 0.1, 1 and 5% low degree partial
12 melts of Archaean SCLM (Cousens et al., 2001) before undergoing 32.32% FC of olivine.
13 Also plotted is the analysis of East Bull Lake Suite feeder dyke sample 234 (Vogel et al.,
14 1998b). Primitive Mantle normalising values from McDonough & Sun (1995).
15
16
17

18
19 Fig. 16. Variation of ϵ_{Ndt} vs. ϵ_{Hft} for the Matachewan LIP layered intrusions analysed in this
20 study. For comparison fields for other Archean-Paleoproterozoic components are plotted: ISB
21 = Isua Supracrustal Belt conglomerates, turbidites and gneisses (Blichert-Toft et al., 1999);
22 WIC = Windimurra Igneous Complex gabbros (Nebel et al., 2013); OP = Peridotite mantle
23 xenoliths from O'ahu (Bizimis et al., 2007); ASAG = Archean lower crustal South African
24 granulites (Schmitz et al., 2004). Values calculated for $t = 2.46$ Ga.
25
26
27
28
29

30
31 Fig. 17. Variation of $\Delta^{33}\text{S}$ versus geological age (modified after Johnson et al., 2011). Note
32 the prevalence of mass-independent fractionation of sulphur isotopes in rocks older than 2450
33 Ma and subsequent absence in rocks deposited since the early Proterozoic. This change in the
34 geological record is argued to signify the first sustained appearance of oxygen in Earth's
35 atmosphere during the Great Oxidation Event. Also plotted are age estimates for each of the
36 individual Matachewan LIP suites. References: A – Krogh et al. (1984), B – Easton et al.
37 (1999), C – Lauri et al. (2012), D – Dahl et al. (2006), E – Heaman (1997), F – Halls et al.
38 (2005), G – Heaman (1994), H – Sandeman et al. (2013), I – Mertanen et al. (1999), J –
39 Ketchum et al. (2013), K – Amelin et al. (1995), L – Puchtel et al. (1997), M – Chashchin et
40 al. (2008), N – Anbar et al. (2007), O – Schopf (1993).
41
42
43
44
45
46
47
48
49
50
51
52
53
54
55
56
57
58
59
60

Table 1. Summary of reported ages for constituent Matachewan LIP suites. Locations in parentheses indicate undated suites that have been interpreted as cogenetic with associated suites (see text for discussion). Abbreviations: bad – baddeleyite, zir – zircon, tit – titanite.

Suite	Age (Ma)	Analysis type	Reference
Mafic Dyke Swarms			
Matachewan	2446 ± 3	bad + zir	Heaman (1997)
	2473 ^{+16, -9}	bad	Heaman (1997)
	2459 ± 5	bad	Halls et al. (2005)
Kaminak (Spi Group)	2450 ± 2	bad	Heaman (1994)
	2498 ± 1	bad	Sandeman et al. (2013)
Viianki	2446 ± 5	bad	Mertanen et al. (1999)
Flood Basalt Provinces			
Thessalon Formation	2439 ± 9	zir	Krogh et al. (1984)
	2435 ± 3	zir	Ketchum et al. (2013)
Seidorechka Formation			
Seidorechka	2431 ± 15	bad + zir	Bayanova & Balashov (1995)
Imandra	2442 ± 2	bad	Amelin et al. (1995)
Paanajärvi	2432 ± 2	zir	Buiko et al. (1995)
Lekhta	2443 ± 5	zir	Levchenkov et al. (1994)
Vetreny Belt	2437 ± 3	zir	Puchtel et al. (1997)
Sakiamaa	2438 ± 11	zir	Räsänen & Huhma (2001)
Rookkiaapa	2438 ± 14	zir	Manninen et al. (2001)
Khibiny	2448 ± 8	zir	Chashchin et al. (2008)
Layered Intrusions			
Blue Draw Metagabbro	2480 ± 6	bad + zir	Dahl et al. (2006)
East Bull Lake Suite (Streich dykes)			
East Bull Lake	2480 ^{+10, -5}	bad + zir	Krogh et al. (1984)
Agnew	2491 ± 5	zir	Krogh et al. (1984)
River Valley	2476 ^{+2, -1}	bad + zir	Unpub. in Easton et al. (1999)
Fennoscandian Intrusions	2424 ± 5 – 2470 ± 9	bad + zir	Comp. in Lauri et al. (2012)
	2432 ± 6 – 2496 ± 10	bad + zir	Comp. in Hanski et al. (2001)

47
48
49
50
51
52
53
54
55
56

46
47
48
49
50
51
52
53
54
55
56
57
58
59
60

Table 2. Summary of the nature and sources of data collated during this study for each of the Matachewan LIP suites.

Suite	Analysis type	# analyses	Data Source
Mafic Dyke Swarms			
Matachewan	Majors + Traces	60	This study
Kaminak	Majors + Traces	57	This study
	Sm - Nd	9	Sandeman et al. (2013)
Viianki	Majors + Traces	6	Vogel et al. (1998a)
	Sm-Nd	5	Mertanen et al. (1999)
Streich	Majors + Traces	4	Vogel et al. (1998a)
Flood Basalt Provinces			
Thessalon Formation	Majors + Traces	79	Tomlinson (1996); Ketchum et al. (2013)
	Sm - Nd	12	Jolly et al. (1992)
Seidorechka Formation	Majors + Traces	100	Mints et al. (1996); Puchtel et al. (1997);
	Sm - Nd	38	Puchtel et al. (1997)
Spi Group	Majors + Traces	8	Sandeman & Ryan (2008)
	Sm - Nd	5	Sandeman & Ryan (2008)
Layered Intrusions			
Blue Draw Metagabbro	Majors + Traces	16	This study
	Sm - Nd	6	This study
	Lu - Hf	6	This study
East Bull Lake Suite	Majors + Traces	38	This study
	Sm - Nd	11	This study
	Lu - Hf	11	This study
Fennoscandian Intrusions	Sm - Nd	168	Hrv'na et al. (1990); Balashov et al. (1993); Iljina (1994); Amelin & Shtenov (1996); Puchtel et al. (1997); Lobach-Zhukhenko et al. (1998); Hanski et al. (2001)

Table 3. Summary of the key geochemical ranges and averages of the Matachewan LIP suites. † - estimate of Blue Draw Metagabbro parent magma from Ciborowski et al. (2013). N denotes normalisation to Primitive Mantle of Sun & McDonough (1989). Sources of data are described in Table 2.

Suite	MgO (wt.%)	Fe ₂ O ₃ (wt.%)	SiO ₂ (wt.%)	Alkali (wt.%)	Ni (ppm)	Cr (ppm)	(La/Sm) _N	(Gd/Yb) _N	Eu/Eu*	Nb/Th	Zr/Nb	Zr/Y	Nb/Y	Nb/Nb*	Ti/Ti*	Zr/Zr*	Y/Y*
Mafic Dyke Swarms																	
Matachewan																	
Group 1	2.2-8.8	11.0-18.0	48.4-55.7	2.2-5.6	8-170	9-476	2.0	1.1	0.9	3.0	19.8	3.6	0.2	0.5	0.8	1.0	1.1
Group 2	23.0-5.9	11.2-14.6	48.3-53.5	4.1-7.5	8-817	5-339	2.8	2.2	0.9	1.5	21.7	6.6	0.3	0.2	0.6	0.9	1.1
Kaminak	2.2-6.3	13.5-17.1	45.4-54.0	3.2-5.4	2-200	4-89	2.9	1.5	1.0	1.5	20.9	4.7	0.2	0.2	0.8	0.9	1.1
Flood Basalts																	
Thessalon Formation																	
Group 1	4.1-7.1	10.1-17.0	45.2-56.6	2.2-8.2	49-152	23-100	2.4	1.5	0.9	1.7	21.1	4.3	0.2	0.3	0.6	0.9	0.9
Group 2	1.5-8.2	10.2-16.7	47.8-61.7	3.3-7.4	1-205	1-44	2.7	2.9	0.9	3.6	14.5	7.7	0.5	0.6	0.5	0.7	0.8
Group 3	8.4-9.9	12.5-14.6	50.1-52.9	2.8-3.9	302-357	997-1080	2.5	2.5	0.9	5.5	10.3	6.2	0.6	0.7	0.5	0.8	0.9
Group 4	3.7-5.2	9.7-13.3	53.1-58.1	3.1-6.5	63-78	27-30	3.6	1.5	0.7	0.7	16.7	5.2	0.3	0.2	0.4	0.8	0.9
Seidorechka Formation	0.5-20.8	4.2-12.3	48.2-76.0	2.8-7.2	0-700	0-1400	3.4	1.6	0.8	-	31.2	6.3	0.2	0.3	0.6	1.2	1.0
Spi Group	2.5-3.5	12.6-13.9	49.3-53.8	3.5-54.9	41-66	28-39	3.1	1.7	0.8	1.4	18.7	5.9	0.3	0.2	0.7	0.9	1.0
Layered Intrusion parent magmas																	
Blue Draw Metagabbro†	13	10.2	52.9	3.9	20-1357	20-3131	3.2	1.5	0.9	0.8	11.8	5.3	0.2	0.1	0.5	1.0	1.0
Fennoscandian Intrusion feeders (Viianki dykes)	8.2-17.2	9.9-11.5	50.7-53.4	1.7-3.8	209-510	520-1708	3.0	1.7	1.0	1.3	17.3	5.4	0.2	0.2	0.6	1.0	0.9
East Bull Lake Suite feeders (Streich dykes)	7.5-8.0	10.0-10.5	49.1-50.4	2.6-3.7	27-709	10-604	2.1	1.1	1.3	2.1	27.1	3.4	1.3	0.3	0.8	1.0	1.0

Table 4. New Sm-Nd and Lu-Hf isotope data for selected Matachewan LIP layered intrusions. ϵNd_i and ϵHf_i calculated for 2460 Ma, $(^{147}\text{Sm}/^{144}\text{Nd})_{\text{CHUR}} = 0.1967$ and $(^{176}\text{Lu}/^{177}\text{Hf})_{\text{CHUR}} = 0.0332$.

Suite	Sample	Rb	Sr	$^{87}\text{Sr}/^{86}\text{Sr}$	$^{87}\text{Rb}/^{86}\text{Sr}$	$(^{87}\text{Sr}/^{86}\text{Sr})_i$	Nd	Sm	$^{147}\text{Sm}/^{144}\text{Nd}$	$^{143}\text{Nd}/^{144}\text{Nd}$	ϵNd_i	Lu	Hf	$^{176}\text{Lu}/^{177}\text{Lu}$	$^{176}\text{Hf}/^{177}\text{Hf}$	ϵHf_i
Blue Draw Metagabbro	BD096	6.9	142.1	0.707821	0.0011	0.707781	1.757	0.547	0.1881	0.511947	-10.83	0.107	1.393	0.0109	0.282261	19.09
	BD091	13.9	132.8	0.710585	0.0014	0.710535	3.570	0.935	0.1582	0.511743	-5.31	0.137	1.305	0.0150	0.282154	8.47
	BD078	0.2	134.3	0.712903	0.0008	0.712875	1.149	0.485	0.2550	0.512854	-14.31	0.106	0.994	0.0151	0.282707	27.91
	BD037	0.3	1.3	0.728534	0.0008	0.728506	0.503	0.108	0.1296	0.511394	-3.04	0.024	0.375	0.0089	0.281975	12.18
	BD044	0.2	26.5	0.710054	0.0011	0.709987	0.973	0.410	0.2550	0.512815	-15.09	0.063	0.589	0.0151	0.283396	52.34
	BD065	46.9	217.4	0.716918	0.0011	0.716904	8.787	1.862	0.1280	0.511399	-2.46	0.218	2.570	0.0121	0.281706	-2.64
East Bull Lake	EB002	5.9	655.8	0.704678	0.026017	0.703753	1.238	1.608	0.1342	0.511618	-0.14	0.242	0.963	0.0357	0.282670	-7.73
	EB003	12.2	131.9	0.707692	0.267563	0.698180	2.238	0.714	0.1981	0.512481	-3.53	0.158	0.605	0.0370	0.283127	6.24
	EB005	16.2	363.0	0.707081	0.129090	0.702491	1.577	0.377	0.1497	0.511842	-0.67	0.074	0.445	0.0237	0.282415	3.11
	EB006	14.4	143.2	0.709568	0.290944	0.699225	2.144	0.545	0.1554	0.511863	-2.06	0.123	0.909	0.0192	0.282172	2.06
Agnew	AG003	4.8	279.0	0.704965	0.049754	0.703196	3.591	0.395	0.1505	0.511857	-0.61	0.134	0.992	0.0193	0.282212	3.36
	AG004	35.8	397.2	0.706368	0.260692	0.697101	1.811	0.473	0.1577	0.511913	-1.81	0.118	0.731	0.0230	0.282448	5.58
	AG006	13.8	200.8	0.706171	0.198775	0.699105	4.055	1.067	0.1591	0.511990	-0.74	0.219	0.976	0.0318	0.282791	2.94
	AG007	27.0	259.8	0.710113	0.300703	0.699423	0.759	0.286	0.2214	0.512637	-9.78	0.086	0.354	0.0347	0.282922	2.91
River Valley	RV006	15.0	277.5	0.707949	0.156369	0.702390	3.789	0.925	0.1474	0.511310	-0.57	0.146	0.674	0.0307	0.282732	2.78
	RV009	16.8	763.1	0.706268	0.063676	0.704004	3.425	0.918	0.1620	0.512009	-0.72	0.168	0.554	0.0432	0.283386	5.15
	RV014	20.8	424.2	0.705460	0.141833	0.702048	2.426	0.496	0.1235	0.511460	-1.00	0.113	0.846	0.0190	0.282171	2.41

Table 5. Whole-rock geochemical data for samples of Matachewan LIP layered intrusions analysed by this study for Rb-Sr, Sm-Nd and Lu-Hf isotopes.

	Blue Draw Metagabbro						East Bull Lake Intrusion				Agnew Intrusion				River Valley Intrusion		
	BD037	BD044	BD065	BD078	BD091	BD096	EB002	EB003	EB005	EB006	AG003	AG004	AG006	AG007	RV006	RV009	RV014
Majors (wt.%)																	
SiO ₂	37.45	50.58	55.06	54.40	52.75	44.91	49.24	48.54	48.50	45.32	50.28	49.18	50.19	50.24	50.63	48.64	53.01
TiO ₂	0.12	0.28	0.62	0.25	0.37	0.30	0.38	0.33	0.18	0.25	0.47	0.33	0.38	0.20	0.34	0.60	0.19
Al ₂ O ₃	2.43	3.44	13.89	8.94	8.40	15.19	22.77	11.89	24.44	14.81	24.58	24.21	13.26	15.82	22.44	9.35	17.10
Fe ₂ O ₃	10.84	8.24	10.71	7.89	10.74	7.13	5.93	14.41	4.86	13.37	6.29	6.35	13.65	8.90	4.79	13.89	9.43
MnO	0.13	0.18	0.17	0.15	0.18	0.13	0.09	0.21	0.09	0.21	0.09	0.08	0.18	0.15	0.10	0.17	0.14
MgO	38.94	19.88	6.15	12.06	13.38	7.79	0.65	11.03	4.18	11.62	2.89	3.10	7.40	8.50	3.48	13.67	6.33
CaO	0.10	13.07	9.42	10.06	10.22	10.71	18.26	9.63	12.77	8.23	12.96	11.27	12.25	10.18	12.77	9.89	8.15
Na ₂ O	0.01	0.99	2.82	0.73	1.64	2.47	1.37	1.35	2.38	1.18	2.36	2.79	1.67	2.35	3.30	1.73	3.40
K ₂ O	0.00	0.03	1.31	0.22	0.5	0.28	0.19	0.46	0.64	0.31	0.31	1.03	0.31	0.40	0.48	0.71	0.86
P ₂ O ₅	0.01	0.02	0.08	0.01	0.2	0.05	0.06	0.02	0.02	0.03	0.04	0.02	0.04	0.01	0.04	0.15	0.01
LOI	11.18	3.58	0.63	4.41	1.98	0.73	1.08	1.86	1.71	3.61	0.80	1.33	0.75	1.71	1.38	2.04	1.72
Total	101.20	100.29	100.86	99.11	100.14	100.69	100.01	99.74	99.77	98.95	101.08	99.70	100.09	98.47	99.74	100.84	100.35
Traces (ppm)																	
Sc	8.9	45.2	28.7	37.9	34.1	23.5	9	37.2	16.9	15.0	17.7	11.7	43.9	24.8	22.4	40.0	17.3
Zr	14.6	20.4	97.7	21.4	47.7	37.6	51.0	22.2	22.0	28.9	38.5	24.7	38.8	12.9	25.5	19.2	30.4
V	43.4	225.9	203.3	208.2	245.8	149.2	151.7	65.7	87.4	106.2	121.5	88.8	189.8	325.6	110.4	226.2	59.1
Cr	3390.9	1567.1	110.3	641.9	628.7	130.3	10.4	25.3	412.1	64.5	103.6	82.6	164.1	187.1	153.1	604.2	139.8
Co	127.3	46.0	39.1	32.2	57.8	31.0	6.1	7.5	22.8	79.8	22.8	26.7	49.7	47.3	23.2	66.4	47.4
Ni	1236.7	365.0	168.5	160.6	199.5	130.8	26.6	27.7	119.7	450.3	68.1	175.6	107.9	253.9	41.3	347.9	708.5
Cu	34.8	37.7	47.0	90.5	39.8	27.8	27.5	82.1	45.8	62.5	47.5	143.2	88.6	57.8	70.0	473.7	2911.8
Ga	3.7	5.3	16.6	10.9	10.3	12.6	26.0	11.9	15	11.9	16.6	17.7	15.7	14.8	16.1	14.6	15.8
Rb	0.3	0.2	46.9	0.2	13.9	6.9	5.9	12.2	16.2	14.1	4.8	35.8	13.8	27.0	15.0	16.8	20.8
Sr	1.1	27.3	217.4	145.1	128.6	142.5	649.3	130.5	363.4	146.4	305.8	420.2	214.5	275.9	284.7	742.5	450.6
Y	3.2	7.0	15.7	7.0	10.1	7.2	16.0	9.2	5.0	6.9	9.2	7.9	16.0	5.8	9.2	9.8	6.5
Nb	46.43	10.28	329.60	15.08	205.87	85.63	39.88	167.39	107.80	116.2	77.34	211.98	130.69	231.98	238.48	325.48	269.12
La	2.08	3.27	16.46	3.61	8.16	6.45	14.65	5.59	5.62	5.53	5.10	6.50	7.44	4.21	4.57	4.38	7.45
Ce	3.31	6.17	34.10	7.68	17.77	12.52	19.75	6.00	5.43	8.27	9.7	9.49	12.53	4.94	8.66	7.78	13.53
Pr	0.38	0.82	4.07	0.99	2.22	1.58	2.44	0.81	0.68	1.04	1.22	1.04	1.68	0.80	1.14	1.10	1.57
Nd	1.58	3.50	15.40	4.12	8.33	5.82	9.72	3.65	2.81	4.16	5.06	3.4	7.23	3.18	4.54	4.95	5.78
Sm	0.38	0.89	3.25	0.98	1.98	1.28	2.28	1.06	0.73	1.00	1.23	1.05	1.92	0.81	1.17	1.31	1.11
Eu	0.12	0.27	0.96	0.32	0.59	0.39	1.01	0.45	0.40	0.38	0.50	0.67	0.76	0.44	0.50	0.64	0.67
Gd	0.36	1.02	3.20	0.98	1.90	1.22	2.23	1.05	0.65	0.94	1.24	1.22	2.00	0.73	1.23	1.25	0.91
Tb	0.07	0.17	0.49	0.16	0.30	0.19	0.38	0.19	0.10	0.15	0.21	0.19	0.36	0.12	0.20	0.21	0.16
Dy	0.45	1.16	2.98	1.12	1.99	1.32	2.49	1.38	0.73	1.00	1.40	1.24	2.38	0.81	1.28	1.37	0.95
Ho	0.08	0.23	0.54	0.23	0.38	0.25	0.51	0.29	0.16	0.21	0.28	0.24	0.48	0.17	0.26	0.29	0.20
Er	0.25	0.67	1.63	0.63	1.14	0.75	1.52	0.87	0.45	0.61	0.82	0.70	1.40	0.47	0.80	0.85	0.62
Tm	0.04	0.11	0.27	0.11	0.17	0.11	0.25	0.15	0.07	0.10	0.13	0.11	0.23	0.08	0.13	0.14	0.09
Yb	0.28	0.69	1.69	0.64	1.13	0.74	1.69	1.00	0.48	0.65	0.89	0.77	1.58	0.54	0.92	1.01	0.80
Lu	0.04	0.10	0.25	0.10	0.17	0.11	0.28	0.16	0.07	0.10	0.13	0.12	0.25	0.09	0.12	0.14	0.13
Hf	0.33	0.49	2.53	0.66	1.55	0.94	1.32	0.51	0.50	0.70	1.15	0.65	1.05	0.36	0.58	0.48	0.82
Ta	0.05	0.05	0.37	0.07	0.17	0.15	0.11	0.02	0.03	0.06	0.10	0.07	0.08	0.06	0.07	0.04	0.12
Pb	1.21	0.94	12.98	2.88	5.21	3.32	8.29	2.51	4.86	45.73	5.12	13.34	2.74	6.42	8.99	6.35	6.95
Th	0.72	0.86	5.94	1.06	2.93	2.02	1.56	0.28	0.34	0.67	0.78	0.51	0.92	0.35	0.60	0.23	1.97
U	0.17	0.21	1.71	0.27	0.70	0.47	0.54	0.09	0.12	0.18	0.22	0.18	0.24	0.33	0.14	0.11	0.95

1
2
3
4
5
6
7
8
9
10
11
12
13
14
15
16
17
18
19
20
21
22
23
24
25
26
27
28
29
30
31
32
33
34
35
36
37
38
39
40
41
42
43
44
45
46
47
48
49

For Peer Review

Table 6. Primary magma compositions for different Matachewan LIP suites as calculated by PRIMELT2. T – eruption temperature; T_p – mantle potential temperature; F – degree of melting; Fo – forsterite content of olivine in equilibrium with the melt; % ol – percentage of olivine added to sample composition needed to obtain primary magma composition.

Sample	Suite	SiO ₂	TiO ₂	Al ₂ O ₃	Cr ₂ O ₃	Fe ₂ O ₃	FeO	MnO	MgO	CaO	Na ₂ O	K ₂ O	NiO	P ₂ O ₅	T (°C)	T_p (°C)	F	Fo	% ol
91113	Seidorechka Formation	49.03	0.56	10.78	0.02	1.14	9.13	0.18	17.04	9.76	1.78	0.24	0.07	0.08	1390	1508	31.1	91.5	7.3
234	Streich Dykes	47.06	0.35	12.82	0.02	0.5	10.04	0.18	18.69	8.94	1.47	0.43	0.16	0.01	1422	1545	30.3	92.4	32.3

Table 7. Model parameters used in PELE for investigation of fractional crystallisation models.

Model	Pressure	H ₂ O content	Oxygen buffer
Model 1	1 kbar	0%	QFM
Model 2	1 kbar	1%	QFM
Model 3	3 kbar	0%	QFM
Model 4	7 kbar	0%	QFM
Model 5	10 kbar	0%	QFM

For Peer Review

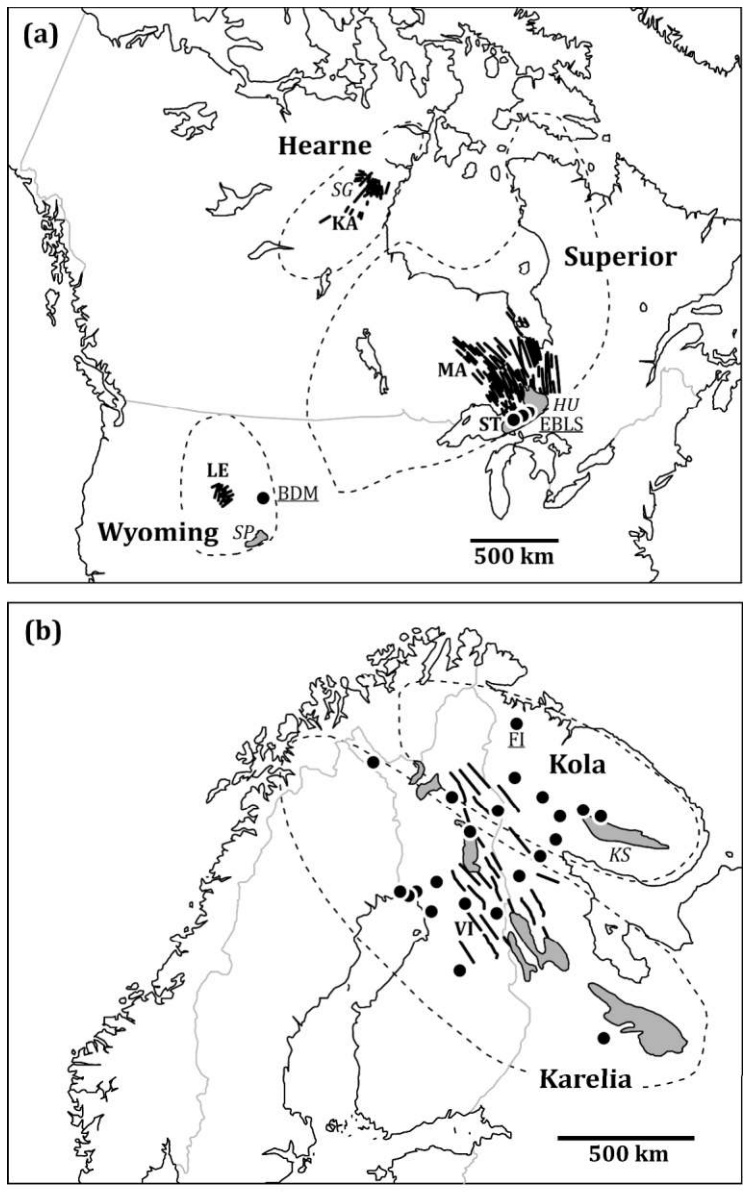
Table 8. Summary of the modelling showing the MgO content of the parent magma, most successful model parameters, predicted crystallisation sequence, the degree of fractionation required to account for the geochemical variation observed and the preferred mechanism for each of the Matachewan LIP suites studied. Abbreviations: sp – spinel, ol – olivine, cpx – clinopyroxene, plg – plagioclase, opx – orthopyroxene, or – orthoclase, qz – quartz, FC – fractional crystallisation, AFC – assimilation-fractional crystallisation.

Suite	MgO cont. parent	Pressure (kbar)	1 wt.% H ₂ O	Liquidus temp. (°C)	Crystallisation sequence	% FC recorded	Preferred mechanism
Matachewan Dykes (Grp. 1)	8.8	7		1375	sp, ol, cpx, plg	60	FC
East Bull Lake Suite	6.6-7.7	3		1267-1251	sp, plg, ol, cpx, opx, qz, or	100	AFC
Thessalon Formation (Grp. 1)	6.7	1		1245	sp, ol, plg, cpx	30	AFC
Thessalon Formation (Grp. 2)	6.8	10		1378	sp, opx, cpx, plg	60	AFC
Blue Draw Metagabbro	5.5	3		1446	ol, sp, plg, cpx, opx, or, qz	100	AFC
Kaminak Dykes	6.3	7		1283	sp, cpx, plg	60	AFC
Viianki Dykes	8.0			1475	sp, ol, cpx	30	AFC
Seidorechka Formation	20.8	1		1479	ol, opx, sp, cpx, plg, qz	90	AFC

Element (ppm)	DMM	EM1	PM	C _S DMM F = 0.3	C _S EM1 F = 0.3	C _S PM F = 0.3
Th	0.01	0.03	0.09	0.00008	0.00027	0.00081
Nb	0.15	0.38	0.71	0.00100	0.00260	0.00480
Ta	0.01	0.03	0.04	0.00007	0.00018	0.00028
La	0.19	0.60	0.69	0.00600	0.01800	0.02000
Ce	0.55	1.75	1.78	0.02900	0.09400	0.09500
Pr	0.11	0.29	0.28	0.00900	0.02300	0.02200
Nd	0.58	1.47	1.35	0.06200	0.15700	0.14500
Zr	5.00	13.00	11.00	0.64300	1.58900	1.41800
Hf	0.16	0.36	0.31	0.02200	0.05100	0.04400
Sm	0.24	0.52	0.44	0.05000	0.10700	0.09200
Eu	0.10	0.20	0.17	0.02300	0.04900	0.04100
Ti	716	1433	1300	198	396	360
Gd	0.36	0.72	0.60	0.09300	0.18700	0.15600
Tb	0.07	0.13	0.11	0.01900	0.03700	0.03000
Dy	0.71	0.92	0.74	0.14800	0.27000	0.21600
Y	3.33	5.77	4.55	0.91100	1.58000	1.24600
Ho	0.15	0.20	0.16	0.03700	0.06600	0.05300
Er	0.35	0.60	0.48	0.12200	0.21200	0.16900
Tm	0.05	0.09	0.07	0.02000	0.03400	0.02700
Yb	0.37	0.62	0.49	0.12100	0.20400	0.16300
Lu	0.06	0.10	0.07	0.02000	0.03300	0.02600

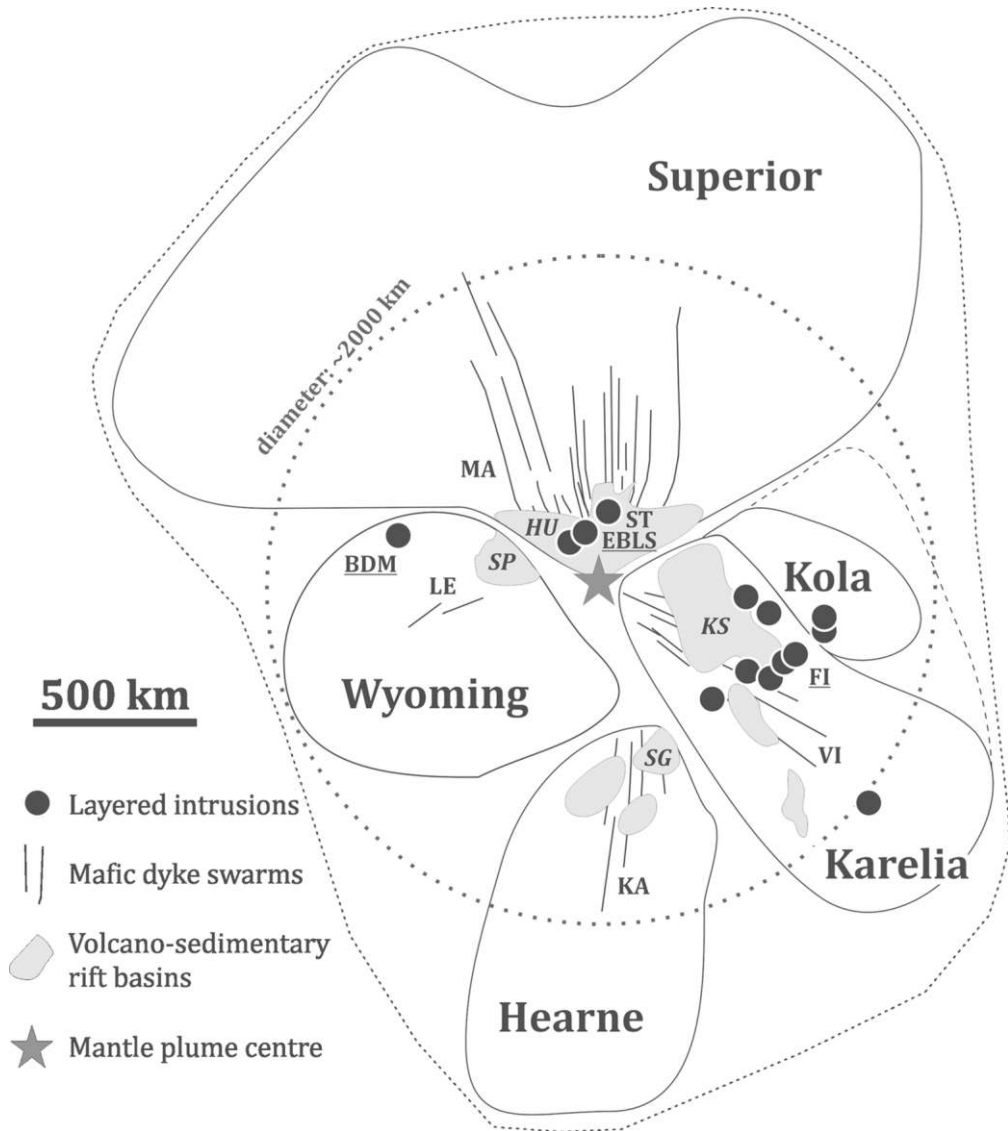
Table 9. Trace element compositions of mantle end-members modelled in this study. Data sources: DMM – Workman & Hart (2005), EM1 – Willbold & Stracke (2006), PM – McDonough & Sun (1995). Also shown are the trace element compositions of the mantle end-member residues (C_S) following 30% batch partial melting of spinel lherzolite.

1
2
3
4
5
6
7
8
9
10
11
12
13
14
15
16
17
18
19
20
21
22
23
24
25
26
27
28
29
30
31
32
33
34
35
36
37
38
39
40
41
42
43
44
45
46
47
48
49
50
51
52
53
54
55
56
57
58
59
60

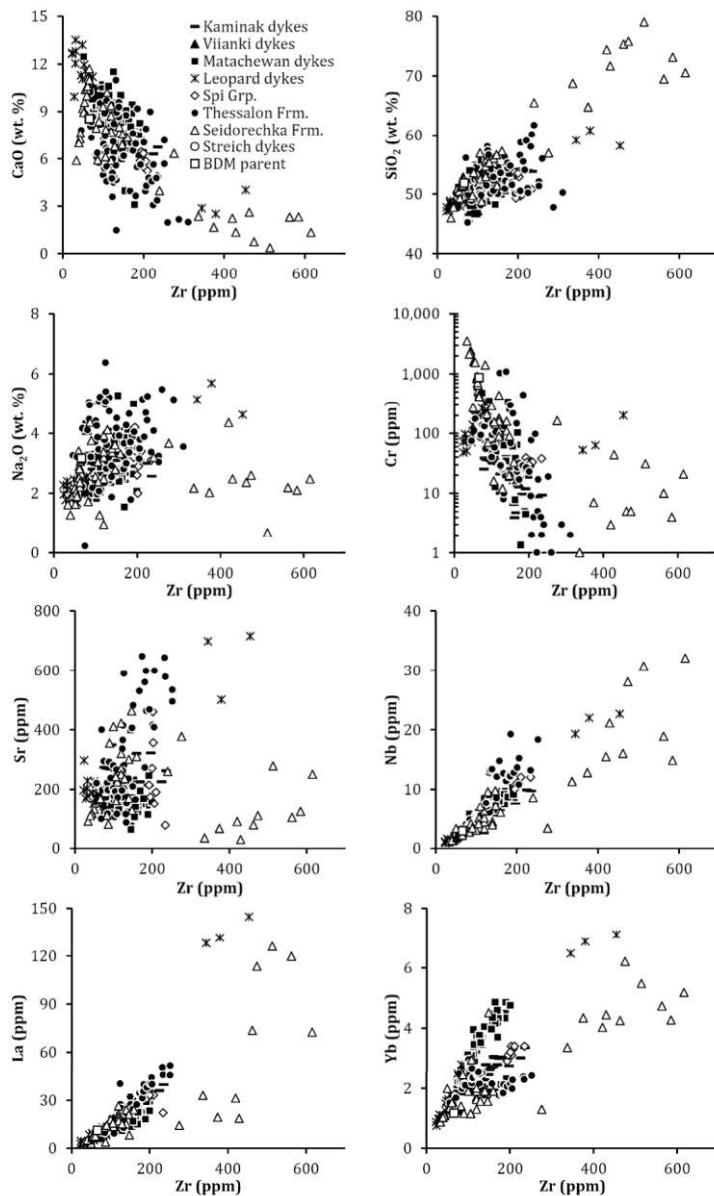


272x443mm (300 x 300 DPI)

1
2
3
4
5
6
7
8
9
10
11
12
13
14
15
16
17
18
19
20
21
22
23
24
25
26
27
28
29
30
31
32
33
34
35
36
37
38
39
40
41
42
43
44
45
46
47
48
49
50
51
52
53
54
55
56
57
58
59
60

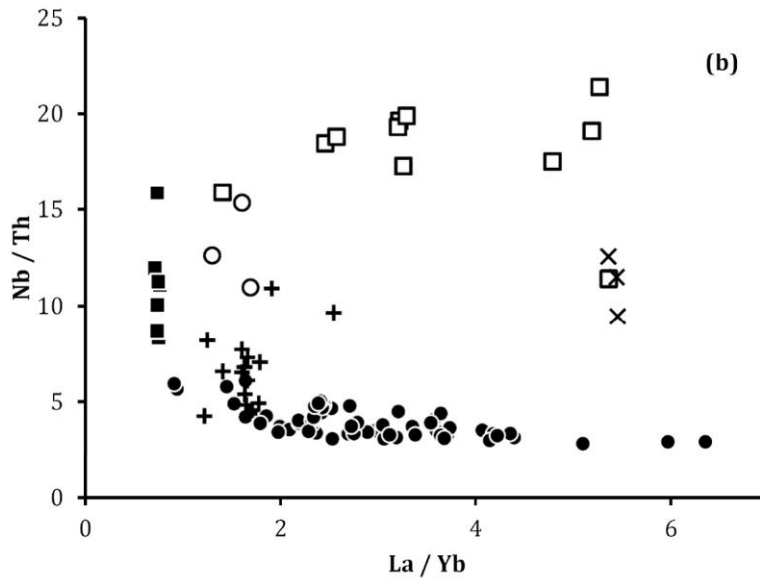
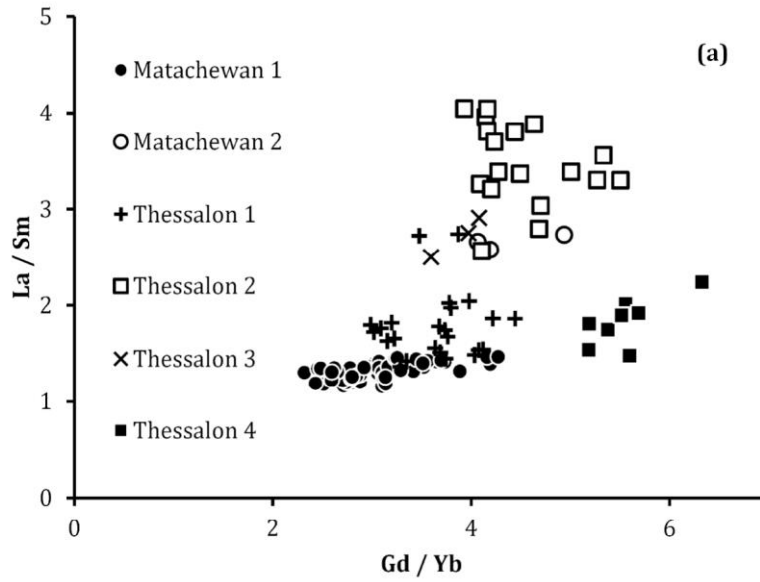


113x127mm (300 x 300 DPI)



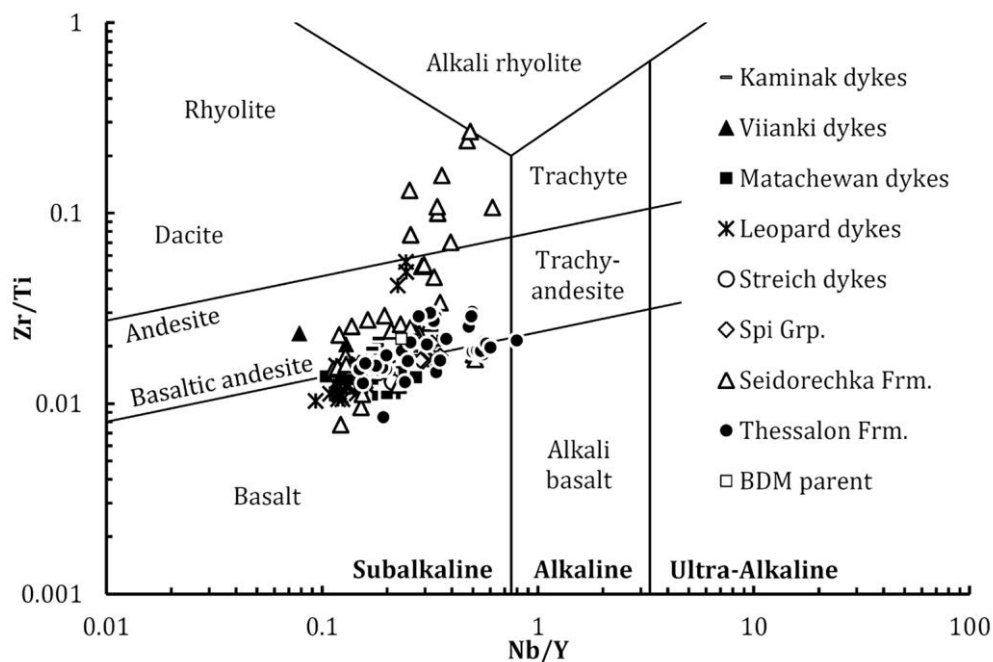
299x497mm (300 x 300 DPI)

1
2
3
4
5
6
7
8
9
10
11
12
13
14
15
16
17
18
19
20
21
22
23
24
25
26
27
28
29
30
31
32
33
34
35
36
37
38
39
40
41
42
43
44
45
46
47
48
49
50
51
52
53
54
55
56
57
58
59
60



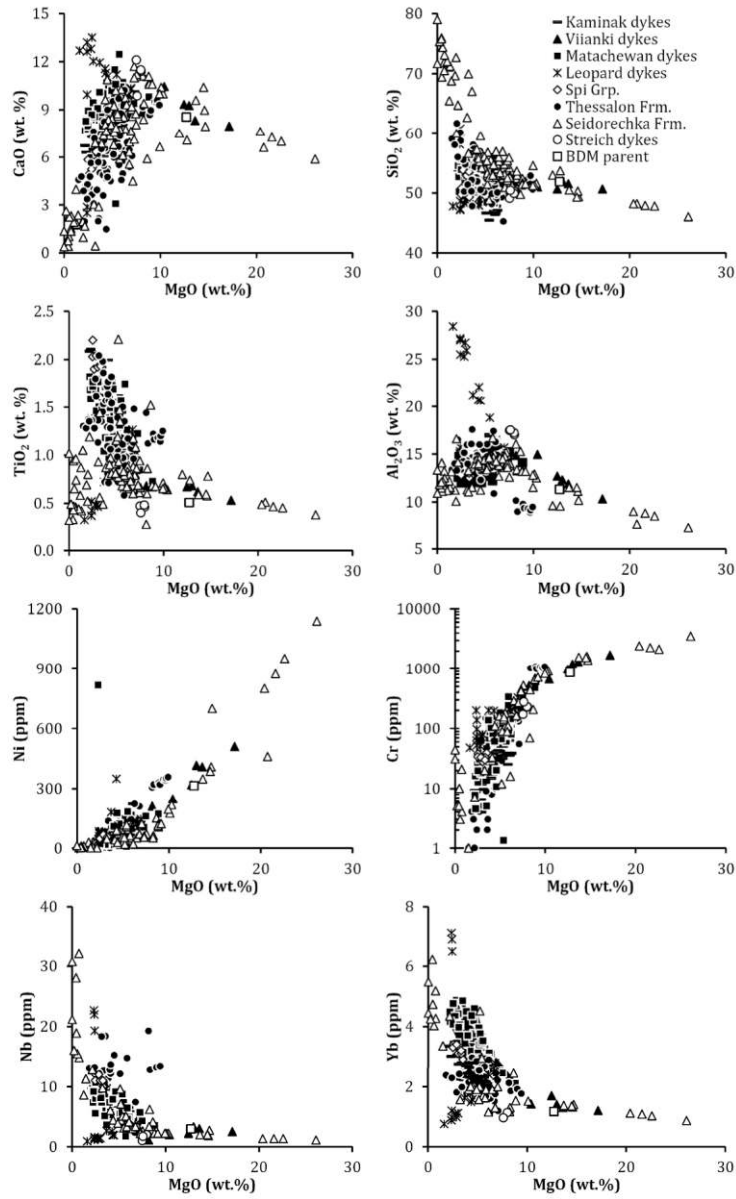
305x467mm (300 x 300 DPI)

1
2
3
4
5
6
7
8
9
10
11
12
13
14
15
16
17
18
19
20
21
22
23
24
25
26
27
28
29
30
31
32
33
34
35
36
37
38
39
40
41
42
43
44
45
46
47
48
49
50
51
52
53
54
55
56
57
58
59
60



135x91mm (300 x 300 DPI)

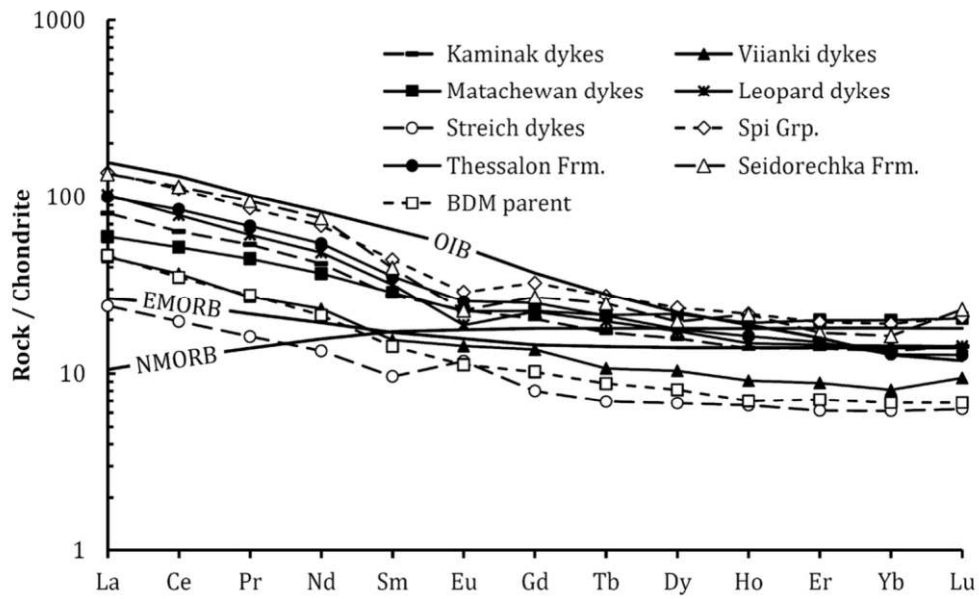
Review



294x480mm (300 x 300 DPI)

45
46

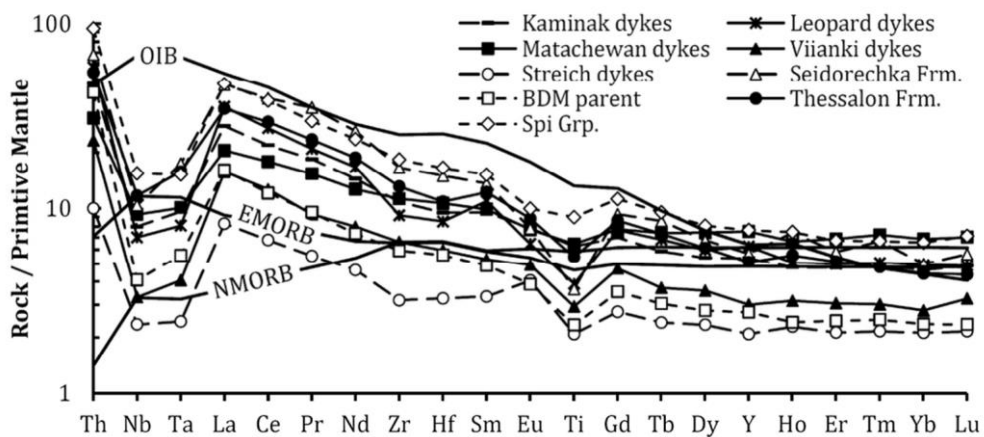
45
46
47
48
49
50
51
52
53
54
55
56
57
58
59
60



121x73mm (300 x 300 DPI)

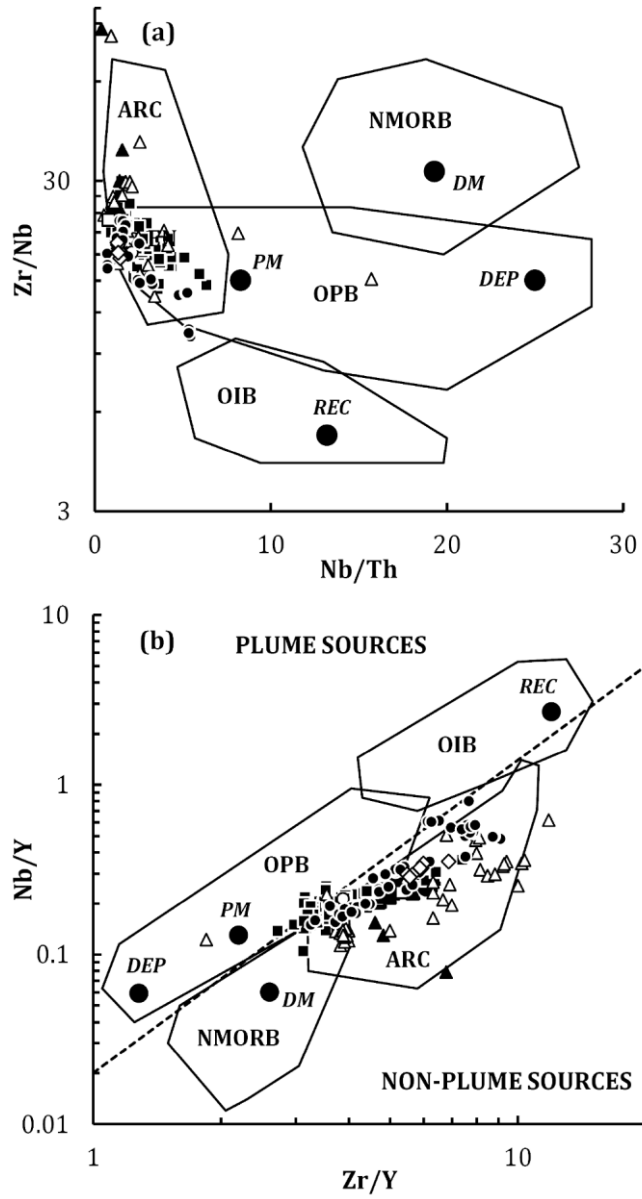
Review

294x480mm (300 x 300 DPI)

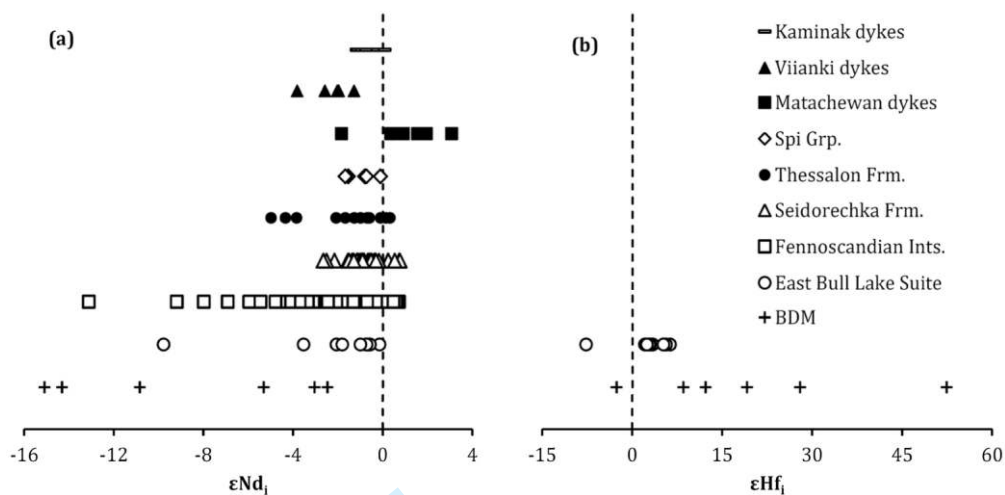


90x40mm (300 x 300 DPI)

366x670mm (300 x 300 DPI)

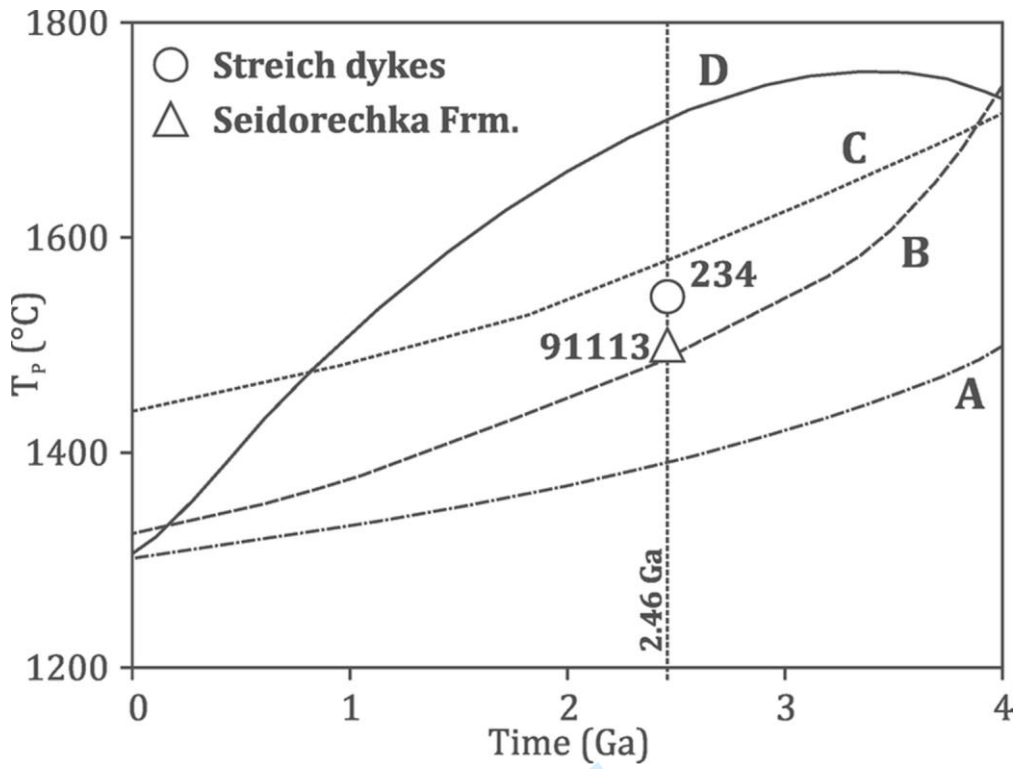


1
2
3
4
5
6
7
8
9
10
11
12
13
14
15
16
17
18
19
20
21
22
23
24
25
26
27
28
29
30
31
32
33
34
35
36
37
38
39
40
41
42
43
44
45
46
47
48
49
50
51
52
53
54
55
56
57
58
59
60



155x80mm (300 x 300 DPI)

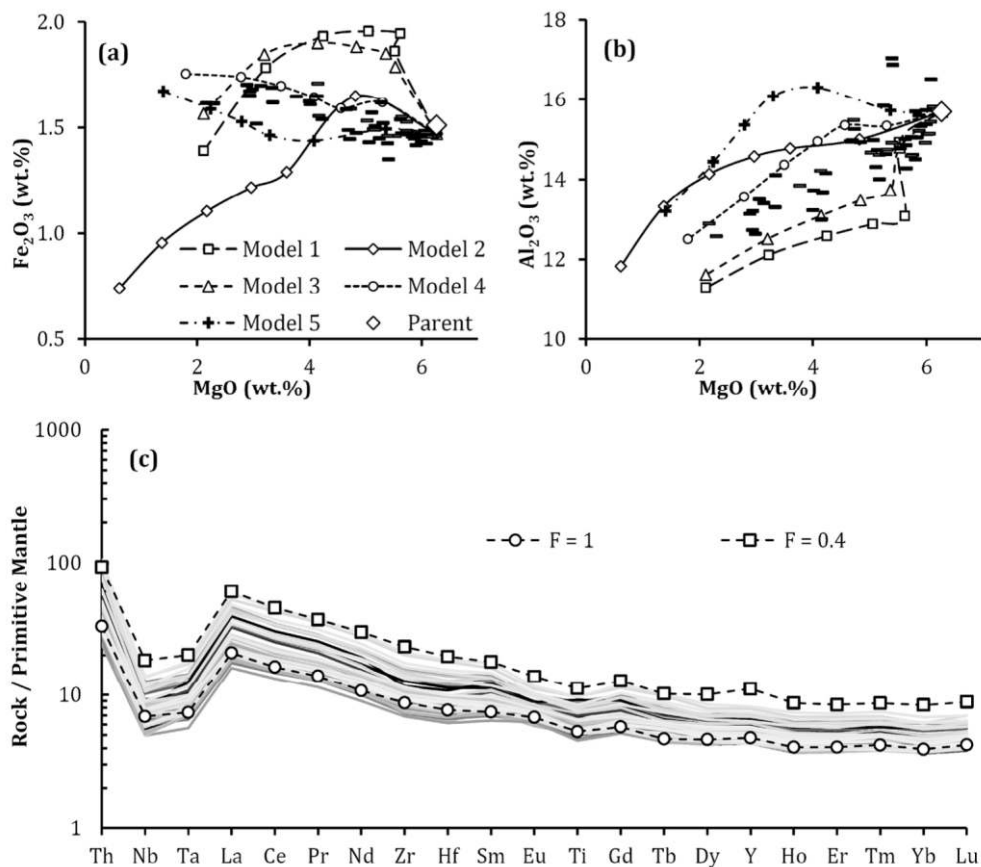
366x670mm (300 x 300 DPI)



70x52mm (300 x 300 DPI)

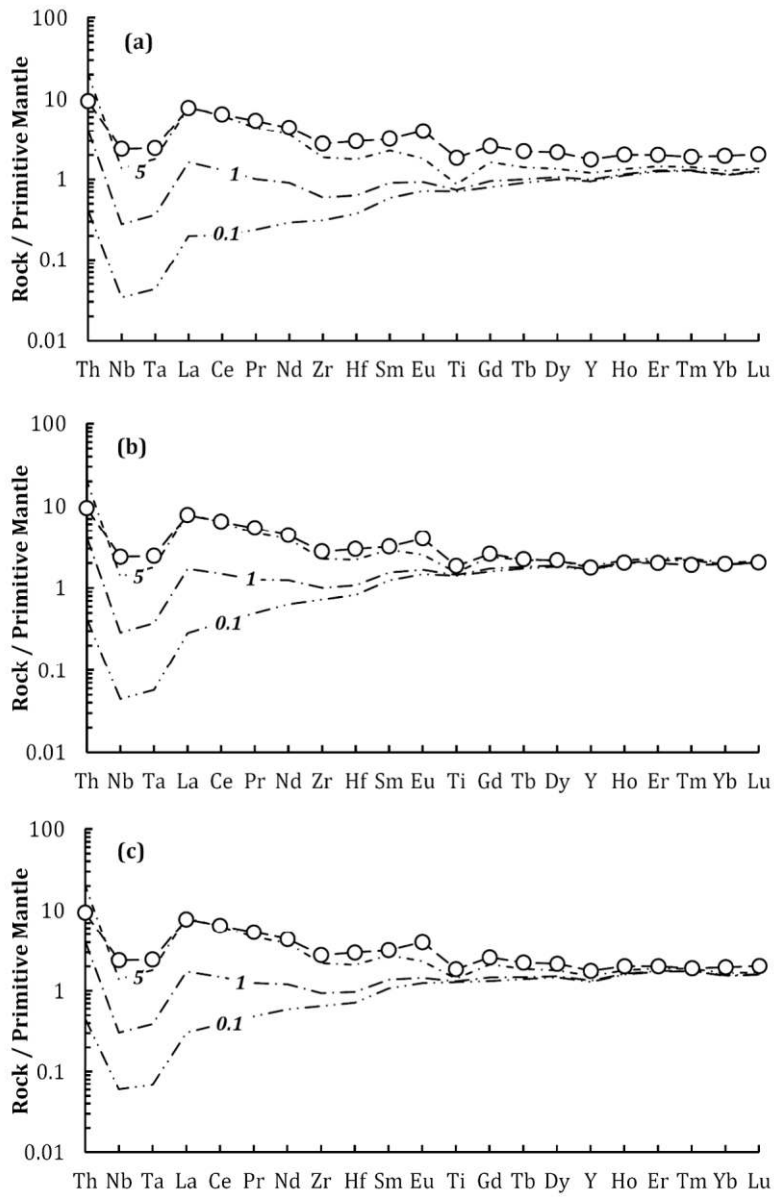
Review

1
2
3
4
5
6
7
8
9
10
11
12
13
14
15
16
17
18
19
20
21
22
23
24
25
26
27
28
29
30
31
32
33
34
35
36
37
38
39
40
41
42
43
44
45
46
47
48
49
50
51
52
53
54
55
56
57
58
59
60

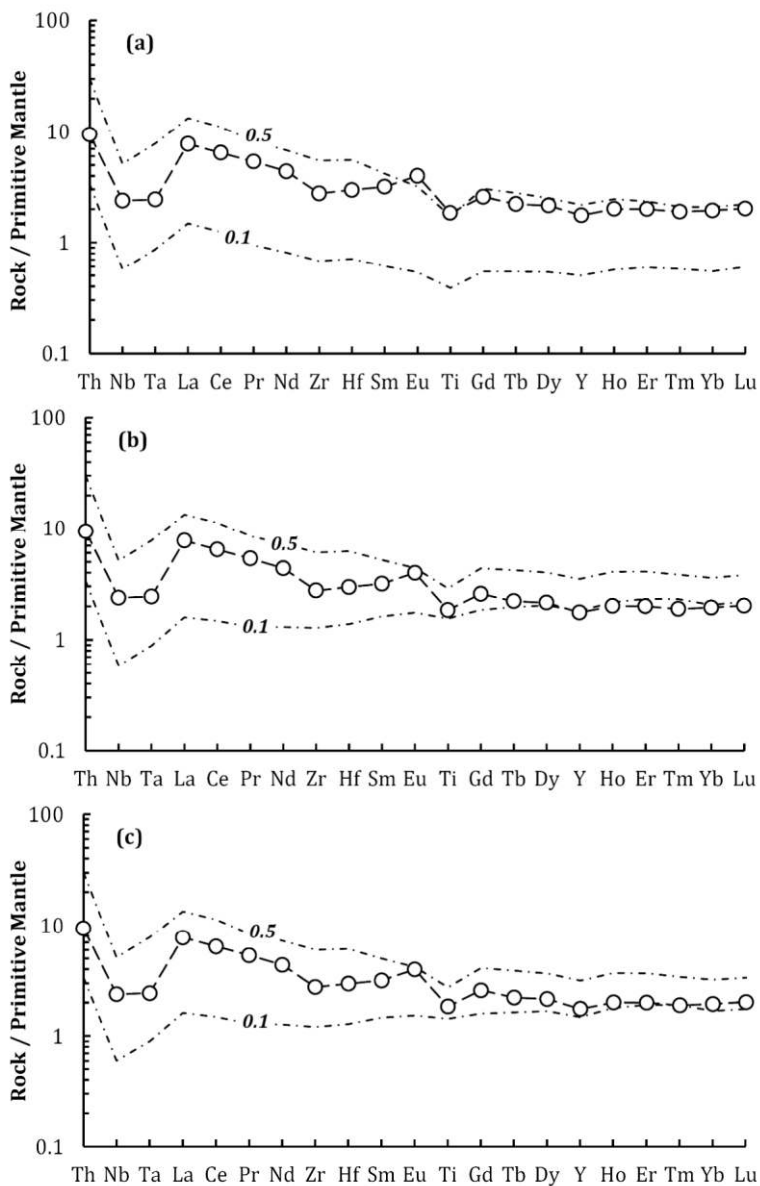


175x153mm (300 x 300 DPI)

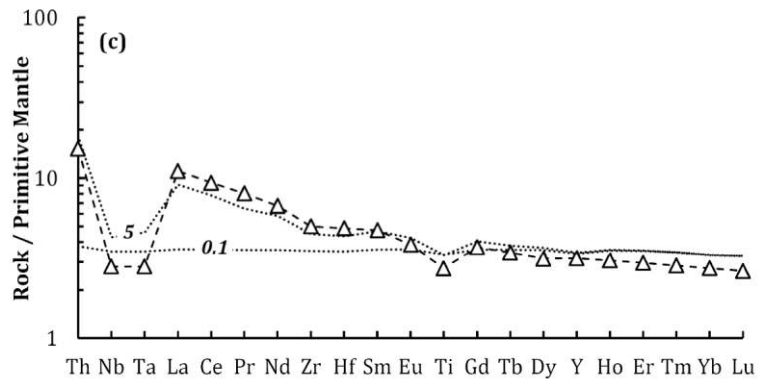
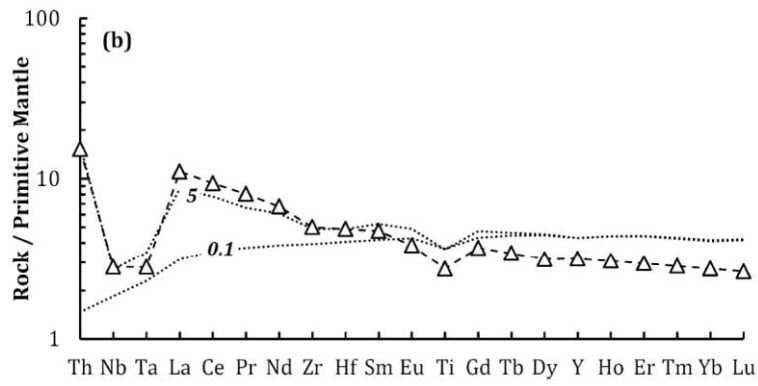
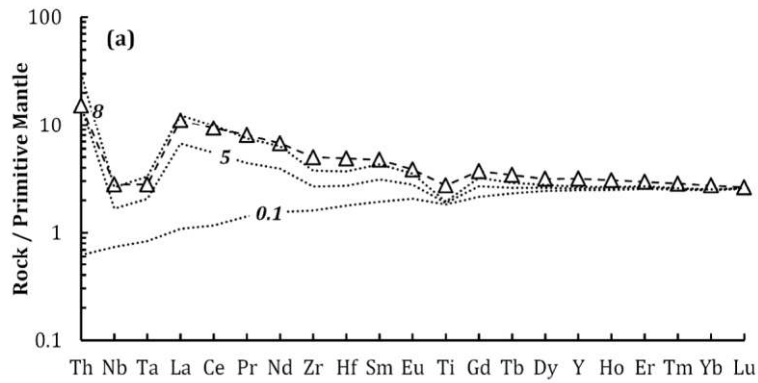
1
2
3
4
5
6
7
8
9
10
11
12
13
14
15
16
17
18
19
20
21
22
23
24
25
26
27
28
29
30
31
32
33
34
35
36
37
38
39
40
41
42
43
44
45
46
47
48
49
50
51
52
53
54
55
56
57
58
59
60

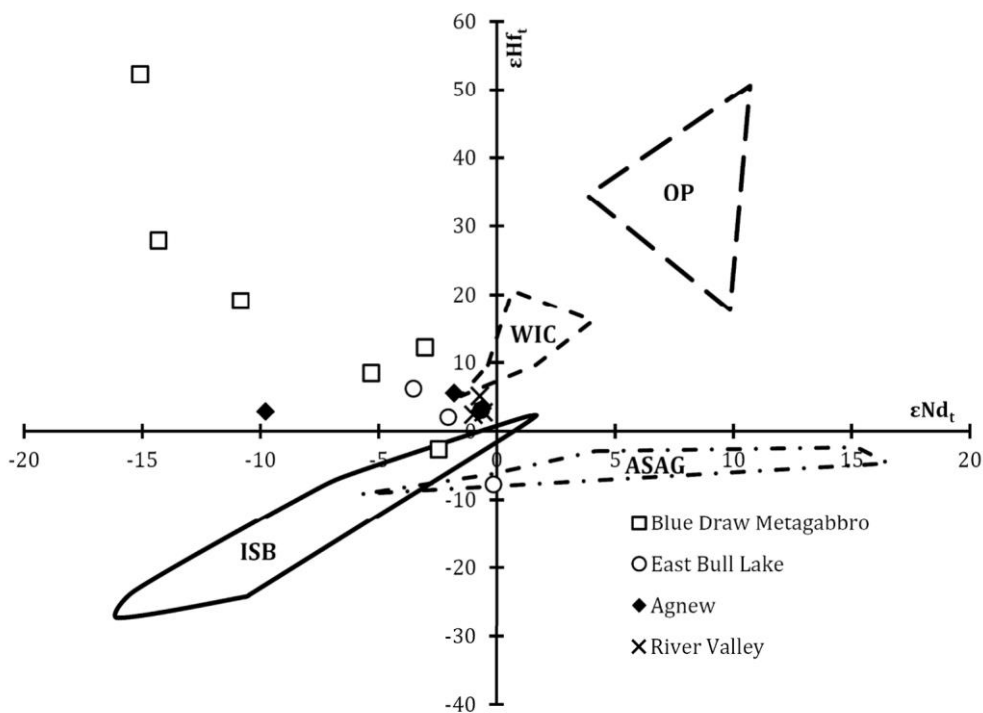


312x488mm (300 x 300 DPI)



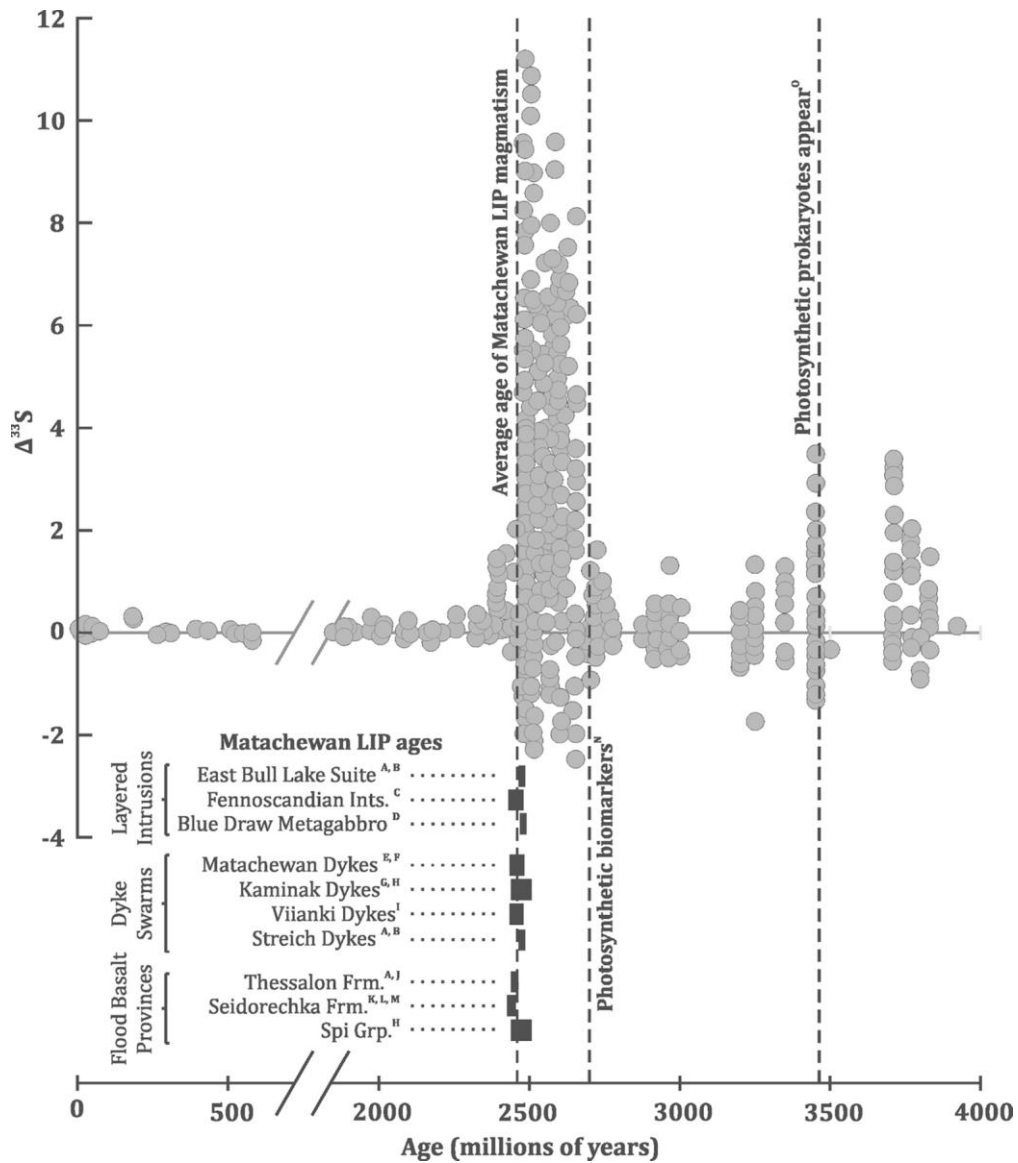
304x464mm (300 x 300 DPI)





222x164mm (300 x 300 DPI)

315x496mm (300 x 300 DPI)



113x130mm (300 x 300 DPI)